LA-11367-MS

Cross Sections for Neutron-Producing Reactions Induced by 14.1 MeV Neutrons Incident on ^{6}Li, ^{7}Li, ^{10}B, ^{11}B, and Carbon

Los Alamos

Los Alamos National Laboratory is operated by the University of California for the United States Department of Energy under contract W-7405-ENG-36.

Prepared by Noel R. Sanchez, Group P-3

An Affirmative Action/Equal Opportunity Employer

LA-11367-MS

UC-700
Issued: October 1988

LA--11367-MS

DE89 002104

Cross Sections for Neutron-Producing Reactions Induced by 14.1 MeV Neutrons Incident on ^{6}Li, ^{7}Li, ^{10}B, ^{11}B, and Carbon

M. Drosg*
P. W. Lisowski
D. M. Drake
R. A. Hardekopf
M. Muellner

*Consultant at Los Alamos. Institut für Experimental Physik, University of Vienna, Strudlhofgasse 4, A-1090, Wien, AUSTRIA.

Los Alamos National Laboratory
Los Alamos, New Mexico 87545

Cross Sections for Neutron-Producing Reactions Induced by 14.1 MeV Neutrons Incident on ^{6}Li, ^{7}Li, ^{10}B, ^{11}B, and Carbon

by

M. Drosg, P. W. Lisowski, D. M. Drake,
R. A. Hardekopf, and M. Muellner

ABSTRACT

Using the time-of-flight technique, we have measured neutron emission spectra for ^{6}Li, ^{7}Li, ^{10}B, ^{11}B and carbon at an incident neutron energy of 14.1 MeV and at 10 angles between 30° and 143°. Double differential cross sections and their integrated values have been extracted and are presented in tables and graphs. The nonelastic portion of the neutron emission spectra is noticeably higher than expected which may be due to uncertainties in the input library (ENDF/B-IV) used in the Monte Carlo correction for multiple scattering. In particular, the library for ^{11}B appears to be very unrealistic with an integrated elastic cross section which should be higher by 50%.

I. INTRODUCTION

The measurement of continuous neutron spectra requires sources of monoenergetic neutrons unless a very long flight path is used between source and sample[1] at the expense of counting rate. At 14.1 MeV a relatively intense neutron source is available using neutrons from the $^{3}H(d,n)^{4}He$ reaction at 90°. This source has been used before to measure fusion relevant double-differential neutron emission cross sections of light elements[2,3]. The present work complements previous work at 6 and 10 MeV on the two stable lithium isotopes[4] and boron isotopes[5]. In addition, carbon was measured for reference purposes.

II. EXPERIMENTAL DETAILS

A. Neutron Source

Fig. 1 compares the specific neutron yield of various sources near 14 MeV when gas targets are employed. The best source, $^{1}H(t,n)^{3}He$, could not be used, because at the time of the experiment there were no bunched

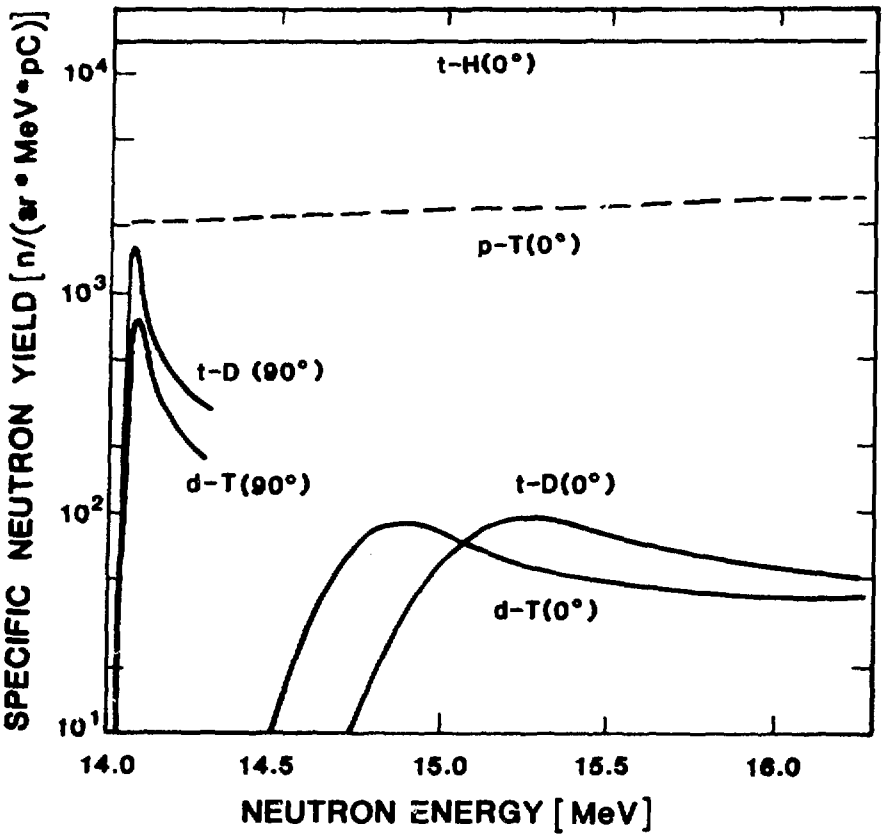

Fig. 1. Comparison of neutron yield of sources near 14 MeV when gas targets are employed.

tritons with an energy of 21 MeV available. The $^{3}H(p,n)^{3}He$ reaction is not monoenergetic at 14 MeV and therefore cannot be used. The striking feature of this figure is the compression of neutrons from the $^{3}H(d,n)^{4}He$ and the $^{2}H(t,n)^{4}He$ reaction into a narrow energy window if the sample is located at 90°. This results in an increase of the specific neutron yield by an order of magnitude. The $^{2}H(t,n)^{4}He$ reaction has been used in a similar experiment on beryllium before[6]. However, the 1.5 times higher specific yield of this source is offset by a lower triton current from the vertical Van-de-Graaff, which was used in this experiment. In addition, the higher zero-degree energy from the $^{2}H(t,n)^{4}He$ source would give a higher room background. So the experiment was performed with neutrons from the $^{3}H(d,n)^{4}He$ reaction at about 90° using a gas target.

A beam of about 0.7 μA of bunched deuterons from the vertical Van-de-Graaff with a time spread of about 1 ns and an energy of 1.3 MeV was stopped inside a tritium gas target to produce monoenergetic neutrons via the $^{3}H(d,n)^{4}He$ reaction. The target was a cell of 3 cm length, an entrance window of 5.3 mg/cm^{2} molybdenum and filled with tritium gas at a pressure of about 2 atm so that the deuteron beam was stopped in the middle of the gas cell. Under these conditions the nominal neutron energy is 14.1 MeV with an energy distribution having a FWHM energy spread of about 0.3 MeV and a high energy tail extending beyond 14.7 MeV.

B. Geometry

The cylindrical samples had their symmetry axis parallel to the beam direction and were rotated at a distance of 11.9 cm from the beam in a plane through the center of the target at 90° with respect to the beam direction. The heavily shielded detector, collimator, and tungsten shadow bar[6] were lifted hydraulically so that the center of the collimator was always aligned with the center of the sample. At the same time, this hydraulic lift adjusted the position of the shielded detector in such a way that the sample-to-detector distance remained constant at 251 cm.

At 30° the sample-to-source distance had to be changed to 14.5 cm to provide room for the shadow bar. In this case, the flight-path was 249 cm. The resulting change in solid angles was taken care of by calculation.

C. Samples

The samples were rectangular cylinders of highly enriched material. The Li-isotopes were canned in thin-walled aluminum cans (2.7 cm height, 1.98 cm diameter, 0.02 cm wall thickness and a mass of 1.4 g). The ^{6}Li sample had 0.573 moles with a purity of 99.05%. The ^{7}Li sample had 0.578 moles with a purity of 99.96%. The ^{10}B, ^{11}B and carbon samples were not encased. There were 1.025 moles of ^{10}B (96.19% pure, 4 cm high, 1.5 cm diameter), 0.980 moles of ^{11}B (97.15% pure, 3.7 cm high, 1.52 cm diameter) and 0.990 moles of carbon in its natural composition (3.81 cm high, 1.27 cm diameter). To check the validity of the multiple scattering correction, a low density graphite sample was used in addition (at 30° and 40°). This sample had a height of 2.54 cm and a diameter of 1.3 cm. It contained 0.236 moles of carbon.

D. Detector and Electronics

The general layout of the measuring system has been described before[4,6]. The pulse-height bias of the neutron detector (NE213) was set in the minimum between the two peaks of a ^{241}Am gamma-ray spectrum. The energy dependence of the neutron detection efficiency of the detector at this bias (0.29 MeV) has been reported before[7]. However, a closer examination showed that all time-of-flight spectra had their low energy cutoff at 0.235 MeV. Therefore the data were corrected for this difference in bias by the following simplified energy-dependent relation:

$$(E_n - B_c)/(E_n - B_a), \text{ where } B_c = 0.29 \text{ MeV and } B_a = 0.235 \text{ MeV} \quad .$$

A special feature of the electronics was the use of a time digitizer which resulted in a dead time of less than 1%. The dynamic range of the neutron-gamma discrimination circuit was increased by a factor of four by employing a special dynamic-range-expander[8]. The bias of this discriminator was so chosen that some γ-ray pulses were accepted but no neutron pulses lost.

The use of a constant-fraction discriminator in this experiment where a rather wide dynamic range is needed proved to be detrimental to the time resolution. It was only noticed toward the end of the experiment that big pulses were saturated which resulted in an overall time resolution of the constant fraction discriminator of about 5 ns. However, this affects only the energy resolution of the high energy portion of the spectrum and not continua or the integral of the nonelastic events.

E. Experimental Procedure

At each angle spectra of 7 samples were taken: ^{6}Li, ^{7}Li, casing of Li, ^{10}B, ^{11}B, carbon, no sample (as background runs for ^{10}B, ^{11}B and carbon). At 30° and 40° data were taken also with carbon foam and polyethylene for normalization to the ^{1}H(n,n)^{1}H cross section[9]. (The polyethylene sample had dimensions of 2.54 cm height, 1.3 cm diameter and had a mass of 2.924 g.) All runs were normalized to the counts of a monitor detector (5.0 cm diameter x 2.5 cm height, NE213) viewing the gas target (at an angle of 10° from a distance of 7.8 m) and, at the same time to the integrated beam charge. After correction for pressure and temperature changes of the gas in the target, the two methods agreed to better than 0.5%.

III. DATA REDUCTION

A. Time-of-Flight Spectra

At each angle the data of all samples were measured relative to each other, and at 30° and 40° relative to hydrogen as well. Net time-of-flight spectra were obtained by subtracting the corresponding background runs (see Sec. II. E) from the foreground runs. (For ^{6}Li, ^{10}B, and ^{11}B the appropriate portion of the other isotope was also subtracted to correct for its admixture.) The region where no neutrons were expected (for flight times corresponding to neutrons below the detection bias) was checked for consistency with a zero signal, otherwise an appropriate (small) "white" time background was added or subtracted to give zero counts in a region where there should be none.

B. Energy Spectra, Normalization and Corrections

The time spectra were converted into energy spectra and corrected for the energy dependence of the neutron detection efficiency of the detector[7] (see II.D. for the bias correction). Then the scale was calibrated by using scattering from hydrogen at 30° and 40° as a cross section reference[9], i.e., by using the ratio (or quasiabsolute) method to establish the cross section scale.

These calibrated spectra were corrected for multiple scattering using the Los Alamos National Laboratory code MCNP[10] to perform a Monte Carlo simulation. For these calculations the cross section library ENDF/B-IV was used. In this simulation the scattered neutrons were tallied by energy and angle according to the reaction type that created

them: single elastic, double elastic, elastic-inelastic, single inelastic, double inelastic and inelastic-elastic processes. However, in most cases, this simulation does not give realistic results as can be seen in Figs. A1 through A52 of the Appendix. There the actually measured spectra (full curves) are compared with the results of the simulation (dotted curves). Obviously, a poor simulation of the spectrum will result in a poorly calculated multiple scattering correction. Because an improvement of the input library (ENDF/B-IV) was beyond the scope of this work, the following procedure was believed to give a first-order improvement: the elastic and the inelastic portions of the simulated spectra were adjusted individually so that their integrals agreed with those of the corresponding portions of the measured spectra, changing the original simulation (dotted curves in the graphs of the Appendix) to the piecewise adjusted solution (dashed curves). The same adjustment factors were then applied to the corrections so that the energy shape of the corrections remained unchanged. Because of the generally poor agreement in shape, the corrections were done additively rather than in the usual multiplicative way. Thus at least the corrected integral is a better replica of the actual value.

There was no need to correct for neutrons from the deuterium contamination of the tritium gas in the target. The d-D neutron yield (with a mean neutron energy of 2.6 MeV) is only about 1/30 of the d-T yield. From the elastic scattering of these 2.6 MeV neutrons from carbon and hydrogen a deuterium admixture of less than 6% was deduced, i.e. the actual d-D neutron yield was only 0.2% of the total yield.

IV. RESULTS

A. Double Differential Cross sections

Tables I through VI give the multiple-scattering corrected double differential cross sections measured in this experiment. Because of the questionable quality of the multiple scattering correction, especially in the inelastic region, angular distributions of scattering from the excited states were not extracted except for the first excited state in ^{12}C.

B. Differential Elastic Cross sections

The multiple scattering correction of the elastically scattered neutrons (perhaps, with the exception of ^{11}B) should be quite reliable. Therefore, differential cross sections for elastic scattering were extracted. In most cases the worse time resolution at higher energies (see Sec. II.D) did not allow the separation of scattering from the low-lying excited states. Therefore, Table VII gives the differential laboratory cross section of the highest energy peak rather than elastic cross sections.

TABLE I

DOUBLE DIFFERENTIAL NEUTRON EMISSION CROSS SECTIONS FOR 14.1 MEV NEUTRONS ON LITHIUM-6 [DATA AND ERRORS IN mb/(sr*MeV)]

LAB.ANGLE [Deg]	30.0		40.0		50.1		63.6		80.3		89.8		99.3		115.0		130.0		143.0	
E-RANGE [MeV]																				
0.35- 0.50	31.8	6.5	19.8	4.4	14.9	5.9	18.8	5.1	20.0	4.7	10.2	3.5	9.2	4.2	7.8	4.3	5.6	4.3	6.2	4.6
0.50- 0.65	30.4	4.2	20.1	2.8	11.8	3.8	6.4	3.2	17.1	3.0	10.9	2.2	6.4	2.7	8.1	2.7	6.4	2.8	7.1	3.0
0.65- 0.80	21.5	3.4	17.2	2.3	14.9	3.2	10.5	2.6	12.8	2.5	10.4	1.8	7.8	2.2	3.3	2.2	8.1	2.3	5.3	2.5
0.80- 0.95	16.8	3.0	15.8	2.0	13.6	2.8	12.7	2.3	12.4	2.2	9.7	1.6	5.2	2.0	10.7	2.0	5.8	2.0	11.4	2.2
0.95- 1.10	14.8	2.7	12.8	1.9	10.4	2.6	10.9	2.2	12.9	2.0	9.0	1.5	9.2	1.8	6.7	1.9	6.5	1.9	6.4	2.0
1.10- 1.25	16.7	2.5	13.3	1.7	10.0	2.4	6.7	2.0	8.4	1.9	5.9	1.4	8.0	1.7	4.7	1.7	8.1	1.7	6.8	1.9
1.25- 1.40	13.1	2.4	13.5	1.7	11.3	2.3	7.6	1.9	7.1	1.8	7.2	1.3	6.2	1.6	4.6	1.6	7.9	1.6	1.9	1.8
1.40- 1.55	14.7	2.3	9.0	1.6	8.8	2.2	5.6	1.9	6.8	1.8	6.0	1.3	3.9	1.5	5.9	1.6	5.9	1.6	3.6	1.7
1.55- 1.70	10.2	2.2	10.4	1.5	10.0	2.1	9.1	1.8	7.3	1.7	6.7	1.3	5.6	1.5	5.9	1.5	5.4	1.5	3.2	1.6
1.70- 1.85	12.1	2.1	10.7	1.5	11.3	2.1	8.0	1.7	6.7	1.7	4.9	1.2	4.9	1.4	3.7	1.5	4.7	1.5	4.5	1.6
1.85- 2.00	13.0	2.1	7.3	1.5	8.7	2.0	7.0	1.7	6.9	1.6	4.0	1.2	3.9	1.4	3.1	1.4	1.8	1.4	1.9	1.5
2.00- 2.20	10.9	1.8	8.2	1.2	5.3	1.7	7.1	1.5	6.4	1.4	4.7	1.0	3.5	1.2	2.7	1.2	3.8	1.2	4.5	1.3
2.20- 2.40	11.3	1.8	8.1	1.2	7.2	1.7	2.5	1.5	3.7	1.4	4.2	1.0	3.6	1.2	2.8	1.2	0.1	1.2	6.1	1.3
2.40- 2.60	7.2	1.8	5.8	1.3	2.3	1.7	5.2	1.5	5.1	1.4	3.5	1.0	2.2	1.2	4.5	1.2	3.9	1.3	4.5	1.3
2.60- 2.80	9.2	1.8	5.3	1.2	4.5	1.7	2.8	1.4	2.2	1.3	3.2	1.0	2.0	1.1	4.0	1.2	4.4	1.2	5.0	1.3
2.80- 3.00	10.5	1.8	7.7	1.3	7.3	1.6	6.1	1.4	3.5	1.3	4.0	1.0	2.6	1.1	1.8	1.2	3.8	1.2	0.3	1.2
3.00- 3.20	7.3	1.8	5.2	1.2	7.4	1.6	4.4	1.4	3.6	1.3	4.1	0.9	5.0	1.1	3.6	1.1	1.2	1.2	1.4	1.2
3.20- 3.40	8.0	1.7	5.3	1.2	2.8	1.5	3.6	1.4	3.4	1.3	3.1	0.9	2.2	1.1	4.3	1.2	1.7	1.2	2.5	1.2
3.40- 3.60	2.9	1.7	4.2	1.2	5.0	1.6	4.6	1.3	5.6	1.2	1.0	0.9	1.6	1.1	1.4	1.1	3.4	1.1	5.1	1.2
3.60- 3.80	4.6	1.7	4.4	1.2	5.6	1.5	3.2	1.3	2.8	1.2	2.3	0.9	3.6	1.0	3.3	1.1	3.9	1.1	4.9	1.1
3.80- 4.00	5.9	1.7	4.4	1.2	3.0	1.5	6.2	1.3	3.3	1.2	1.7	0.9	1.6	1.0	5.9	1.1	3.0	1.1	3.2	1.1
4.00- 4.25	7.8	1.5	5.6	1.0	4.5	1.3	2.8	1.1	3.1	1.0	3.1	0.8	2.5	0.9	3.4	1.0	3.5	1.0	2.9	1.0
4.25- 4.50	8.4	1.4	5.6	1.0	4.6	1.3	3.7	1.1	3.2	1.0	1.5	0.7	2.3	0.9	1.9	1.0	2.3	1.0	5.9	1.0
4.50- 4.75	8.7	1.4	5.8	1.0	3.5	1.3	3.8	1.1	2.7	1.0	4.3	0.7	3.0	0.9	3.2	1.0	3.5	1.0	3.9	1.1
4.75- 5.00	8.2	1.5	4.7	1.0	3.7	1.3	3.8	1.1	3.8	1.0	4.2	0.7	4.2	0.9	2.0	1.0	2.3	1.0	3.9	1.0
5.00- 5.25	7.7	1.5	5.3	1.0	3.3	1.3	2.2	1.1	3.7	1.0	3.5	0.7	2.0	0.9	1.4	1.0	2.0	1.0	4.0	1.0
5.25- 5.50	6.9	1.4	5.1	1.0	5.9	1.3	2.7	1.1	2.2	1.0	4.4	0.7	4.1	0.9	3.5	1.0	2.4	1.0	1.1	1.0
5.50- 5.75	7.3	1.3	5.3	1.0	4.5	1.3	2.8	1.1	5.0	1.0	3.2	0.7	2.8	0.9	0.7	1.0	2.2	0.9	2.1	1.0
5.75- 6.00	4.8	1.3	5.6	0.9	5.8	1.3	2.5	1.1	5.1	1.0	3.0	0.7	3.8	0.9	2.9	1.0	3.0	0.9	4.1	1.0
6.00- 6.25	4.8	1.3	5.3	0.9	6.4	1.3	4.2	1.0	4.2	1.0	4.1	0.7	2.7	0.8	2.3	1.0	4.0	0.9	2.7	0.9
6.25- 6.50	8.2	1.3	5.6	0.9	6.9	1.2	5.4	1.0	3.5	0.9	4.2	0.7	0.1	0.9	3.3	0.9	3.8	0.9	1.9	0.9

LAB.ANGLE [Deg]	30.0		40.0		50.1		63.6		80.3		89.8		99.3		115.0		130.0		143.0	
E-RANGE [MeV]																				
6.50- 6.75	8.7	1.3	5.9	0.9	7.1	1.2	5.5	1.0	5.4	0.9	2.9	0.7	3.0	0.8	3.9	0.9	1.6	0.9	1.5	0.9
6.75- 7.00	7.0	1.3	7.0	0.9	5.8	1.3	5.3	1.0	3.7	1.0	2.6	0.7	3.1	0.9	3.8	0.9	0.5	0.9	0.8	0.9
7.00- 7.25	11.7	1.3	8.2	0.9	8.8	1.3	7.4	1.0	6.3	1.0	3.2	0.7	4.9	0.9	3.5	0.9	0.5	0.9	0.2	0.9
7.25- 7.50	8.9	1.3	8.3	0.9	8.0	1.2	6.7	1.0	4.7	0.9	2.8	0.7	4.9	0.9	0.8	0.9	3.3	0.9	0.3	1.0
7.50- 7.75	9.5	1.2	8.0	0.9	8.1	1.2	6.8	1.0	3.1	0.9	3.5	0.7	4.3	0.8	0.2	0.8	1.8	0.8	2.3	0.9
7.75- 8.00	9.4	1.2	8.0	0.8	8.8	1.1	5.3	0.9	4.3	0.9	5.1	0.7	3.1	0.8	1.8	0.8	4.8	0.9	2.1	0.8
8.00- 8.30	11.0	1.1	9.0	0.8	8.9	1.1	5.8	0.9	5.4	0.8	5.8	0.7	3.4	0.7	4.4	0.8	3.9	0.8	2.5	0.8
8.30- 8.60	13.9	1.2	10.4	0.8	8.9	1.1	5.7	0.9	7.4	0.9	5.0	0.7	2.5	0.7	7.4	0.8	3.1	0.8	0.5	0.8
8.60- 8.90	14.0	1.2	11.2	0.9	10.0	1.1	6.6	0.9	7.1	1.0	2.9	0.6	3.6	0.7	6.7	0.8	0.2	0.8	0.5	0.7
8.90- 9.20	12.4	1.1	11.4	0.8	9.3	1.0	6.7	0.8	6.4	0.8	3.4	0.5	4.4	0.7	4.1	0.7	0.3	0.7		
9.20- 9.50	11.0	1.0	10.5	0.8	10.2	1.0	7.7	0.8	4.9	0.7	3.7	0.5	5.3	0.7	2.0	0.7				
9.50- 9.80	13.6	1.1	12.0	0.8	10.4	1.1	9.3	0.9	3.7	0.7	6.0	0.6	5.6	0.8	0.1	0.7				
9.80-10.10	15.1	1.2	12.9	0.8	11.9	1.1	8.6	0.9	4.7	0.7	8.1	0.7	4.5	0.7						
10.10-10.40	14.8	1.1	12.5	0.9	10.7	1.1	7.6	0.8	4.3	0.8	6.5	0.6	3.3	0.6						
10.40-10.70	16.3	1.2	12.2	0.9	12.1	1.1	7.0	0.8	4.2	0.8	5.1	0.6	0.5	0.6						
10.70-11.00	22.7	1.3	17.1	1.0	14.2	1.1	6.6	0.8	5.8	0.7	3.5	0.5	0.5	0.6						
11.00-11.30	31.5	1.4	20.0	1.0	15.7	1.1	6.7	0.8	5.3	0.7	2.0	0.5	0.7	0.6						
11.30-11.60	43.3	1.6	28.3	1.0	20.7	1.2	8.5	0.8	3.2	0.6	0.4	0.5	0.7	0.5						
11.60-11.90	62.0	1.8	39.3	1.2	23.6	1.2	8.4	0.8	1.0	0.6	0.5	0.4								
11.90-12.20	80.8	2.0	49.3	1.3	23.8	1.3	8.7	0.8												
12.20-12.50	98.3	2.3	54.3	1.5	28.9	1.5	8.4	0.8												
12.50-12.80	108.2	2.6	60.8	1.6	31.9	1.6	5.1	0.8												
12.80-13.10	125.2	2.9	68.5	1.8	32.3	1.6	4.3	0.9												
13.10-13.40	134.0	3.2	72.8	1.8	27.5	1.6	3.1	0.9												
13.40-13.70	138.4	3.3	71.5	1.7	25.2	1.7	3.3	0.9												
13.70-14.00	123.9	3.2	57.1	1.6	17.6	1.6	1.4	1.1												
14.00-14.50	91.7	2.4	38.1	1.1	8.3	1.3	0.5	0.6												
14.50-15.00	51.1	1.8	18.0	0.9	6.3	1.3														
15.00-15.50	19.7	1.2	8.4	0.7	4.9	1.1														
15.50-16.00	9.4	0.8	2.6	0.5	4.0	0.9														
16.00-16.50	3.4	0.6	1.3	0.4	2.0	0.8														
16.50-17.00	1.5	0.6	0.9	0.4																

TABLE II

DOUBLE DIFFERENTIAL NEUTRON EMISSION CROSS SECTIONS FOR 14.1 MEV NEUTRONS ON LITHIUM-7 [DATA AND ERRORS IN mb/(sr*MeV)]

LAB.ANGLE [Deg]	30.0		40.0		50.1		63.6		80.3		89.8		99.3		115.0		130.0		143.0	
E-RANGE [MeV]																				
0.35- 0.50	27.9	6.5	24.6	4.4	20.0	5.9	15.9	5.6	16.4	5.0	10.5	3.5	5.7	4.2	11.0	4.3	7.0	4.4	11.5	4.6
0.50- 0.65	36.7	4.2	27.6	2.9	13.1	3.8	12.7	3.6	11.7	3.2	11.0	2.2	8.6	2.7	10.0	2.8	9.9	2.8	11.2	3.1
0.65- 0.80	26.0	3.5	20.5	2.4	13.8	3.1	9.9	2.9	11.2	2.6	10.2	1.8	12.3	2.3	9.0	2.2	7.3	2.3	3.3	2.5
0.80- 0.95	27.7	3.1	17.4	2.1	9.0	2.8	12.0	2.6	11.1	2.3	7.9	1.6	6.7	2.0	7.5	2.0	4.9	2.0	7.2	2.2
0.95- 1.10	18.7	2.8	9.2	1.9	9.7	2.6	7.8	2.4	12.7	2.2	8.8	1.5	8.6	1.8	4.4	1.8	5.0	1.9	3.4	2.1
1.10- 1.25	17.8	2.6	11.2	1.8	7.3	2.4	8.5	2.2	7.6	2.0	4.1	1.4	6.0	1.7	3.9	1.7	3.1	1.7	4.3	1.9
1.25- 1.40	11.8	2.5	10.9	1.7	10.6	2.3	6.3	2.1	6.2	1.9	4.0	1.3	5.5	1.6	5.1	1.6	6.1	1.6	2.8	1.8
1.40- 1.55	10.6	2.3	9.6	1.6	10.8	2.2	6.8	2.1	3.5	1.9	4.9	1.3	5.7	1.5	6.2	1.6	7.2	1.6	3.7	1.7
1.55- 1.70	13.0	2.2	9.5	1.6	9.5	2.1	5.9	2.0	6.2	1.8	5.3	1.2	5.3	1.5	5.8	1.5	4.0	1.5	5.5	1.6
1.70- 1.85	10.3	2.1	8.8	1.5	7.3	2.0	5.2	1.9	6.5	1.8	4.4	1.2	5.5	1.4	4.9	1.5	1.5	1.5	4.8	1.6
1.85- 2.00	8.9	2.1	7.4	1.5	6.2	2.0	3.8	1.9	7.0	1.7	5.4	1.2	4.7	1.4	2.8	1.4	1.7	1.5	1.4	1.5
2.00- 2.20	8.9	1.8	8.0	1.2	3.4	1.7	3.6	1.6	6.0	1.5	4.3	1.0	2.2	1.2	3.3	1.2	2.4	1.2	5.2	1.3
2.20- 2.40	9.9	1.7	8.0	1.2	6.3	1.7	3.2	1.6	2.1	1.4	3.9	1.0	2.4	1.1	4.7	1.2	1.0	1.2	3.5	1.3
2.40- 2.60	7.3	1.8	5.1	1.2	1.9	1.7	4.3	1.6	6.0	1.4	3.8	1.0	2.3	1.2	4.8	1.2	4.8	1.2	3.6	1.3
2.60- 2.80	7.1	1.7	5.3	1.2	3.8	1.6	4.7	1.6	0.9	1.4	2.3	1.0	2.3	1.1	4.4	1.2	3.7	1.2	4.5	1.3
2.80- 3.00	8.6	1.8	6.7	1.2	5.2	1.6	4.4	1.5	2.5	1.4	3.8	0.9	3.2	1.1	2.4	1.2	3.1	1.2	0.3	1.2
3.00- 3.20	7.6	1.7	4.3	1.2	7.2	1.5	3.4	1.5	3.8	1.3	3.7	0.9	4.5	1.1	3.5	1.1	3.1	1.2	2.9	1.2
3.20- 3.40	5.4	1.6	4.7	1.2	2.9	1.5	1.8	1.5	1.8	1.3	2.8	0.9	2.3	1.1	4.3	1.1	1.8	1.2	1.6	1.2
3.40- 3.60	6.5	1.6	6.2	1.2	4.8	1.5	5.3	1.4	3.6	1.3	2.0	0.9	2.2	1.1	2.3	1.1	4.3	1.1	4.7	1.2
3.60- 3.80	6.5	1.7	5.0	1.2	5.7	1.5	3.4	1.4	0.4	1.3	1.8	0.9	2.9	1.0	3.6	1.1	3.8	1.1	3.2	1.1
3.80- 4.00	9.0	1.8	5.3	1.2	2.8	1.4	4.4	1.4	2.8	1.2	2.3	0.8	1.4	1.0	4.4	1.1	1.4	1.1	2.7	1.1
4.00- 4.25	7.1	1.6	6.5	1.0	2.0	1.3	2.7	1.2	2.3	1.	2.7	0.7	3.2	0.9	3.8	1.0	2.9	1.0	1.9	1.0
4.25- 4.50	5.7	1.4	4.6	1.0	3.7	1.3	3.1	1.2	2.6	1.1	0.7	0.7	2.7	0.9	1.3	1.0	1.9	1.0	4.1	1.0
4.50- 4.75	8.9	1.5	6.0	1.1	1.5	1.3	2.3	1.2	3.3	1.1	3.5	0.7	3.6	0.9	2.5	1.0	2.4	1.0	5.6	1.0
4.75- 5.00	8.0	1.5	4.7	1.1	3.5	1.3	5.4	1.2	4.2	1.1	3.5	0.7	3.6	0.9	2.5	1.0	6.7	1.0	7.6	1.0
5.00- 5.25	7.3	1.6	6.1	1.0	3.1	1.3	3.2	1.2	3.6	1.1	3.4	0.7	2.7	0.9	5.1	1.0	7.0	1.0	4.5	1.0
5.25- 5.50	6.9	1.5	6.4	1.0	5.7	1.3	3.5	1.2	1.7	1.1	3.5	0.7	3.7	0.9	8.2	1.0	3.5	1.0	1.7	1.0
5.50- 5.75	7.6	1.4	7.1	1.0	5.4	1.3	2.6	1.2	1.7	1.0	3.2	0.7	4.4	0.9	4.1	1.0	1.5	0.9	1.5	1.1
5.75- 6.00	7.3	1.4	6.0	1.0	5.9	1.3	3.2	1.2	2.9	1.0	3.8	0.7	7.5	0.9	4.6	0.9	0.6	0.9	0.2	1.0
6.00- 6.25	5.6	1.4	5.9	1.0	6.0	1.2	3.7	1.1	4.2	1.0	6.0	0.7	6.7	0.9	1.6	0.9	0.1	0.9	0.8	0.9
6.25- 6.50	10.1	1.4	6.6	1.0	3.4	1.2	2.9	1.1	5.4	1.0	8.8	0.7	2.8	0.9	1.6	0.9	0.0	0.8	0.3	0.9

LAB.ANGLE [Deg]	30.0		40.0		50.1		63.6		80.3		89.8		99.3		115.0		130.0		143.0	
E-RANGE [MeV]																				
6.50- 6.75	7.4	1.3	5.6	0.9	4.4	1.2	4.2	1.1	8.8	1.0	7.2	0.7	4.7	0.8	1.0	0.8	0.0	0.8	0.2	1.0
6.75- 7.00	8.2	1.4	7.9	1.0	3.3	1.2	5.3	1.1	9.6	1.1	5.0	0.7	1.9	0.9	2.1	0.9	0.0	0.9	0.2	1.0
7.00- 7.25	9.8	1.4	7.5	1.0	7.6	1.2	7.7	1.2	8.7	1.1	2.6	0.7	0.1	0.8	1.2	0.9	0.6	0.9	0.5	1.0
7.25- 7.50	9.3	1.4	6.5	0.9	6.7	1.2	11.3	1.2	3.8	1.0	1.0	0.6	0.5	0.8	1.1	0.9	0.6	0.9	0.8	1.0
7.50- 7.75	9.1	1.3	8.5	0.9	8.7	1.2	10.9	1.1	2.3	0.9	0.3	0.6	0.2	0.7	0.6	0.9	0.4	0.8	0.8	0.9
7.75- 8.00	10.7	1.2	9.2	0.9	11.9	1.2	8.4	1.1	0.9	0.9	1.2	0.6	0.5	0.7	0.6	0.9	1.9	0.8	2.4	0.9
8.00- 8.30	13.5	1.2	12.1	0.9	13.0	1.1	6.5	1.0	1.8	0.8	0.1	0.5	1.5	0.7	3.3	0.8	3.2	0.8	6.5	0.8
8.30- 8.60	15.4	1.2	15.4	0.9	11.8	1.1	3.6	0.9	1.0	0.8	0.5	0.5	0.6	0.7	7.4	0.8	6.3	0.8	5.8	0.9
8.60- 8.90	17.1	1.3	14.3	0.9	8.2	1.1	2.6	0.9	0.4	0.8	0.8	0.6	2.9	0.7	8.2	0.8	6.2	0.8	3.7	0.8
8.90- 9.20	13.9	1.2	9.3	0.8	5.8	1.0	1.7	0.8	1.5	0.8	1.5	0.5	5.9	0.7	8.6	0.8	4.6	0.7	0.7	0.7
9.20- 9.50	11.3	1.1	6.4	0.7	4.3	0.9	1.6	0.8	2.0	0.8	3.3	0.5	8.4	0.7	10.3	0.8	2.3	0.7	1.2	0.7
9.50- 9.80	8.8	1.1	3.6	0.7	3.2	1.0	3.0	0.8	1.8	0.8	6.8	0.5	10.6	0.8	7.4	0.8	0.3	0.7	1.0	0.7
9.80-10.10	6.8	1.1	4.2	0.7	1.6	0.9	0.8	0.8	5.5	0.8	9.4	0.6	12.6	0.9	4.7	0.7	0.8	0.7	0.4	0.7
10.10-10.40	6.9	1.0	2.9	0.7	1.1	0.9	0.5	0.8	6.9	0.8	11.6	0.6	12.5	0.8	2.7	0.7				
10.40-10.70	7.5	1.0	2.4	0.7	2.5	0.9	3.3	0.8	7.4	0.8	12.0	0.7	8.7	0.7	1.8	0.6				
10.70-11.00	12.5	1.1	7.2	0.7	6.3	1.0	5.6	0.8	9.7	0.8	11.3	0.6	4.7	0.7	1.2	0.6				
11.00-11.30	21.7	1.2	12.4	0.8	13.6	1.1	7.7	0.9	10.3	0.9	8.9	0.5	2.5	0.6	1.1	0.6				
11.30-11.60	38.7	1.4	25.1	1.0	20.3	1.2	11.6	0.9	9.5	0.8	4.9	0.5	0.9	0.6						
11.60-11.90	60.9	1.7	40.6	1.2	26.1	1.2	12.3	1.0	6.1	0.8	2.3	0.5	0.7	0.5						
11.90-12.20	87.1	2.1	53.0	1.3	30.0	1.4	13.4	1.0	3.5	0.7	1.4	0.5								
12.20-12.50	110.8	2.4	61.7	1.5	37.2	1.5	14.9	1.0	1.6	0.7	0.5	0.4								
12.50-12.80	123.4	2.8	69.4	1.7	41.8	1.7	12.6	1.0	0.9	0.7										
12.80-13.10	138.2	3.1	82.1	1.9	42.6	1.8	8.0	1.0												
13.10-13.40	154.6	3.4	89.6	2.0	39.4	1.8	6.1	1.0												
13.40-13.70	162.8	3.7	87.2	2.0	33.5	1.8	6.9	1.0												
13.70-14.00	153.6	3.6	71.4	1.8	23.5	1.7	3.0	1.0												
14.00-14.50	113.6	2.8	49.0	1.3	15.1	1.3	1.1	0.8												
14.50-15.00	64.4	2.1	28.0	1.0	8.2	1.3														
15.00-15.50	28.3	1.4	11.0	0.7	3.4	1.1														
15.50-16.00	11.9	0.9	3.7	0.5	1.9	0.9														
16.00-16.50	5.1	0.7	1.6	0.4	1.2	0.7														
16.50-17.00	2.9	0.6	1.4	0.4																

TABLE III

DOUBLE DIFFERENTIAL NEUTRON EMISSION CROSS SECTIONS FOR 14.1 MEV NEUTRONS ON BORON-10 [DATA AND ERRORS IN mb/(sr*MeV)]

LAB.ANGLE [Deg]	30.0		40.0		50.1		63.6		80.3		89.8		99.3		115.0		130.0		143.0	
E-RANGE [MeV]																				
0.35- 0.50	50.4	3.7	27.6	2.2	20.9	3.3	20.0	3.1	14.6	2.8	17.7	2.8	14.7	2.3	11.4	2.4	12.9	2.4	8.3	2.5
0.50- 0.65	40.6	2.4	25.0	1.4	18.0	2.1	15.9	2.0	13.6	1.8	11.3	1.8	11.4	1.5	11.5	1.5	7.3	1.5	10.9	1.7
0.65- 0.80	34.0	1.9	21.6	1.2	15.6	1.7	13.2	1.6	11.0	1.5	10.1	1.5	8.6	1.3	6.9	1.2	6.3	1.3	7.6	1.4
0.80- 0.95	21.2	1.7	14.9	1.0	12.1	1.5	9.1	1.4	6.6	1.3	8.5	1.3	8.0	1.1	5.5	1.1	3.6	1.1	6.8	1.2
0.95- 1.10	18.3	1.5	12.3	1.0	7.7	1.4	9.4	1.3	5.7	1.2	6.4	1.2	4.1	1.0	2.8	1.0	3.2	1.0	4.7	1.1
1.10- 1.25	13.6	1.4	11.3	0.9	9.4	1.3	6.4	1.2	5.8	1.1	5.6	1.1	3.4	0.9	3.5	1.0	5.0	1.0	6.4	1.0
1.25- 1.40	12.7	1.7	8.3	0.8	4.3	1.3	6.1	1.2	3.3	1.1	4.6	1.0	4.3	0.9	5.2	0.9	3.3	0.9	5.4	1.0
1.40- 1.55	9.4	1.6	6.4	0.8	2.5	1.2	3.4	1.1	4.1	1.0	2.6	1.0	3.0	0.8	2.9	0.9	3.2	0.9	6.0	0.9
1.55- 1.70	10.7	1.5	5.8	0.8	2.9	1.2	5.7	1.1	5.4	1.0	4.4	1.0	5.1	0.8	4.3	0.8	3.8	0.8	5.1	0.9
1.70- 1.85	8.8	1.4	4.9	0.7	4.7	1.1	4.6	1.1	3.6	1.0	3.9	1.0	5.0	0.8	2.7	0.8	2.7	0.8	2.6	0.9
1.85- 2.00	10.4	1.4	5.8	0.7	2.9	1.1	3.0	1.1	4.0	1.0	4.2	1.0	2.5	0.8	2.9	0.8	3.6	0.8	3.5	0.8
2.00- 2.20	6.5	1.5	4.2	0.7	2.7	1.0	4.3	0.9	4.2	0.8	3.3	0.8	3.2	0.7	3.6	0.7	2.5	0.7	1.6	0.7
2.20- 2.40	6.1	1.7	5.5	0.8	5.7	1.0	5.0	0.9	3.6	0.8	4.1	0.8	3.3	0.7	2.9	0.7	2.7	0.7	3.1	0.7
2.40- 2.60	6.1	1.5	5.0	0.9	4.6	1.0	4.3	0.9	3.7	0.8	3.5	0.8	2.6	0.7	2.7	0.7	2.8	0.7	2.8	0.7
2.60- 2.80	7.0	1.2	5.4	0.9	3.8	1.0	3.5	0.9	3.7	0.8	3.0	0.8	3.7	0.7	2.9	0.7	1.8	0.7	2.3	0.7
2.80- 3.00	5.5	1.2	5.0	1.0	2.3	0.9	4.1	0.9	4.3	0.8	4.1	0.8	1.6	0.6	1.9	0.7	0.8	0.7	1.2	0.7
3.00- 3.20	7.3	2.0	5.1	0.9	1.8	0.9	3.1	0.9	4.1	0.8	3.4	0.7	2.4	0.6	1.4	0.6	1.2	0.7	2.2	0.7
3.20- 3.40	6.7	1.9	4.6	0.8	3.8	0.9	4.8	0.9	4.1	0.8	3.6	0.7	1.9	0.6	2.1	0.7	1.2	0.7	2.5	0.7
3.40- 3.60	6.8	2.0	4.2	0.8	4.7	0.8	3.8	0.8	3.1	0.8	1.9	0.7	1.5	0.6	1.5	0.7	1.0	0.6	1.6	0.7
3.60- 3.80	7.9	2.0	4.5	0.8	4.1	0.9	3.0	0.8	2.7	0.7	1.5	0.7	0.9	0.6	1.4	0.7	0.9	0.6	0.7	0.7
3.80- 4.00	6.4	1.6	5.6	0.9	4.0	0.8	3.8	0.8	1.9	0.7	2.4	0.7	1.5	0.6	1.4	0.6	1.1	0.6	2.3	0.6
4.00- 4.25	7.3	1.6	3.9	0.7	2.1	0.7	2.7	0.7	2.0	0.6	1.4	0.7	1.4	0.5	2.4	0.5	2.1	0.6	2.4	0.6
4.25- 4.50	4.2	1.6	3.4	0.6	2.0	0.7	2.0	0.7	2.1	0.7	1.9	0.6	2.0	0.5	1.8	0.6	1.3	0.5	4.0	0.7
4.50- 4.75	5.7	2.0	3.1	0.6	1.5	0.7	2.3	0.7	0.7	0.7	1.9	0.6	1.6	0.5	1.9	0.6	2.6	0.6	5.8	0.7
4.75- 5.00	4.7	1.5	3.2	0.7	1.5	0.8	1.6	0.7	2.2	0.7	1.4	0.6	1.7	0.5	4.0	0.6	6.4	0.7	6.3	0.8
5.00- 5.25	5.5	1.9	2.8	0.6	2.3	0.7	3.1	0.7	1.4	0.6	1.4	0.6	2.3	0.5	6.1	0.8	6.4	0.8	3.5	0.7
5.25- 5.50	4.2	1.5	3.3	0.7	2.0	0.8	2.0	0.7	1.8	0.6	2.2	0.6	4.4	0.6	6.6	0.8	3.1	0.6	2.4	0.6
5.50- 5.75	5.1	2.0	3.2	0.7	1.3	0.7	1.9	0.7	2.5	0.6	4.4	0.7	6.0	0.7	3.4	0.7	1.8	0.6	1.2	0.5
5.75- 6.00	4.8	1.6	3.4	0.7	2.2	0.7	3.7	0.7	4.6	0.7	7.2	0.8	4.5	0.8	1.8	0.6	1.9	0.5	1.0	0.5
6.00- 6.25	4.2	1.8	2.8	0.7	2.2	0.7	3.7	0.6	6.4	0.9	6.5	0.9	2.4	0.6	1.4	0.5	1.9	0.5	0.8	0.5
6.25- 6.50	6.2	1.3	3.2	0.6	3.2	0.7	4.9	0.8	6.5	1.0	3.1	0.7	2.3	0.5	1.1	0.5	1.3	0.5	2.0	0.5

LAB.ANGLE [Deg]	30.0		40.0		50.1		63.6		80.3		89.8		99.3		115.0		130.0		143.0	
E-RANGE [MeV]																				
6.50- 6.75	6.6	1.5	3.8	0.6	2.7	0.8	5.7	1.0	5.0	0.8	2.4	0.6	1.0	0.5	0.9	0.5	1.7	0.5	1.8	0.5
6.75- 7.00	8.3	1.7	6.5	0.9	5.8	1.0	7.3	1.3	3.4	0.7	2.1	0.5	1.4	0.5	2.0	0.5	1.7	0.5	1.3	0.5
7.00- 7.25	11.2	2.6	7.8	1.3	7.2	1.2	5.7	1.0	2.1	0.6	1.2	0.5	1.0	0.5	1.9	0.5	0.8	0.5	1.2	0.5
7.25- 7.50	11.1	3.0	9.3	1.6	6.8	1.2	2.4	0.7	1.6	0.6	1.1	0.5	0.7	0.4	0.8	0.5	1.1	0.5	0.2	0.5
7.50- 7.75	11.3	3.6	8.2	1.4	4.1	0.9	2.6	0.6	1.3	0.5	1.0	0.5	0.8	0.4	1.4	0.4	0.4	0.4	0.7	0.5
7.75- 8.00	10.0	3.1	6.2	1.0	3.5	0.7	1.9	0.6	1.4	0.5	1.6	0.4	1.5	0.4	0.1	0.4	0.9	0.4	0.8	0.5
8.00- 8.30	7.1	2.3	5.2	0.6	2.9	0.6	2.0	0.5	2.0	0.4	0.5	0.4	0.6	0.4	0.4	0.4	1.2	0.4	1.0	0.4
8.30- 8.60	7.1	1.6	4.4	0.6	3.5	0.6	2.1	0.5	0.8	0.5	0.4	0.4	1.1	0.4	0.6	0.4	1.0	0.4	1.6	0.4
8.60- 8.90	6.3	1.1	4.2	0.5	3.5	0.6	1.5	0.5	1.0	0.5	0.0	0.4	0.5	0.4	0.9	0.4	1.6	0.4	2.3	0.5
8.90- 9.20	6.6	0.9	4.3	0.4	3.2	0.5	0.7	0.4	0.4	0.4	0.8	0.4	0.3	0.3	1.9	0.4	2.2	0.4	2.3	0.4
9.20- 9.50	5.9	0.8	3.8	0.4	1.8	0.5	1.5	0.5	0.5	0.4	0.9	0.4	1.5	0.3	3.5	0.4	3.5	0.4	3.0	0.4
9.50- 9.80	4.6	0.7	3.3	0.4	2.6	0.5	0.7	0.5	0.3	0.4	1.0	0.4	2.9	0.4	5.5	0.4	4.5	0.4	5.0	0.5
9.80-10.10	4.6	0.7	2.4	0.4	2.0	0.5	0.3	0.4	1.3	0.4	1.6	0.4	5.3	0.4	7.3	0.5	5.8	0.5	5.2	0.5
10.10-10.40	4.4	0.7	2.3	0.4	1.2	0.5	1.0	0.4	1.7	0.4	3.9	0.4	7.4	0.5	8.3	0.5	6.6	0.5	3.8	0.4
10.40-10.70	4.4	0.7	3.0	0.3	2.0	0.5	0.8	0.4	3.4	0.4	5.2	0.5	9.5	0.5	10.4	0.6	5.2	0.4	2.9	0.4
10.70-11.00	6.8	0.7	2.6	0.3	2.1	0.5	2.6	0.4	5.6	0.5	7.2	0.5	10.2	0.5	10.1	0.5	3.0	0.4	2.1	0.4
11.00-11.30	9.7	0.7	5.5	0.4	2.8	0.5	3.5	0.4	7.2	0.5	9.2	0.6	12.3	0.6	7.6	0.5	1.8	0.4	1.2	0.4
11.30-11.60	19.7	0.9	10.1	0.5	5.6	0.6	4.8	0.5	8.9	0.5	12.4	0.6	11.6	0.6	4.9	0.4	1.1	0.3	0.6	0.3
11.60-11.90	35.0	1.3	16.4	0.7	9.0	0.6	5.9	0.5	10.7	0.6	13.2	0.6	9.3	0.5	3.5	0.4	1.2	0.3	0.4	0.3
11.90-12.20	51.3	1.7	24.7	0.9	12.8	0.7	7.0	0.5	11.2	0.6	12.7	0.6	6.4	0.4	1.4	0.3	0.2	0.3		
12.20-12.50	71.5	2.2	35.0	1.1	15.7	0.8	8.8	0.6	10.7	0.6	9.4	0.5	4.5	0.4	0.4	0.3				
12.50-12.80	88.3	2.7	42.0	1.3	18.3	0.9	9.7	0.6	9.5	0.6	6.4	0.5	3.0	0.4	0.6	0.3				
12.80-13.10	98.4	3.2	47.4	1.5	22.3	1.0	9.8	0.6	6.9	0.5	4.8	0.4	1.8	0.3	0.9	0.3				
13.10-13.40	108.3	3.6	53.0	1.7	25.4	1.1	8.2	0.6	3.5	0.5	3.2	0.4	0.7	0.3						
13.40-13.70	122.9	4.2	58.8	1.8	25.6	1.1	6.2	0.6	1.6	0.5	1.7	0.4	0.5	0.4						
13.70-14.00	125.8	4.2	59.1	1.6	22.1	1.1	4.8	0.6	0.9	0.5	0.6	0.4								
14.00-14.50	103.8	3.5	47.3	1.3	14.4	0.8	3.2	0.4	0.4	0.4										
14.50-15.00	68.4	2.7	29.2	0.9	8.3	0.7	1.1	0.4												
15.00-15.50	35.0	1.9	14.2	0.6	4.8	0.6	0.5	0.3												
15.50-16.00	16.4	1.0	5.4	0.3	1.9	0.5														
16.00-16.50	5.1	0.5	1.5	0.2																
16.50-17.00	2.7	0.3																		

TABLE IV

DOUBLE DIFFERENTIAL NEUTRON EMISSION CROSS SECTIONS FOR 14.1 MEV NEUTRONS ON BORON-11 [DATA AND ERROR IN mb/(sr*MeV)]

LAB.ANGLE [Deg]	30.0		40.0		50.1		63.6		80.3		89.8		99.3		115.0		130.0		143.0	
E-RANGE [MeV]																				
0.35- 0.50	49.3	3.7	17.4	2.5	21.5	3.3	22.2	3.1	13.4	2.9	13.3	2.8	9.8	2.3	5.8	2.4	5.0	2.4	5.7	2.5
0.50- 0.65	32.1	2.4	17.6	1.6	14.3	2.1	16.9	2.0	12.2	1.8	10.6	1.8	9.0	1.5	5.4	1.5	4.0	1.5	7.7	1.7
0.65- 0.80	26.1	1.9	14.9	1.3	15.1	1.8	13.3	1.6	11.5	1.5	11.5	1.5	9.1	1.3	9.0	1.3	8.6	1.3	11.6	1.4
0.80- 0.95	22.2	1.7	13.0	1.2	16.0	1.6	12.2	1.5	10.7	1.3	12.9	1.3	9.6	1.1	8.9	1.1	5.6	1.1	9.0	1.3
0.95- 1.10	18.6	1.6	10.7	1.0	9.7	1.4	9.4	1.3	8.1	1.2	10.9	1.2	6.6	1.0	4.4	1.0	4.5	1.0	6.5	1.1
1.10- 1.25	14.2	1.4	9.4	1.0	9.7	1.3	7.8	1.2	6.1	1.1	9.1	1.1	5.2	0.9	2.8	1.0	3.7	1.0	5.6	1.0
1.25- 1.40	11.9	1.3	9.1	0.9	5.7	1.3	7.3	1.2	7.2	1.1	8.3	1.1	4.1	0.9	3.6	0.9	3.1	0.9	4.3	1.0
1.40- 1.55	10.4	1.3	6.1	0.9	6.1	1.2	7.3	1.2	7.0	1.1	4.8	1.0	4.2	0.9	4.3	0.9	3.3	0.9	6.0	0.9
1.55- 1.70	8.0	1.2	6.5	0.9	7.9	1.2	5.3	1.1	5.1	1.0	4.6	1.0	5.5	0.8	5.1	0.9	4.4	0.8	4.0	0.9
1.70- 1.85	9.9	1.2	6.0	0.8	4.3	1.1	6.6	1.1	5.1	1.0	3.7	1.0	4.1	0.8	3.4	0.8	1.9	0.8	3.4	0.9
1.85- 2.00	9.6	1.2	5.1	0.8	6.4	1.1	2.9	1.1	4.0	1.0	4.9	0.9	5.4	0.8	3.2	0.8	4.2	0.8	3.4	0.8
2.00- 2.20	7.9	1.0	4.9	0.7	4.0	0.9	5.6	0.9	6.0	0.8	4.4	0.8	4.6	0.7	3.8	0.7	1.9	0.7	1.8	0.7
2.20- 2.40	7.2	1.0	4.3	0.7	5.6	0.9	4.8	0.9	5.1	0.8	5.1	0.8	2.5	0.6	1.9	0.7	1.5	0.7	2.7	0.7
2.40- 2.60	7.1	1.0	3.5	0.7	6.0	0.9	5.5	0.9	3.9	0.8	3.9	0.8	1.9	0.7	1.4	0.7	2.8	0.7	5.5	0.7
2.60- 2.80	8.2	1.0	5.3	0.7	5.2	0.9	5.7	0.9	4.2	0.8	2.0	0.8	1.8	0.6	3.6	0.7	3.9	0.7	3.1	0.7
2.80- 3.00	7.4	1.0	5.5	0.7	4.1	0.9	4.1	0.8	3.3	0.8	2.5	0.7	2.2	0.6	2.9	0.7	2.1	0.7	2.4	0.7
3.00- 3.20	7.5	1.0	5.2	0.7	4.1	0.9	2.5	0.8	3.2	0.8	4.1	0.7	5.0	0.6	3.1	0.6	3.0	0.7	2.4	0.7
3.20- 3.40	6.2	0.9	5.4	0.7	3.6	0.8	3.5	0.8	3.6	0.8	5.7	0.7	4.1	0.6	2.4	0.6	2.1	0.6	1.5	0.7
3.40- 3.60	6.9	0.9	3.7	0.6	4.9	0.8	3.9	0.8	4.8	0.8	4.2	0.7	2.2	0.6	2.1	0.6	1.2	0.6	1.7	0.7
3.60- 3.80	6.4	0.9	2.9	0.6	2.5	0.8	6.5	0.8	4.0	0.7	2.1	0.7	0.9	0.6	0.8	0.6	0.9	0.6	0.9	0.7
3.80- 4.00	5.6	0.9	4.1	0.6	4.8	0.8	5.5	0.8	3.2	0.7	2.5	0.7	1.8	0.6	1.3	0.6	1.2	0.6	2.3	0.7
4.00- 4.25	5.0	0.8	5.3	0.6	4.6	0.7	4.0	0.7	2.6	0.6	1.1	0.6	1.0	0.5	2.2	0.5	1.5	0.5	2.7	0.6
4.25- 4.50	6.9	0.8	5.3	0.6	5.1	0.7	3.0	0.7	1.6	0.6	1.6	0.6	1.8	0.5	2.3	0.6	2.4	0.6	4.5	0.6
4.50- 4.75	6.4	0.8	3.8	0.5	3.3	0.7	2.9	0.7	1.1	0.6	1.9	0.6	2.7	0.5	2.4	0.6	4.5	0.6	3.4	0.6
4.75- 5.00	5.4	0.8	3.0	0.5	2.2	0.7	2.2	0.7	2.1	0.6	2.6	0.6	1.8	0.5	3.4	0.6	2.4	0.6	1.3	0.6
5.00- 5.25	5.2	0.8	2.1	0.5	2.9	0.7	1.8	0.7	2.6	0.6	3.1	0.6	2.5	0.5	2.3	0.6	1.5	0.5	0.7	0.6
5.25- 5.50	4.6	0.8	2.1	0.5	1.5	0.7	2.6	0.7	3.5	0.6	3.7	0.6	2.4	0.5	1.2	0.5	1.3	0.5	1.7	0.6
5.50- 5.75	4.2	0.8	2.2	0.5	0.9	0.7	2.2	0.7	3.6	0.6	3.6	0.6	1.4	0.5	0.1	0.5	1.7	0.5	2.6	0.6
5.75- 6.00	4.3	0.8	2.1	0.5	2.2	0.7	4.5	0.7	3.1	0.6	1.9	0.6	0.6	0.5	1.0	0.5	2.4	0.5	3.2	0.6
6.00- 6.25	5.8	0.8	2.9	0.5	2.2	0.7	4.9	0.6	1.7	0.6	0.5	0.5	0.7	0.5	1.1	0.5	4.0	0.5	4.5	0.6
6.25- 6.50	7.9	0.8	4.4	0.5	4.0	0.7	3.4	0.6	1.4	0.6	0.8	0.5	1.2	0.5	2.7	0.5	4.3	0.5	4.6	0.6

LAB.ANGLE [Deg]	30.0		40.0		50.1		63.6		80.3		89.8		99.3		115.0		130.0		143.0	
E-RANGE [MeV]																				
6.50- 6.75	7.9	0.8	5.5	0.6	4.0	0.7	1.6	0.6	1.6	0.5	1.7	0.5	2.8	0.5	4.1	0.5	3.9	0.5	2.8	0.6
6.75- 7.00	9.1	0.8	5.8	0.6	3.1	0.7	1.5	0.6	2.4	0.6	2.1	0.5	2.8	0.5	4.3	0.5	3.0	0.5	2.4	0.6
7.00- 7.25	7.6	0.8	3.7	0.5	1.9	0.7	2.6	0.6	2.2	0.6	3.1	0.6	4.4	0.5	2.8	0.5	0.9	0.5	1.6	0.5
7.25- 7.50	4.6	0.8	3.0	0.5	1.6	0.7	2.0	0.6	3.1	0.6	4.5	0.6	3.1	0.5	1.2	0.5	0.1	0.5	1.9	0.5
7.50- 7.75	4.9	0.7	2.4	0.5	1.6	0.7	3.8	0.6	4.0	0.6	4.9	0.5	2.4	0.4	1.0	0.5	0.5	0.5	0.7	0.5
7.75- 8.00	5.9	0.7	3.6	0.5	2.5	0.6	3.8	0.6	3.4	0.5	3.4	0.5	2.5	0.4	0.4	0.5	0.9	0.4	0.9	0.5
8.00- 8.30	7.0	0.7	5.6	0.5	4.5	0.6	4.7	0.5	3.8	0.5	1.4	0.5	1.2	0.4	0.7	0.4	1.1	0.4	1.5	0.5
8.30- 8.60	9.2	0.7	7.4	0.5	6.2	0.7	5.6	0.6	2.3	0.5	1.7	0.5	0.7	0.4	0.5	0.4	1.3	0.4	2.1	0.5
8.60- 8.90	9.9	0.7	7.6	0.5	6.8	0.7	4.1	0.6	2.0	0.5	0.7	0.4	0.7	0.4	0.9	0.4	1.3	0.4	1.4	0.5
8.90- 9.20	10.7	0.7	7.4	0.5	6.1	0.6	2.6	0.5	1.6	0.5	0.7	0.4	0.4	0.4	1.7	0.4	1.3	0.4	1.5	0.4
9.20- 9.50	9.7	0.7	6.1	0.5	4.2	0.6	1.6	0.5	1.1	0.4	1.0	0.4	1.8	0.4	2.1	0.4	2.7	0.4	2.3	0.4
9.50- 9.80	8.3	0.7	4.1	0.5	3.7	0.6	1.7	0.5	0.9	0.5	1.3	0.4	2.4	0.4	4.4	0.4	3.9	0.4	3.4	0.4
9.80-10.10	6.5	0.7	3.4	0.5	3.1	0.6	1.1	0.5	0.8	0.4	1.8	0.4	3.7	0.4	6.2	0.5	3.9	0.4	4.4	0.5
10.10-10.40	5.6	0.7	3.0	0.4	2.3	0.6	1.2	0.5	2.3	0.4	3.5	0.4	6.1	0.4	7.9	0.5	5.8	0.4	4.4	0.5
10.40-10.70	6.7	0.7	3.3	0.4	1.9	0.5	1.3	0.5	3.0	0.4	5.6	0.5	7.9	0.5	8.6	0.5	5.1	0.4	3.6	0.4
10.70-11.00	7.7	0.7	3.2	0.4	2.5	0.5	2.1	0.5	5.3	0.5	7.9	0.5	9.1	0.5	9.4	0.5	4.3	0.4	2.3	0.4
11.00-11.30	10.3	0.7	4.6	0.4	3.4	0.5	3.4	0.5	7.0	0.5	8.2	0.5	11.4	0.5	9.3	0.5	3.5	0.4	1.1	0.4
11.30-11.60	18.6	0.8	9.0	0.5	5.4	0.6	4.8	0.5	8.9	0.5	10.8	0.6	12.4	0.6	7.7	0.4	1.9	0.4	0.7	0.4
11.60-11.90	31.5	1.0	14.7	0.6	8.4	0.6	6.1	0.5	9.6	0.6	11.1	0.6	12.2	0.5	5.2	0.4	0.7	0.3	0.5	0.3
11.90-12.20	47.2	1.3	21.6	0.7	12.1	0.7	6.8	0.5	10.4	0.6	12.8	0.6	9.1	0.5	2.7	0.4	0.4	0.3		
12.20-12.50	65.5	1.5	30.5	0.8	15.0	0.8	7.9	0.6	10.3	0.6	10.7	0.6	6.0	0.4	0.8	0.3	0.1	0.3		
12.50-12.80	74.2	1.8	36.2	0.9	15.4	0.8	8.9	0.6	9.6	0.6	7.7	0.5	4.2	0.4	0.6	0.3				
12.80-13.10	85.0	2.0	39.9	1.0	18.6	0.9	10.1	0.7	7.7	0.6	5.2	0.5	2.9	0.4	0.3	0.3				
13.10-13.40	94.6	2.2	45.2	1.2	22.7	1.0	8.5	0.7	5.3	0.6	3.0	0.4	1.0	0.4						
13.40-13.70	106.4	2.5	50.2	1.2	23.4	1.0	6.2	0.6	3.4	0.5	1.6	0.4	0.5	0.4						
13.70-14.00	108.6	2.6	50.4	1.2	22.0	1.0	4.8	0.6	1.8	0.5	1.3	0.4	0.6	0.4						
14.00-14.50	91.2	2.1	41.4	0.9	15.7	0.8	3.3	0.4	0.8	0.4	0.6	0.4								
14.50-15.00	57.1	1.7	25.4	0.7	9.1	0.7	2.0	0.4	0.4	0.4										
15.00-15.50	29.9	1.2	12.2	0.5	5.8	0.6	1.3	0.4												
15.50-16.00	14.5	0.8	5.3	0.4	3.6	0.5	0.5	0.3												
16.00-16.50	4.7	0.5	1.7	0.3	0.6	0.4														
16.50-17.00	1.8	0.3	0.9	0.2																
17.00-17.50	1.4	0.3																		

TABLE V

DOUBLE DIFFERENTIAL NEUTRON EMISSION CROSS SECTIONS FOR 14.1 MEV NEUTRONS ON CARBON [DATA AND ERROR IN mb/(sr*MeV)]

LAB.ANGLE [Deg]	30.0		40.0		50.1		63.6		80.3		89.8		99.3		115.0		130.0		143.0	
E-RANGE [MeV]																				
0.35- 0.50	56.7	4.0	27.1	2.7	32.0	4.4	23.4	3.3	16.7	3.0	19.6	2.5	19.6	2.5	14.6	2.5	9.1	2.5	10.0	2.7
0.50- 0.65	46.0	2.5	28.2	1.7	25.6	2.9	22.0	2.2	16.9	1.9	15.2	1.6	15.9	1.6	14.7	1.6	10.5	1.6	9.8	1.8
0.65- 0.80	38.6	2.1	22.1	1.4	22.4	2.4	13.3	1.8	12.1	1.6	10.6	1.3	12.2	1.3	8.6	1.3	5.0	1.3	8.1	1.5
0.80- 0.95	30.5	2.4	17.9	1.5	15.4	2.1	13.4	1.6	7.9	1.4	7.2	1.2	10.1	1.3	7.8	1.2	3.3	1.2	4.3	1.3
0.95- 1.10	22.5	2.3	14.6	1.4	10.1	1.9	10.9	1.5	7.2	1.3	6.7	1.1	7.0	1.2	4.5	1.1	3.7	1.1	5.7	1.2
1.10- 1.25	17.8	2.2	12.5	1.3	8.7	1.8	9.2	1.4	6.0	1.2	6.0	1.0	5.9	1.1	5.0	1.0	4.1	1.0	6.6	1.1
1.25- 1.40	17.0	2.0	9.6	1.2	7.7	1.8	7.8	1.3	5.1	1.1	5.3	1.0	5.9	0.9	6.8	1.0	4.0	1.0	4.9	1.0
1.40- 1.55	15.3	1.8	9.0	1.2	8.1	1.7	6.1	1.3	3.7	1.1	3.2	0.9	5.4	0.9	4.9	0.9	4.0	0.9	4.9	1.0
1.55- 1.70	10.8	1.3	7.7	1.1	8.6	1.7	5.2	1.2	6.7	1.1	4.3	0.9	5.3	0.9	6.3	0.9	4.0	0.9	4.8	0.9
1.70- 1.85	10.8	1.3	7.6	1.1	6.0	1.6	4.6	1.2	4.3	1.0	4.8	0.9	4.4	0.8	4.6	0.9	1.5	0.9	2.1	0.9
1.85- 2.00	9.2	1.2	5.7	1.0	5.4	1.5	4.8	1.2	5.0	1.0	5.3	0.9	5.2	0.8	2.9	0.8	3.8	0.8	2.9	0.9
2.00- 2.20	8.2	1.6	4.4	0.9	6.3	1.3	5.4	1.0	4.8	0.9	5.6	0.8	4.0	0.7	3.2	0.7	1.4	0.7	2.9	0.8
2.20- 2.40	7.6	1.6	4.4	0.9	4.7	1.3	4.1	1.0	4.2	0.9	2.6	0.7	3.7	0.7	3.4	0.7	3.2	0.7	5.1	0.8
2.40- 2.60	7.1	1.6	4.3	0.8	5.5	1.3	4.9	1.0	2.5	0.8	3.4	0.7	3.3	0.7	7.0	0.7	4.5	0.7	3.9	0.7
2.60- 2.80	9.7	1.6	4.6	0.7	5.7	1.3	3.7	0.9	4.4	0.8	1.9	0.7	7.4	0.7	6.7	0.7	2.5	0.7	1.9	0.7
2.80- 3.00	6.6	1.5	3.6	0.7	3.6	1.3	2.4	0.9	5.6	0.8	9.0	0.7	7.6	0.7	2.6	0.7	1.5	0.7	1.3	0.7
3.00- 3.20	5.8	1.3	3.5	0.7	1.7	1.2	5.0	0.9	11.4	0.9	10.9	0.7	5.6	0.7	2.6	0.7	1.3	0.7	1.3	0.7
3.20- 3.40	7.1	1.3	3.3	0.7	5.9	1.2	9.4	0.9	10.2	0.8	6.7	0.7	2.7	0.6	0.6	0.6	1.5	0.7	0.3	0.8
3.40- 3.60	7.5	1.4	5.4	0.8	11.8	1.2	11.5	1.0	4.8	0.8	3.4	0.7	1.2	0.7	1.8	0.6	0.6	0.6	0.0	0.8
3.60- 3.80	13.0	1.4	11.4	0.9	12.6	1.2	9.5	0.9	2.5	0.7	0.8	0.6	0.1	0.7	1.7	0.6	0.0	0.7	0.7	0.7
3.80- 4.00	18.1	1.2	13.8	0.8	11.3	1.2	6.0	0.8	1.4	0.7	0.5	0.6	0.3	0.6	0.8	0.6	0.6	0.7	0.4	0.6
4.00- 4.25	12.2	0.9	7.9	0.6	4.7	1.0	2.4	0.7	0.6	0.8	0.4	0.5	0.5	0.5	1.6	0.5	1.0	0.6	0.6	0.6
4.25- 4.50	5.8	0.9	4.1	0.6	3.3	0.9	1.7	0.7	0.1	0.8	0.1	0.5	1.2	0.5	0.7	0.6	0.1	0.6	0.5	0.6
4.50- 4.75	4.1	0.8	1.4	0.5	1.1	1.1	1.1	0.7	0.4	0.6	0.5	0.7	0.3	0.5	0.4	0.5	0.3	0.5	0.9	0.6
4.75- 5.00	2.0	0.8	1.3	0.5	0.2	1.0	0.1	0.8	0.6	0.6	0.0	0.7	0.2	0.5	0.2	0.5	0.5	0.5	0.0	0.6
5.00- 5.25	1.4	0.8	1.1	0.5	1.2	0.9	0.7	0.8	1.1	0.6	0.0	0.6	0.5	0.5	0.3	0.5	1.1	0.5	0.8	0.6
5.25- 5.50	1.3	0.8	0.9	0.5	2.2	0.9	1.6	0.7	0.4	0.6	0.0	0.6	0.0	0.5	0.7	0.5	0.3	0.5	0.5	0.6
5.50- 5.75	2.9	0.7	1.0	0.5	0.7	0.9	0.1	0.7	0.1	0.6	0.2	0.5	0.0	0.5	0.4	0.5	0.8	0.5	0.2	0.6
5.75- 6.00	3.1	0.7	1.9	0.5	0.5	0.9	0.3	0.6	0.1	0.6	0.5	0.5	0.0	0.5	1.1	0.5	1.1	0.5	2.1	0.6
6.00- 6.25	3.4	0.7	1.1	0.5	0.5	0.9	1.1	0.6	0.1	0.6	0.8	0.5	0.2	0.5	0.7	0.5	3.2	0.6	7.5	0.7
6.25- 6.50	2.6	0.7	0.5	0.5	0.3	0.8	1.0	0.6	0.0	0.6	0.8	0.5	0.2	0.5	2.5	0.5	6.9	0.6	13.8	1.0

LAB.ANGLE [Deg]	30.0		40.0		50.1		63.6		80.3		89.8		99.3		115.0		130.0		143.0	
E-RANGE [MeV]																				
6.50- 6.75	2.7	0.7	0.7	0.5	0.3	0.8	0.0	0.7	0.7	0.5	0.5	0.5	1.4	0.5	5.2	0.6	11.3	0.8	15.9	1.4
6.75- 7.00	2.0	0.7	1.3	0.5	0.9	0.8	0.0	0.7	1.8	0.6	0.5	0.5	2.3	0.5	7.9	0.7	11.3	1.0	9.9	1.0
7.00- 7.25	2.5	0.7	0.5	0.5	0.9	0.8	0.2	0.6	0.5	0.6	1.7	0.5	4.6	0.6	9.0	0.9	6.7	0.8	4.3	0.6
7.25- 7.50	1.9	0.7	0.5	0.5	0.4	0.8	0.3	0.6	1.6	0.6	3.5	0.6	6.4	0.7	5.4	0.7	2.4	0.6	0.6	0.6
7.50- 7.75	3.7	0.7	1.8	0.5	1.1	0.8	1.3	0.6	4.7	0.6	6.7	0.7	6.3	0.8	2.9	0.5	0.8	0.5	0.2	0.5
7.75- 8.00	6.3	0.7	2.6	0.5	2.4	0.8	2.9	0.6	6.4	0.8	7.0	0.9	4.3	0.6	0.5	0.5	0.5	0.4	0.2	0.5
8.00- 8.30	10.6	0.7	8.1	0.6	6.3	0.9	7.0	0.7	7.0	0.9	4.3	0.7	2.2	0.5	0.4	0.5	1.1	0.4	0.2	0.4
8.30- 8.60	17.2	0.9	13.0	1.0	13.4	1.4	10.7	0.9	5.1	0.7	2.2	0.5	0.9	0.4	0.4	0.4	0.0	0.5	0.2	0.5
8.60- 8.90	22.4	1.4	18.2	1.4	17.7	2.0	11.1	0.9	2.8	0.5	1.1	0.4	0.6	0.4	0.4	0.4	0.6	0.4	0.7	0.5
8.90- 9.20	25.7	1.9	20.9	1.8	18.6	1.9	5.9	0.7	0.8	0.4	0.1	0.4	0.3	0.4	0.6	0.4	0.7	0.4	0.9	0.4
9.20- 9.50	24.8	2.4	18.2	1.6	13.2	1.4	3.6	0.5	0.7	0.4	0.2	0.4	0.3	0.4	1.5	0.4	2.3	0.4	2.1	0.4
9.50- 9.80	19.8	2.0	14.4	1.2	8.5	0.9	1.4	0.5	0.3	0.5	0.3	0.4	1.1	0.4	3.5	0.4	3.8	0.4	4.9	0.5
9.80-10.10	11.6	1.5	6.7	0.8	6.1	0.8	1.2	0.5	0.3	0.5	0.9	0.4	2.8	0.4	6.4	0.5	5.4	0.5	5.0	0.5
10.10-10.40	7.1	0.9	3.7	0.4	2.8	0.7	0.5	0.5	0.7	0.4	2.6	0.4	5.2	0.4	8.6	0.5	7.0	0.5	5.8	0.5
10.40-10.70	5.0	0.6	2.9	0.4	2.7	0.7	0.8	0.4	1.1	0.4	4.1	0.4	8.1	0.5	9.5	0.5	7.7	0.5	7.3	0.5
10.70-11.00	5.2	0.6	1.8	0.4	1.6	0.6	0.0	0.4	3.6	0.4	7.0	0.4	9.3	0.5	11.6	0.6	8.6	0.5	6.0	0.4
11.00-11.30	7.8	0.6	3.4	0.4	2.8	0.6	1.5	0.4	6.2	0.5	8.7	0.5	11.4	0.5	13.3	0.6	7.0	0.4	3.7	0.4
11.30-11.60	15.7	0.8	6.2	0.4	3.5	0.7	1.8	0.4	7.2	0.5	11.1	0.5	14.3	0.6	11.6	0.5	4.5	0.4	1.5	0.4
11.60-11.90	28.2	1.0	11.2	0.5	5.9	0.7	3.2	0.5	7.5	0.5	13.2	0.6	14.2	0.6	8.5	0.5	3.0	0.4	0.7	0.4
11.90-12.20	43.1	1.3	18.4	0.7	10.2	0.9	4.1	0.5	9.1	0.5	14.3	0.6	12.6	0.6	5.8	0.4	0.8	0.4	0.1	0.3
12.20-12.50	57.7	1.6	26.6	0.9	12.8	1.0	4.7	0.5	10.1	0.6	12.2	0.6	9.4	0.5	3.2	0.4	0.3	0.3		
12.50-12.80	71.2	1.9	31.3	1.0	14.4	1.1	5.4	0.5	9.4	0.6	9.5	0.5	6.6	0.4	1.7	0.4				
12.80-13.10	79.3	2.1	36.8	1.2	15.8	1.2	6.8	0.6	7.8	0.6	6.6	0.5	4.4	0.4	0.7	0.4				
13.10-13.40	87.7	2.4	40.9	1.3	20.6	1.3	8.1	0.6	4.3	0.5	4.1	0.4	1.8	0.4	0.7	0.4				
13.40-13.70	97.7	2.7	47.1	1.5	20.6	1.3	5.9	0.6	3.3	0.5	2.3	0.4	0.8	0.4						
13.70-14.00	99.4	2.9	47.9	1.4	21.9	1.4	4.8	0.6	2.2	0.5	0.7	0.4								
14.00-14.50	84.1	2.5	41.2	1.1	17.9	1.1	3.8	0.5	0.6	0.4										
14.50-15.00	55.7	2.0	26.6	0.9	10.4	1.0	2.5	0.4												
15.00-15.50	29.3	1.5	13.7	0.6	6.9	0.9	0.7	0.4												
15.50-16.00	13.8	1.0	6.3	0.4	4.2	0.7														
16.00-16.50	5.4	0.6	1.9	0.3	1.3	0.6														
16.50-17.00	2.4	0.3	0.9	0.2																
17.00-17.50	1.3	0.3																		

TABLE VI

SAME AS TABLE V, HOWEVER POROUS SAMPLE

LAB.ANGLE [Deg]	30.0		40.0	
E-RANGE [MeV]				
0.35- 0.50	69.3	15.7	28.6	13.1
0.50- 0.65	42.4	9.9	25.5	8.4
0.65- 0.80	33.7	8.1	23.9	6.8
0.80- 0.95	21.6	7.0	15.0	6.0
0.95- 1.10	17.4	6.5	6.3	5.3
1.10- 1.25	8.8	5.9	18.2	5.0
1.25- 1.40	16.0	5.6	9.0	4.7
1.40- 1.55	13.7	5.3	10.0	4.6
1.55- 1.70	10.4	5.1	1.1	4.3
1.70- 1.85	7.4	5.0	6.1	4.2
1.85- 2.00	21.6	4.8	0.8	4.4
2.00- 2.20	8.5	4.2	0.6	3.3
2.20- 2.40	4.0	4.2	0.5	4.8
2.40- 2.60	4.2	4.1	0.1	4.2
2.60- 2.80	9.5	4.4	0.1	4.2
2.80- 3.00	1.4	4.3	0.2	3.7
3.00- 3.20	6.1	3.9	2.6	3.6
3.20- 3.40	0.8	3.9	2.9	3.2
3.40- 3.60	12.9	3.8	1.2	3.2
3.60- 3.80	15.0	3.7	9.9	3.2
3.80- 4.00	17.3	3.8	15.7	3.3
4.00- 4.25	13.2	3.2	6.1	2.8
4.25- 4.50	4.0	3.1	4.2	2.7
4.50- 4.75	5.5	3.3	2.9	2.7
4.75- 5.00	0.4	3.3	2.5	2.6
5.00- 5.25	1.5	3.6	2.8	2.7
5.25- 5.50	0.3	3.6	5.9	2.7
5.50- 5.75	0.3	3.6	2.5	2.6
5.75- 6.00	1.1	3.6	4.0	2.7
6.00- 6.25	2.2	2.8	0.2	2.6
6.25- 6.50	0.8	2.7	3.1	2.5
6.50- 6.75	4.6	2.7	0.8	2.4
6.75- 7.00	1.1	2.8	2.6	2.4
7.00- 7.25	5.3	2.7	1.9	2.4
7.25- 7.50	1.0	2.7	1.8	2.4
7.50- 7.75	6.7	2.6	0.2	2.8
7.75- 8.00	7.2	2.6	0.4	2.8
8.00- 8.30	9.7	2.5	10.0	2.2
8.30- 8.60	18.0	2.5	14.7	2.3
8.60- 8.90	21.7	2.6	20.4	2.5
8.90- 9.20	26.7	2.6	20.6	2.3
9.20- 9.50	26.3	2.6	19.7	2.3
9.50- 9.80	16.6	2.5	12.1	2.1
9.80-10.10	8.3	2.3	3.5	1.9
10.10-10.40	5.3	2.1	2.0	1.8
10.40-10.70	6.0	2.1	6.3	1.9
10.70-11.00	5.5	2.1	0.2	1.9
11.00-11.30	13.6	2.3	5.5	1.8
11.30-11.60	20.1	2.4	6.2	1.9
11.60-11.90	30.7	2.5	10.8	2.0
11.90-12.20	47.0	3.0	20.6	2.3
12.20-12.50	61.6	3.3	25.7	2.5
12.50-12.80	72.7	3.5	30.9	2.7
12.80-13.10	79.9	3.7	34.6	2.9
13.10-13.40	90.7	4.0	38.0	3.1
13.40-13.70	101.2	4.2	44.3	3.3
13.70-14.00	94.9	4.3	50.3	3.5
14.00-14.50	80.2	3.3	37.7	2.6
14.50-15.00	45.1	2.7	23.6	2.3
15.00-15.50	21.3	2.1	13.6	1.9
15.50-16.00	8.6	1.8	3.6	1.5
16.00-16.50	2.3	1.3	2.1	1.3

TABLE VII

ABSOLUTE DIFFERENTIAL LABORATORY CROSS SECTIONS OF THE HIGHEST ENERGY PEAK

REACTION	n-^{6}Li[a]		n-^{7}Li		n-^{10}B		n-^{11}B		n-C	
ANGLE [deg]	SIGMA [mb/sr]	ERROR [%]	SIGMA [mb/sr]	ERROR [%]	SIGMA [mb/sr]	ERROR [%]	SIGMA [mb/sr]	ERROR [%]	SIGMA [mb/sr]	ERROR [%]
30.0	370.2	1.8	436.8	0.8	339.4	1.4	296.4	1.4	273.9	1.0
									264.1[b]	1.6
40.0	183.2	3.3	228.0	0.8	157.2	1.2	135.2	1.3	127.0	1.0
									120.5[b]	2.8
50.1	93.4	4.4	109.0	1.8	63.9	1.0	62.3	2.8	61.1	2.3
63.6	18.3	21.2	32.5	3.8	24.2	1.3	25.4	4.9	17.6	3.3
80.3	8.6	10.6	22.3	4.7	25.3	1.0	26.2	2.7	22.3	2.8
89.8	11.8	6.5	22.6	2.8	28.4	1.5	28.6	4.0	29.4	1.9
99.3	9.3	8.1	21.9	3.7	26.2	1.0	27.5	2.4	31.0	1.8
115.0	7.9	7.9	17.8	5.2	20.4	1.1	20.6	4.6	26.5	2.1
130.0	5.0	12.6	7.9	9.8	12.0	2.8	11.5	7.4	15.5	3.0
143.0	2.3	27.0	7.2	11.6	9.8	2.2	9.0	6.5	11.7	4.2

a) inelastic cross sections of the first excited state at 2.186 MeV subtracted
b) data for porous graphite sample

C. Integrated Cross sections

Table VIII lists the energy integrated angular distributions of the neutron emission cross sections. These data contain extrapolations to zero neutron energy. To account for events below the neutron detection bias, the following simple procedure was set forth: it was assumed that the spectrum below the cutoff of 0.35 MeV was in the average as intense as the spectrum between 0.35 MeV and 2.0 MeV. We assigned an error of 50% to this extrapolation.

The integration of the double differential cross section over both the energy of the emitted neutrons and the solid angle was done in two steps: first, the cross section of the highest energy peak was converted into the center-of-mass system, and then the remainder was integrated over the energy and the solid angle in the laboratory system. In both cases the integration was done by fitting the angular distributions by a series of Legendre polynomials P_i so that the integrated cross sections were obtained from the first coefficient A_0 by $\sigma = 4\pi A_0$.

TABLE VIII

ABSOLUTE DIFFERENTIAL NEUTRON EMISSION CROSS SECTIONS

REACTION ANGLE [deg]	n-^{6}Li SIGMA [mb/sr]	ERROR [%]	n-^{7}Li SIGMA [mb/sr]	ERROR [%]	n-^{10}B SIGMA [mb/sr]	ERROR [%]	n-^{11}B SIGMA [mb/sr]	ERROR [%]	n-C SIGMA [mb/sr]	ERROR [%]
measured data:										
30.0	497.7	1.0	547.8	1.0	435.5	1.5	393.2	1.2	399.1	1.6
									381.2[a]	2.2
40.0	290.4	1.2	315.0	1.1	219.6	1.6	193.5	1.5	206.8	1.8
									196.5[a]	3.2
50.1	175.0	2.0	175.0	2.0	108.3	2.3	114.5	2.3	133.3	2.7
63.6	84.0	3.2	83.2	3.4	65.6	3.2	72.9	3.1	67.9	3.4
80.3	64.0	4.2	61.2	4.2	58.9	3.0	64.2	2.9	58.8	3.4
89.8	51.3	3.7	56.5	3.2	59.1	3.1	64.2	3.0	62.3	3.0
99.3	41.1	4.9	52.3	3.9	52.6	3.1	55.4	2.8	63.8	3.0
115.0	35.3	5.5	47.9	4.3	45.1	3.1	43.4	3.2	57.0	3.1
130.0	30.4	6.1	30.8	5.8	33.6	3.8	32.7	3.8	40.7	3.4
143.0	28.8	6.9	31.2	6.3	34.4	4.4	35.6	4.2	41.2	3.8
calculated data:										
0.0	1072.		1084.		1179.		1082.		1058.	
integrated	1604 mb		1706 mb		1487 mb		1428 mb		1497 mb	

[a] data for porous graphite sample

Removing the elastic portion of the spectrum reduces the forward peaking of the remainder so that fewer coefficients are needed. Further, fitting the elastic portion of the spectra in the center-of-mass allowed a more reliable fit with the 10 data points per angular distribution available. However, as detailed in Sec. VI, the Legendre fits of the present work include also data points of previous work that are in agreement with the present data. Table IX lists the resulting coefficients.

For convenience also Legendre coefficients for describing the angular distribution of the total neutron emission in the laboratory system are given in the same table. These were constructed using the results of fitting the elastic and the nonelastic portions of the spectra under the following constraints:

A_0 was fixed to the sum of the first coefficient of the elastic and of the nonelastic distribution, and

the zero-degree and the 180-degree cross section were taken to be the sum of the corresponding (extrapolated) values of the partial fits.

TABLE IX

LEGENDRE COEFFICIENTS FOR THE PRESENTATION OF THE ANGULAR DISTRIBUTIONS

Isotope:	^{6}Li	^{7}Li	^{10}B	^{11}B	Carbon	
Elastic (C.M.):						4.4 MeV[a]
A_0	72.5	89.8	75.7	68.0	67.7	16.6
A_1	160.3	180.8	147.7	129.3	117.6	10.7
A_2	177.4	195.0	175.5	149.3	148.1	16.7
A_3	139.7	158.8	171.7	152.5	147.7	1.5
A_4	75.4	83.2	121.0	111.1	106.4	-2.0
A_5	30.6	24.5	60.8	57.2	46.9	-2.2
A_6	16.4	9.4	30.9	31.9	36.4	-1.8
A_7	7.1	1.1	14.6	14.6	18.2	
A_8	-1.3	-3.3	6.9	5.1	8.4	
A_9	-8.3	-3.5	3.8	2.5	-2.8	
A_{10}	-6.0	-8.6			-8.5	
A_{11}		-4.4			-3.3	
Nonelastic (lab):						
A_0	55.1	46.0	42.6	45.7	34.8	
A_1	54.3	41.7	35.8	40.5	35.7	
A_2	32.6	29.2	38.9	37.9	30.2	
A_3	9.3	16.8	23.9	24.2	27.0	
A_4	6.9	6.4	30.4	30.1	27.8	
A_5	4.9	-1.2	14.4	23.5	18.1	
A_6		-3.7	11.1	11.6	17.3	
A_7				7.0	14.1	
A_8					1.2	
Total Emission (lab):						
A_0	127.7	135.8	118.3	113.7	119.2	
A_1	223.1	236.0	191.2	179.6	169.5	
A_2	243.6	251.4	230.2	198.0	205.8	
A_3	195.6	220.5	219.5	197.1	191.3	
A_4	142.9	149.2	190.9	170.1	160.2	
A_5	77.7	69.2	111.0	113.0	84.0	
A_6	38.0	28.7	66.4	65.2	63.6	
A_7	17.3	8.7	30.3	36.8	44.2	
A_8	10.4	-9.7	12.8	13.2	17.9	
A_9	7.2	-5.7	8.4	-4.2	9.8	
A_{10}	-12.0				-7.0	

a) coefficients in C.M. for scattering from the 4.4 MeV level of ^{12}C

V. UNCERTAINTIES

A. *Energy and Angle*

The mean incoming neutron energy is uncertain by 0.03 MeV, the zero degree direction by 0.4°. The individual uncertainty of each angle is 0.3°.

B. *Individual Cross Section Errors*

The final error given with each data point of the secondary neutron spectra consists of the counting statistics of the individual spectra plus contributions of various corrections:

- subtraction of white (time-uncorrelated) time-of-flight background
- subtraction of the spectrum of the admixed isotope (if applicable)
- multiple scattering correction

For each point these contributions are uncorrelated and therefore were added quadratically. The fraction of the correction which was used for this purpose, can be seen from Table X. However, the error contributions from the corrections are correlated within each spectrum (to a varying degree), so that combining uncertainties of individual energy bins quadratically will give a distorted combined error.

TABLE X

PERCENT EFFECT OF CORRECTIONS ON THE INTEGRATED VALUES OF THE ELASTIC, NONELASTIC AND TOTAL EMISSION CROSS SECTIONS

Isotope	^{6}Li	^{7}Li	^{10}B	^{11}B	Carbon
Monte Carlo Correction[a] (20%[b]):					
elastic	6.4	5.6	14.7	8.5	12.2
total emission	4.8	3.7	12.4	5.9	8.8
Bias Correction (50%[c]):					
nonelastic	4.1	6.8	10.1	11.1	12.6
total emission	3.3	2.5	5.7	5.8	5.9
Extrapolation of Energy Spectra (50%[d]):					
nonelastic	5.2	7.3	7.1	9.4	8.4
total emission	2.5	2.5	2.6	3.8	3.6
Extrapolation of Angular Range[e] typically 1 to 2%					

a) consisting of multiple scattering, flux attenuation and geometry corrections
b) this fraction of the correction has been added quadratically to the final random errors of the individual points
c) this fraction is expected to account for the uncertainty of the bias correction (see II.D.)
d) this fraction represents the uncertainty in the cutoff (0.35 MeV) correction of the neutron energy spectra and was added quadratically to the error of the energy-integrated data
e) effect on A_0 of the Legendre fit when the zero degree value and the 180 degree value are varied within a reasonable range and the number of coefficients used in the fit is changed by one

To avoid an even stronger masking of the truly random errors, the uncertainty in the neutron detection efficiency which is also strongly correlated is not included. At the secondary neutron energies at which the cross section standard was used (8.3 and 10.6 MeV for the 30° and 40° data, respectively) this uncertainty is even zero. For energies from 11 MeV down to about 0.65 MeV the uncertainty can best be expressed by 2%/10 MeV[7], below that energy it increases strongly due to the steepness of the efficiency curve and the increasing dependence on the stability of the bias. Above 11 MeV the uncertainty is about 1%/MeV. In the present case, the uncertainty in the efficiency is appreciably higher due to the correction for the actual bias (see Sec. II.D) It seems safe to assume that the error contribution is not more than one half of this correction. This would add to the error about 4% at 1 MeV, 8.5% at 0.65 MeV and

appreciably more than that at lower energies. The uncertainty in the dead-time correction is less than 0.1% and was not included.

TABLE XI

CONTRIBUTIONS TO THE SCALE ERROR

1. Systematic Scale Error (errors of the standard)	
mass (weight, purity)	<1.0%
cross section	<1.5%
peak evaluation[a]	0.7%
normalization[b]	<0.5%
geometry[c]	1.7%
Monte Carlo correction[d]	2.6%
2. Individual Contributions (errors of the samples)	
mass (weight, purity)	<1%
Monte Carlo correction[e]: from 0.7 to 3.0%	

a) consists of the combined statistical errors, the error in the dead-time correction and in the background subtraction
b) calibration of the experimental set-up using a detector with a given efficiency curve in a given geometry; it depends on the evaluation of the monitor counts and the beam charge collection
c) difference in the positioning of the sample with regard to the neutron source and the detector; within one angular distribution this uncertainty is uncorrelated, but not for the reference measurement
d) the Monte Carlo simulation corrects for flux attenuation, multiple scattering and finite sample size
e) uncertainties connected with the flux depression in the sample are clearly correlated within each angular distribution; in the present case this systematic error contribution was not extracted from the total uncertainty of this correction

C. *Scale Uncertainty*

Table XI compiles the contributions to the scale error. The common scale error is 3.4%. The closeness in shape and mass of the polyethylene and the carbon foam sample made an accurate background subtraction possible. The difference in flux depression and multiple scattering in the foreground and background runs was corrected for by a Monte Carlo calculation. Measuring at two angles (30° and 40°) reduced those error contributions that are shown with the superscripts a,b and c. The contributions listed under 2. in this table are sample dependent. Neglecting correlations the combined scale errors of the five measurements are between 3.6% and 4.6%.

D. *Uncertainties of Integrated Data*

The uncertainties given in the Tables VII and VIII were obtained by adding quadratically the individual errors disregarding any correlation. To provide more information on possible correlations Table X lists the effect of the corrections on the integrated data together with the percentage which was used for the quadratic addition to the random error of the individual points. More details are given in the footnotes of the table.

VI. DISCUSSION

Table XII compares the integrated cross sections with the values of ENDF/B-V. Analogous to our findings at lower energies[5] also at this energy the ENDF/B-V elastic cross section of ^{11}B is too low. From this table it is obvious that all of our total emission data are high by the order of 10%. These high values are carried over into the total reaction values which include non-neutron cross sections taken from ENDF/B-V.

TABLE XII

COMPARISON OF INTEGRATED CROSS SECTIONS (in barns)

Sample	Elastic		1st Ex.State		Tot. Emission		Tot. Reaction	
	exp[a]	eval[b]	exp[a]	eval[b]	exp[a]	eval[b]	exp[c]	eval[b]
^{6}Li	0.91	0.96			1.60	1.49	1.56	1.44
^{7}Li	1.09[d]	1.01			1.71	1.48	1.67	1.44
^{10}B	0.95[d]	0.95			1.49	1.24	1.70	1.45
^{11}B	0.85	0.60			1.43[e]	1.29	1.46	1.32
C	0.85	0.80	0.21	0.19	1.50	1.22	1.58	1.30

a) this work
b) ENDF/B-V
c) this work, uses ENDF/B-V values for non-neutron reactions
d) cross section of unresolved excited states subtracted
e) this value compares to 1.46 in the recent Japanese work[2]

A. Neutron Emission from ^{6}Li

Our elastic cross sections are higher than practically all other data except those of Hogue et al.[11] and the ENDF/B-V evaluated data. The data of Hogue et al.[11] agree well in scale and reasonably well in shape with ours.

Our double differential cross sections resemble those of Chiba et al.[3] closely, except for energies below about 1 MeV where our spectra show an excess of neutrons which is especially prominent at 30°. Besides our scale is higher by about 10%.

B. Neutron Emission from ^{7}Li

Our differential elastic cross sections are in good agreement, both in scale and shape, with the data of Hogue et al.[11] However they are higher than practically all other data. Especially disturbing is the fact that the value of the total cross section derived from our data is about 15% higher than all reasonable measured or evaluated data (see Table XII). Contrary to that the integrals of the Japanese double differential cross sections[3] are slightly smaller than the ENDF/B-V values. As in the case of ^{6}Li our double differential cross sections are not only higher in scale than the Japanese data[3] but also exhibit a low energy "tail" below 1 MeV. The integrals of the present neutron emission spectra are about 30% higher than those of Morgan et al.[1] which were measured with a low energy cutoff of 0.762 MeV.

C. Neutron Emission from ^{10}B

Our integrated elastic cross section is not only in very good agreement with the ENDF/B-V value but also with two other sets of experimental data[2,12]. Of the latter, the Swiss data[12] also agree very well in the shape of the angular distribution.

The neutron emission spectrum at 85° by Ono et al.[13] is in very good agreement with our data, whereas fractional emission data (between 0.75 and 7.0 MeV) by Mathur et al.[14] at 90° and 14.8 MeV are much too high.

D. Neutron Emission from ^{11}B

The elastic data of ENDF/B-V on ^{11}B are unreasonably low, and we are excluding them from this comparison. The shape of the differential elastic cross section agrees very well with some older Swiss data[15] (scale 4% higher) and quite well with Baba et al.[2] (6% higher).

There is very good agreement (disregarding a tail below 0.5 Mev in our data) with the 85° neutron emission spectrum of the Japanese work[13] and also with their integrated value[2] (see Tab. XII). The fractional data of Mathur et al.[14] (integrated from 0.75 to 7.0 MeV, at 90° and 14.8 MeV) of natural boron (contains 81% ^{11}B) agree just within error bars, the double differential cross sections of Prud'homme et al.[16] (90° and 15 MeV, natural boron) are much higher than ours.

E. Neutron Emission from Carbon

The integrated values for scattering both to the ground state and to the 4.4 MeV state as well as the total cross section derived from our data are higher than the ENDF/B-V values (see Table XII). It is interesting to note that our results from the lower mass sample are lower by about 5%. This indicates the possibility of an overcorrection for multiple scattering.

The integrated elastic data of Glasgow et al.[17] are slightly higher than ours, so are the data by Baba et al.[2] Their double differential cross sections at 45° and 120° agree well with ours. Those of Takahashi[18] at 107° are definitely higher. The spectrum of Prud'homme et al.[16] at 90° for 15 MeV neutrons is also somewhat higher than our corresponding spectrum at 14.1 MeV. Also the result of Mathur et al.[14] (90°, 14.8 MeV) which includes only neutrons between 0.75 and 7.0 MeV is much higher than our result.

One of the few elastic data that are lower than ours are those of Haouat et al.[19] (10% lower). However, these data are the only ones which are compatible with the shape of our angular distribution. In addition the excitation function of Morgan et al.[20] at 125° agrees very well with our value for that angle.

The situation is similar for the data of the first excited state in ^{12}C. Most integrated data are higher, Haouat et al.[19] is lower and there is agreement with Morgan et al.[20] at 125°.

Some of the discrepancies of the carbon data stem from the cross section structure near 14 MeV. But this does not completely explain why up to now there is not even one pair of independent differential elastic cross section measurements that agrees reasonably well.

VII. CONCLUSION

When comparing the present data with previous work one must keep in mind that in the present work all five samples have been measured relative to each other, i. e. part of their scale error is common to all measurements.

Whereas, the scale of the elastic scattering cross sections is supported by previous work, all the neutron emission cross sections appear to be high. The corresponding Japanese data are lower for the lithium isotopes[3], but for carbon[2] even somewhat higher than our data.

A special feature of practically all our neutron emission energy spectra is a low energy "tail". Such a tail is present in some, but not all, of the Japanese data[2,3], as well.

There are the following possible causes for such tails

a) physics (e.g. neutrons produced by charged particles that were produced by the neutron interaction)

b) insufficient correction by the Monte Carlo calculation
c) wrong pulse-height bias
d) presence of a small (positive) white time-of-flight background

In the present case no single cause for these tails and rather high integrated emission cross sections could be tracked down. Although the individual results agree about within error bars with acceptable values the presence of some systematic error is obvious because (according to Table XII) all our total cross sections are high.

REFERENCES

1. G. L. Morgan, "Cross Sections for the $^{7}Li(n,xn)$ and $^{7}Li(n,n'gamma)$ Reactions Between 1 and 20 Mev", Oak Ridge National Laboratory Report ORNL/TM-6247(1978).

2. M. Baba, M. Ono, N. Yabuta, T. Kikuti, and N Hirakawa, "Scattering of 14.1-MeV Neutrons from ^{10}B, ^{11}B, C, N, O, F and Si", p.223 Proc. Int. Conf. on Nuclear Data for Basic and Applied Science, Santa Fe, 1985, published in Radiation Effects, vol. 92-96 (1986) and personal communication by M. Baba.

3. S.Chiba, M. Baba, H. Nakashima, M. Ono, N. Yabuta, S. Yukinori, and N. Hirakawa, J. Nucl. Sci. Techn. 22, 771 (1985).

4. P. W. Lisowski, G. F. Auchampaugh, D. M. Drake, M. Drosg, G. Haouat, N. W. Hill, and L. Nilsson, "Cross Sections For Neutron-Induced, Neutron-Producing Reactions In ^{6}Li and ^{7}Li At 5.96 And 9.83 MeV", Los Alamos Scientific Laboratory Report LA-8342-MS (1980).

5. M. Drosg, P. W. Lisowski, D. M. Drake, R. A. Hardekopf, and M. Muellner, "Cross Sections For Neutron-Producing Reactions Induced by 6.0 and 10.0 MeV Neutrons in Boron", Los Alamos National Laboratory Report LA-10665-MS (1986).

6. D. M. Drake, G. F. Auchampaugh, E. D. Arthur, C. E. Ragan, and P. G. Young, Nucl. Sci. Eng., 63, 401 (1977).

7. M. Drosg, D. M. Drake, and P. Lisowski, Nuclear Inst. Meth. 176, 477 (1980).

8. M. Drosg, Nucl. Instr. Meth. 196, 449 (1982).

9. J. C. Hopkins, and G. Breit, Nucl. Data Tables, A9, 137 (1971).

10. Los Alamos Scientific Laboratory Group X-6, "MCNP -A General Monte Carlo Code for Neutron and Photon Transport", Los Alamos Scientific Laboratory Report LA-7396-M Rev. (Nov. 1979).

11. H. H. Hogue, P. L. von Behren, D. W. Glasgow, S. G. Glendinning, P. W. Lisowski, C. E. Nelson, F. O. Purser, W. Tornow, C. R. Gould, and L. W. Seagondollar, Nucl. Sci. Eng. 69, 22 (1979).

12. B. Vaucher, J. C. Alder, and C. Joseph, Helv. Phys. Acta 43, 237 (1970).

13. M. Ono, M. Baba, N. Yabuta, T. Kikuchi, and N. Hirakawa, "Double-Differential Neutron Emission Cross sections of ^{10}B, ^{11}B, N, O, F and Si at 14.2 MeV", p. 6 of Report NETU-46, Nucl. Eng., Tohoku Univ. (1985).

14. S. C. Mathur, P. S. Buchanan, and L. L. Morgan, Phys. Rev. 186,

1038 (1969).

15. J. C. Alder and B. Vaucher, Nucl. Phys. A147, 657 (1970).

16. J. T. Prud homme, I. L. Morgan, J. H. McCrary, J. B. Ashe, and O. M. Hudson, Jr., "A Study of Neutrons and Gamma Rays from Neutron Induced Reactions in Several Elements", Report AFSWC-TR-60-30, Air Force Special Weapons Center, Kirtland Air Force Base 1960.

17. D. W. Glasgow, F. O. Purser, H. Hogue, J. C. Clement, K. Stelzer, G. Mack, J. R. Boyce, D. E. Epperson, S. G. Buccino, P. W. Lisowski, S. G. Glendinning, E. G. Bilpuch, H. W. Newson, and C. R. Gould, Nucl. Sci. Eng. 61, 521 (1976).

18 A Takahashi, "Double Differential Neutron Emission Cross Sections at 14 MeV Measured at OKTAVIAN", p. 99 of Report JAERI-M 86-029.

19. G. Haouat, J. Lachkar, J. Sigaud, Y. Patin, and F. Cocu, Nucl. Sci. Eng. 65, 331 (1978).

20. G. L. Morgan, T. A. Love, and F. G. Perey, Nucl. Instr. Meth. 128, 125 (1975).

APPENDIX

The following figures are spectra of the uncorrected double differential laboratory cross sections for ^{6}Li, ^{7}Li, ^{10}B, ^{11}B and carbon at 14.1 MeV for angles between 30½ and 143½. The full curves are the experimental results, the dotted curves are the answer of a Monte Carlo simulation using ENDF/B-IV input data when adjusted in the elastic region and the dashed curves are the piecewise adjusted curves used in this paper for determining the multiple scattering correction.

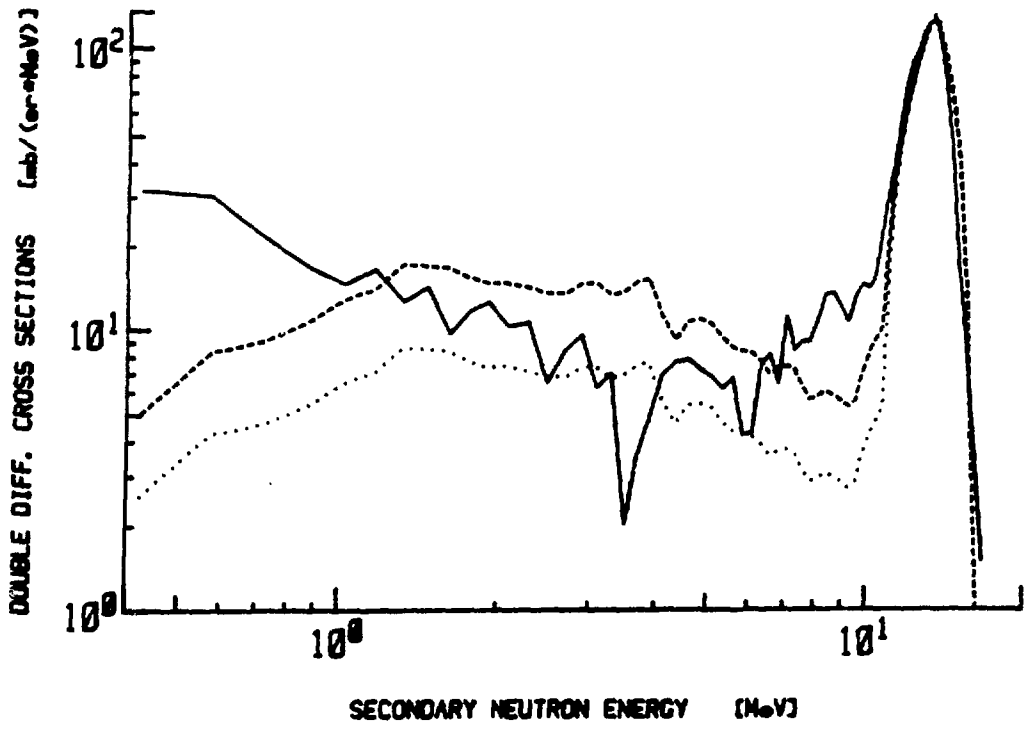

FIG. A-1. LITHIUM-6 30.0 DEG

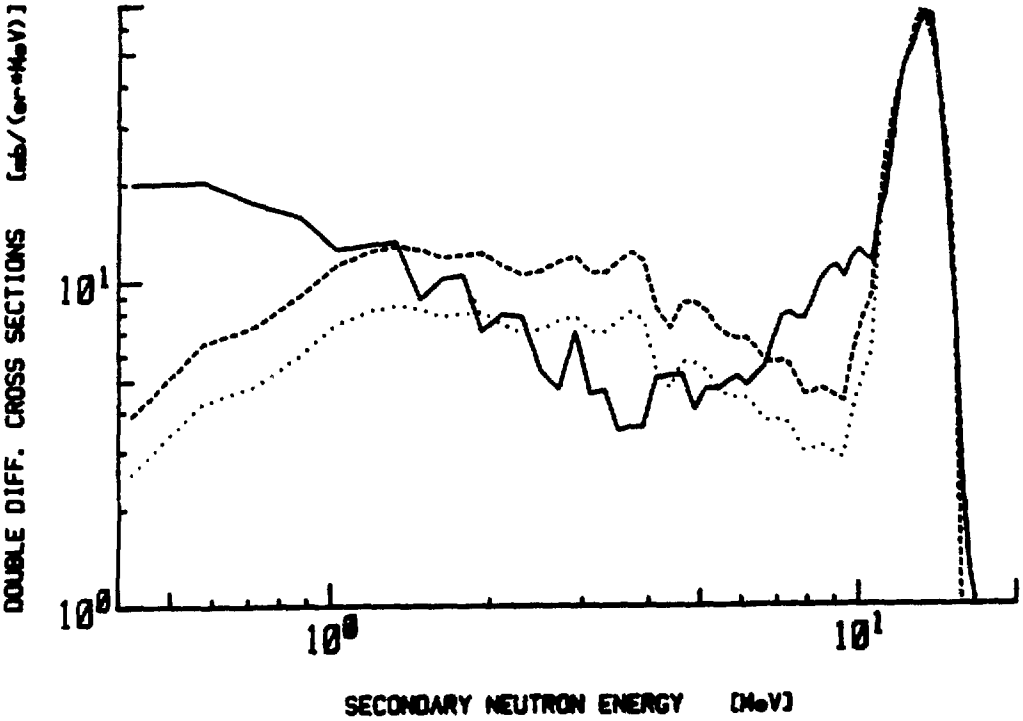

FIG. A-2. LITHIUM-6 40.0 DEG

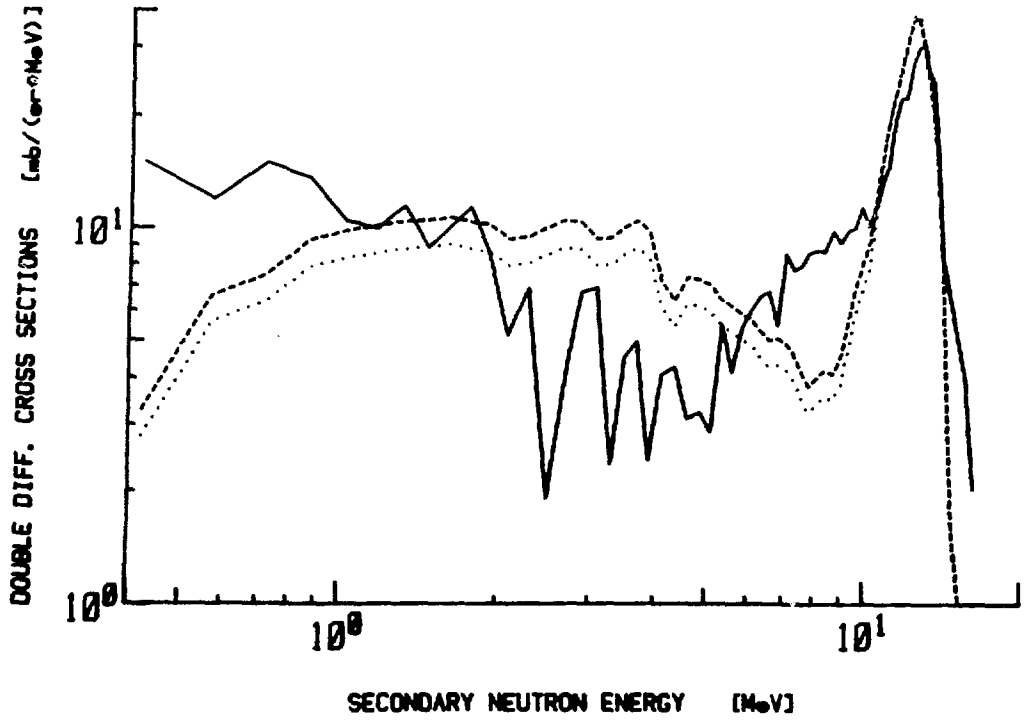

FIG. A-3. LITHIUM-6 50.1 DEG

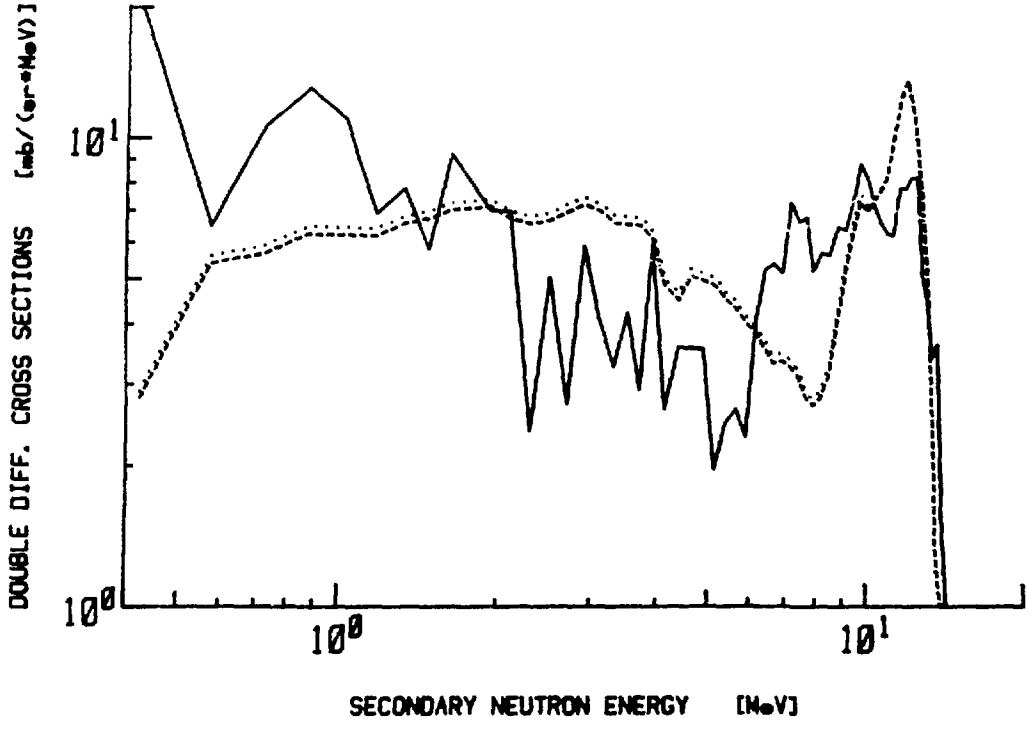

FIG. A-4. LITHIUM-6 63.6 DEG

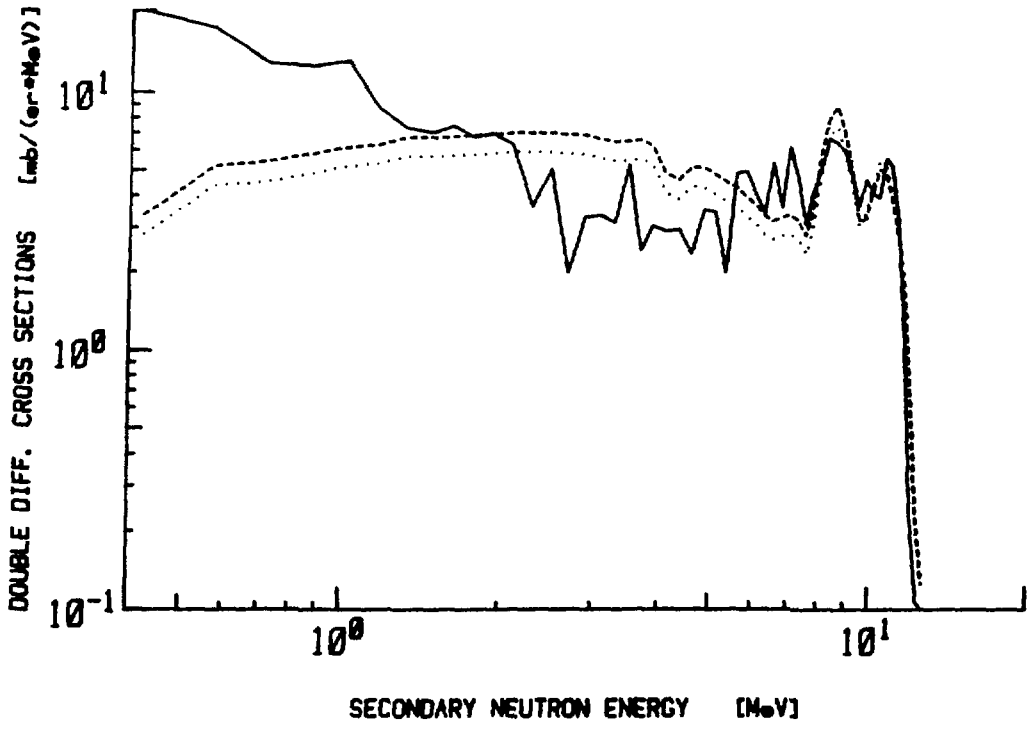

FIG. A-5. LITHIUM-6 80.3 DEG

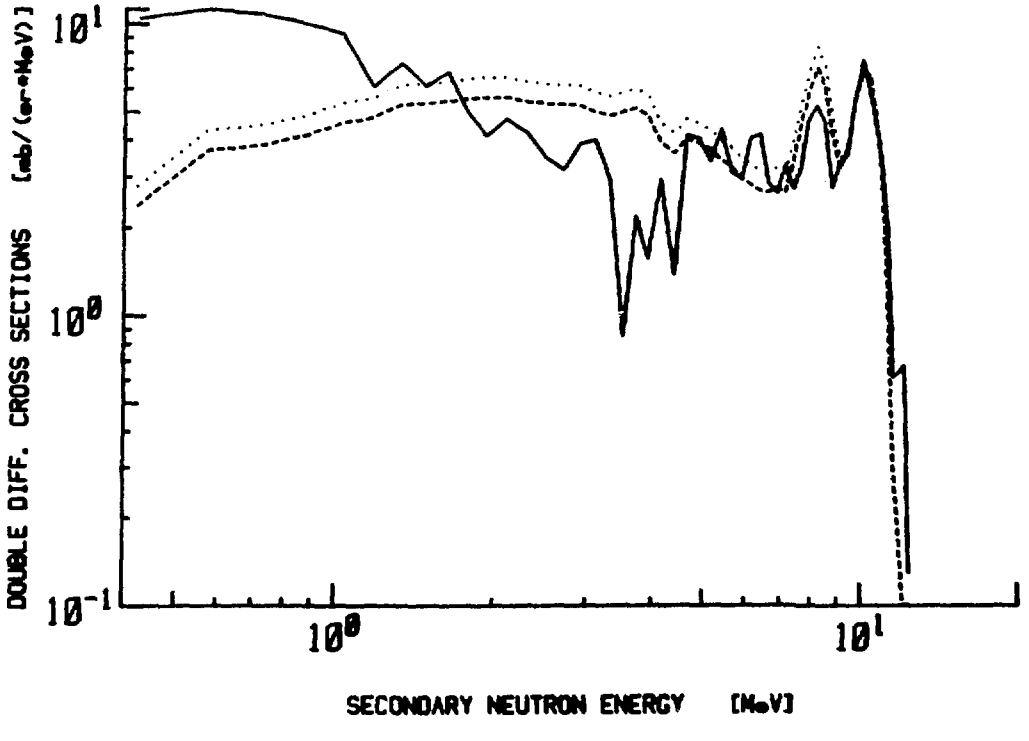

FIG. A-6. LITHIUM-6 89.8 DEG

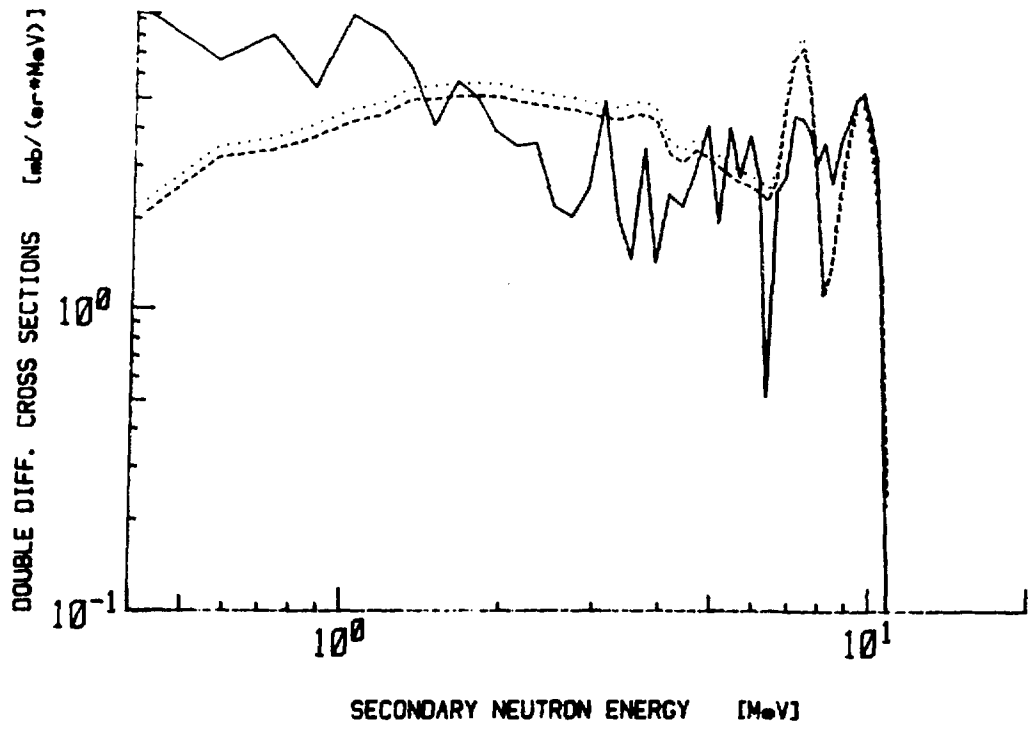

FIG. A-7. LITHIUM-6 99.3 DEG

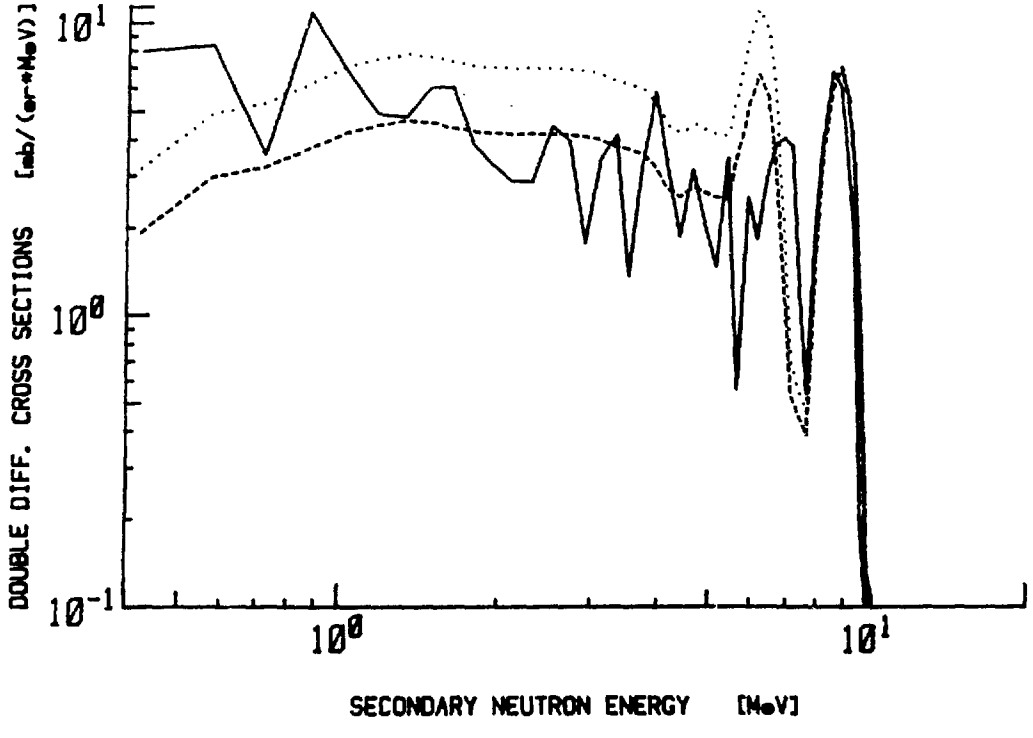

FIG. A-8. LITHIUM-6 115.0 DEG

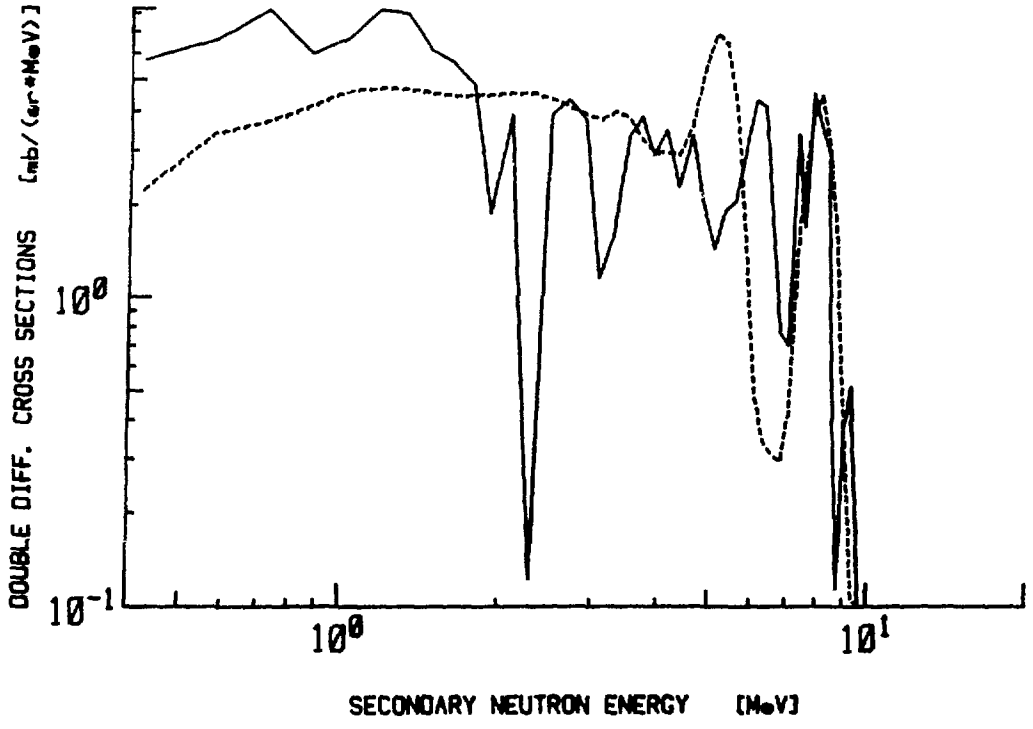

FIG. A-9. LITHIUM-6 130.0 DEG

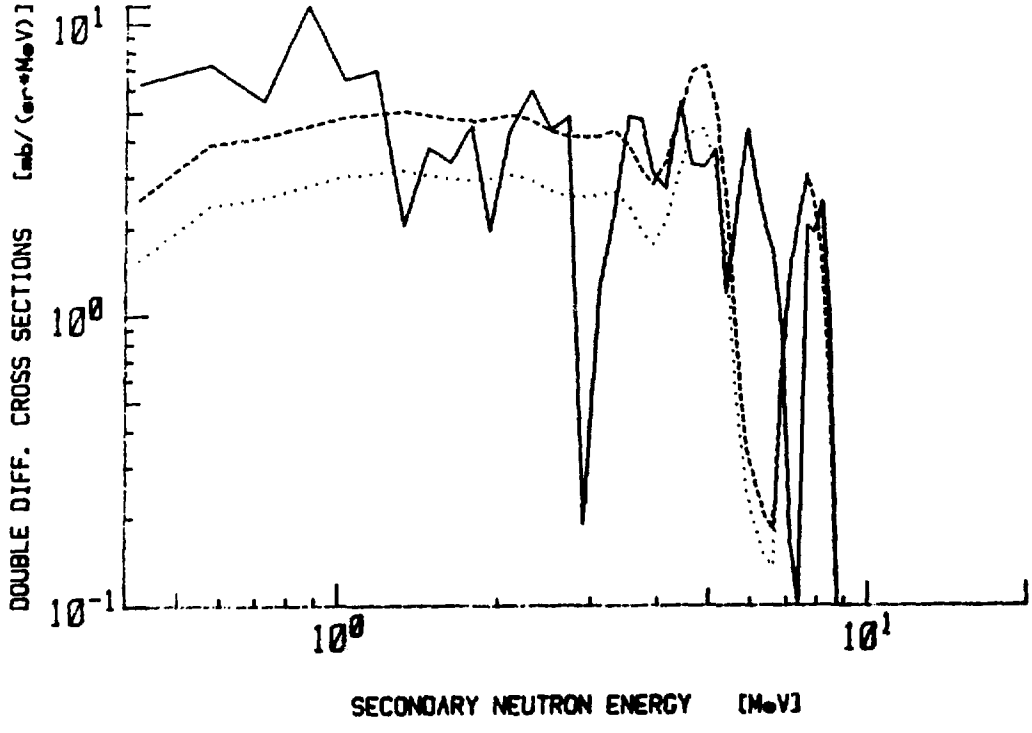

FIG. A-10. LITHIUM-6 143.0 DEG

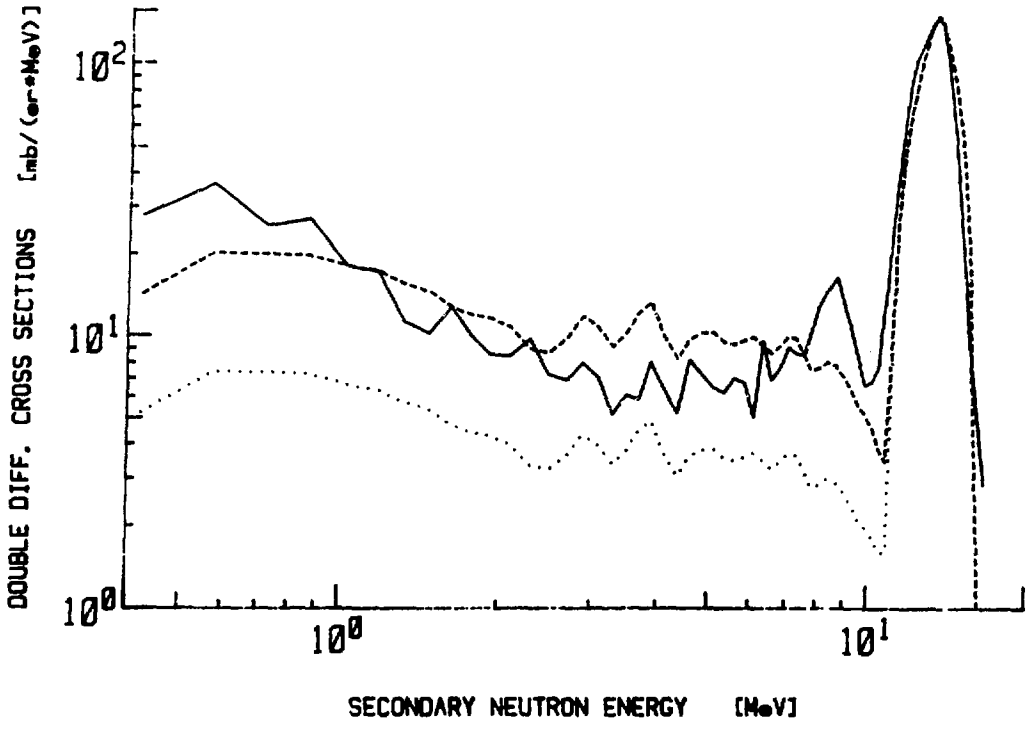

FIG. A-11. LITHIUM-7 30.0 DEG

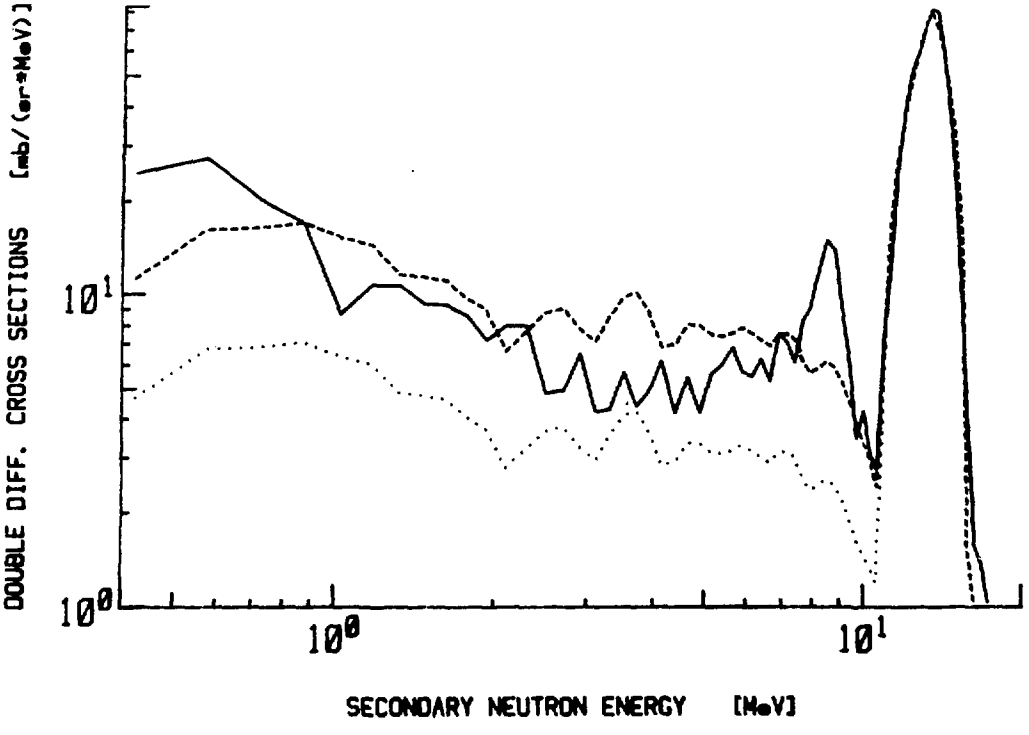

FIG. A-12. LITHIUM-7 40.0 DEG

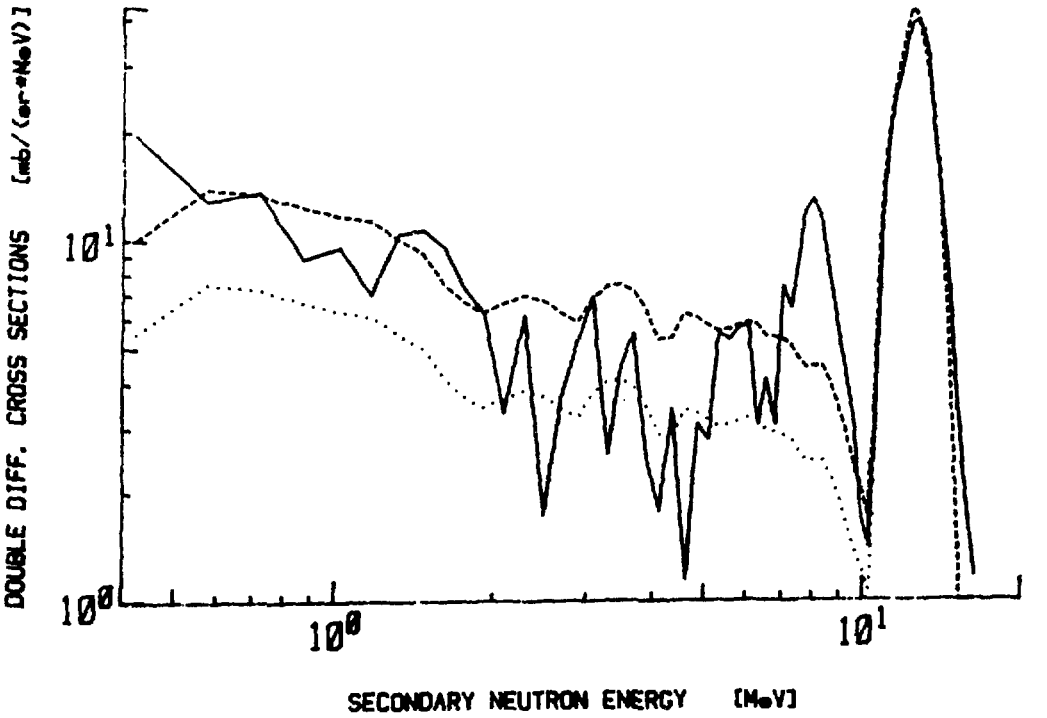

FIG. A-13. LITHIUM-7 50.1 DEG

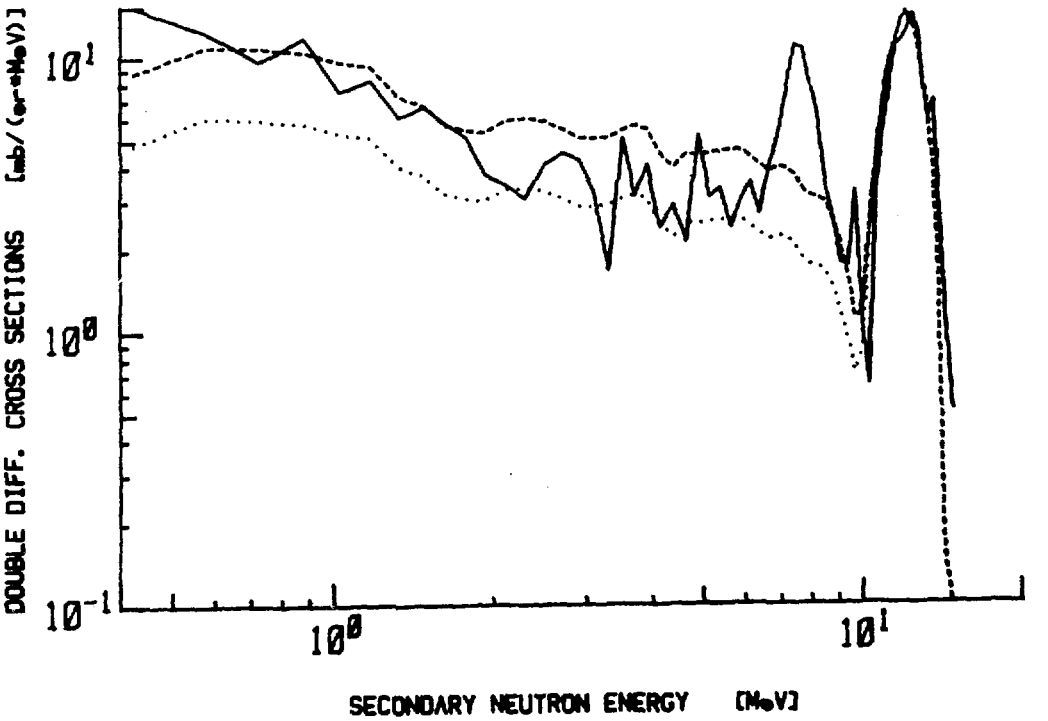

FIG. A-14. LITHIUM-7 63.6 DEG

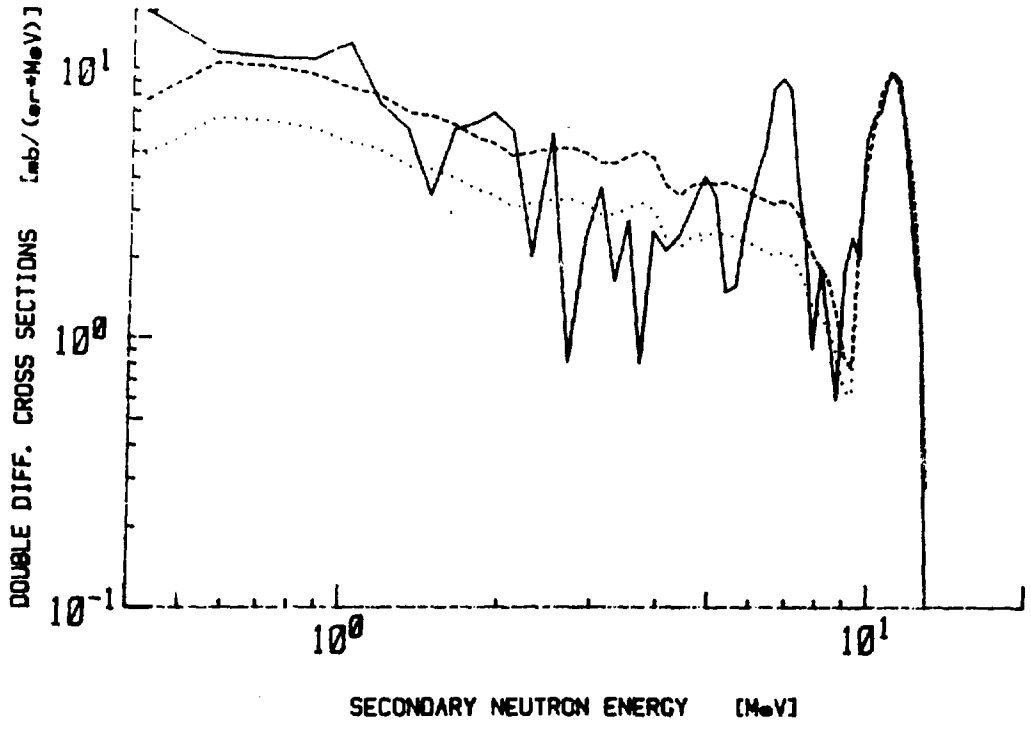

FIG. A-15. LITHIUM-7 80.3 DEG

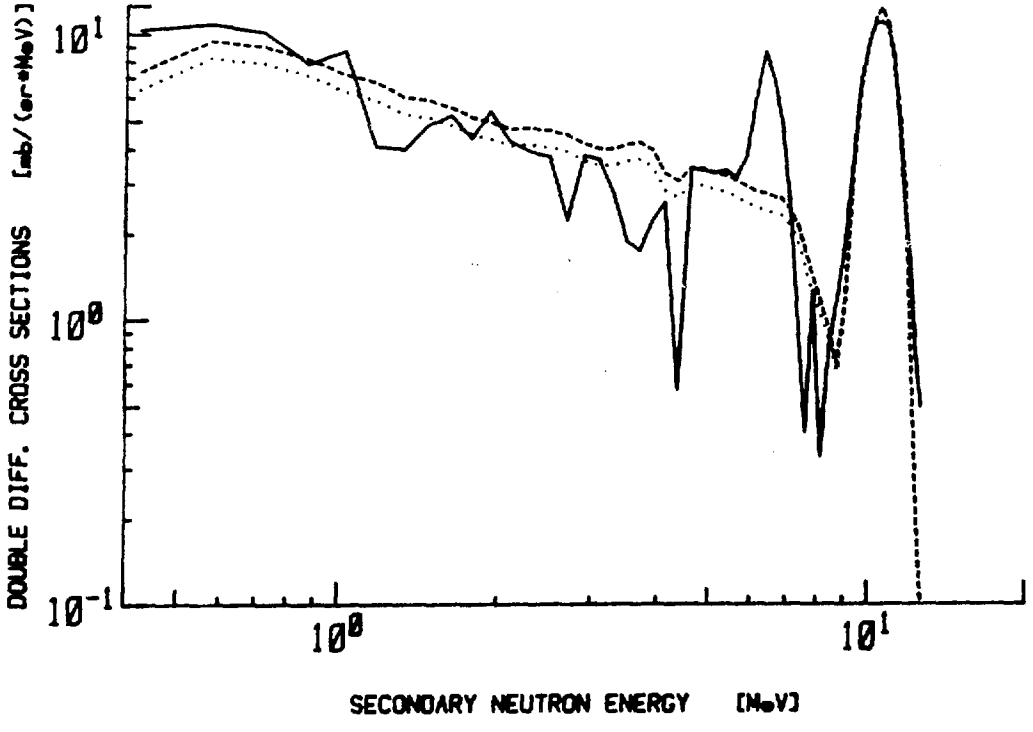

FIG. A-16. LITHIUM-7 89.8 DEG

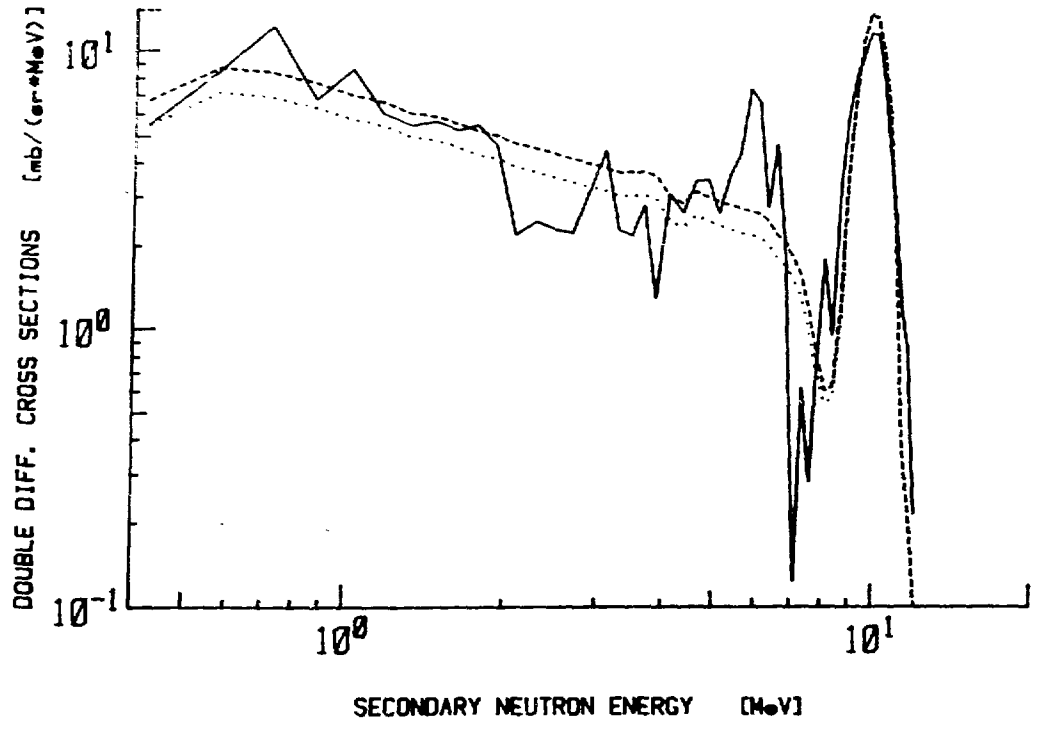

FIG. A-17. LITHIUM-7 99.3 DEG

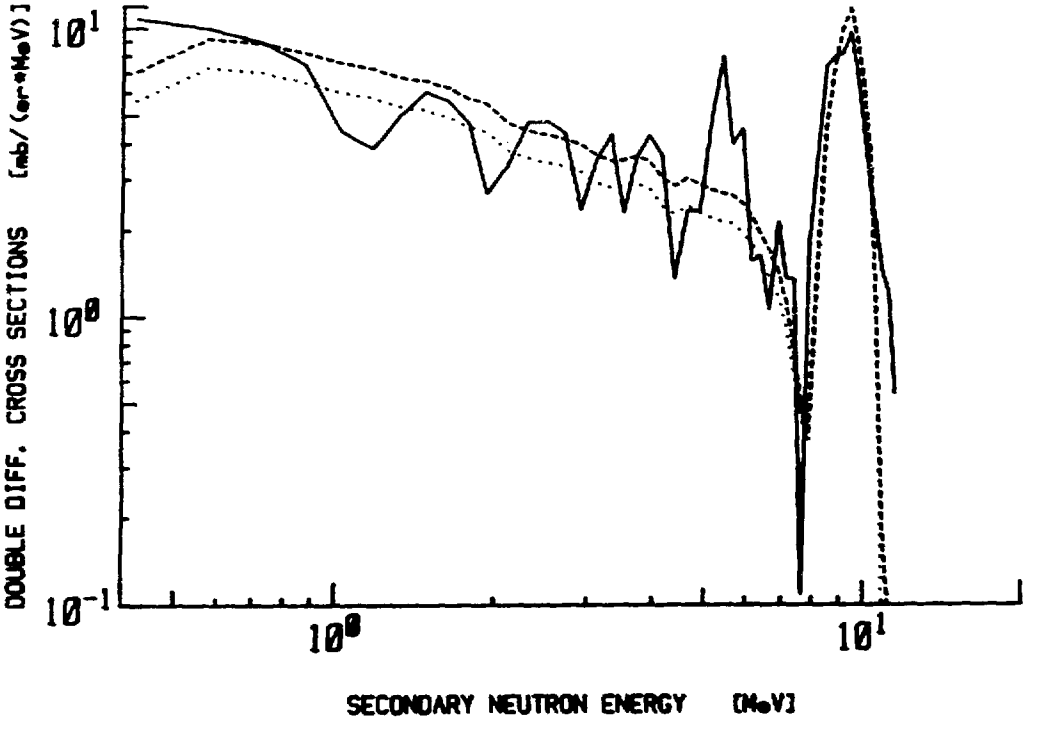

FIG. A-18. LITHIUM-7 115.0 DEG

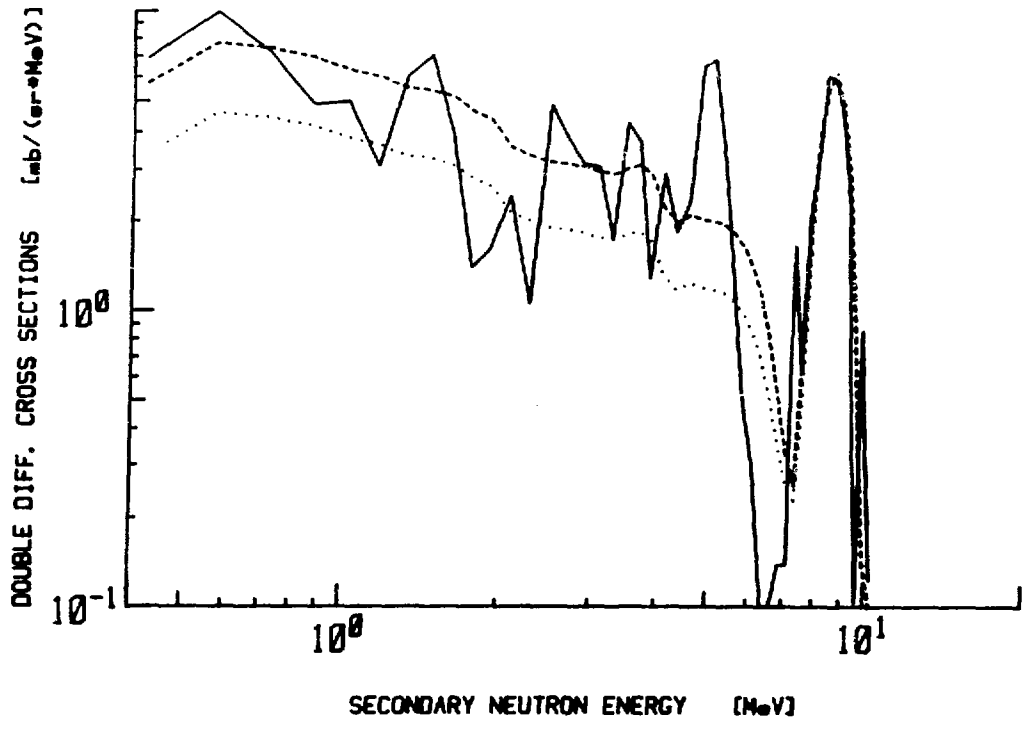

FIG. A-19. LITHIUM-7 130.0 DEG

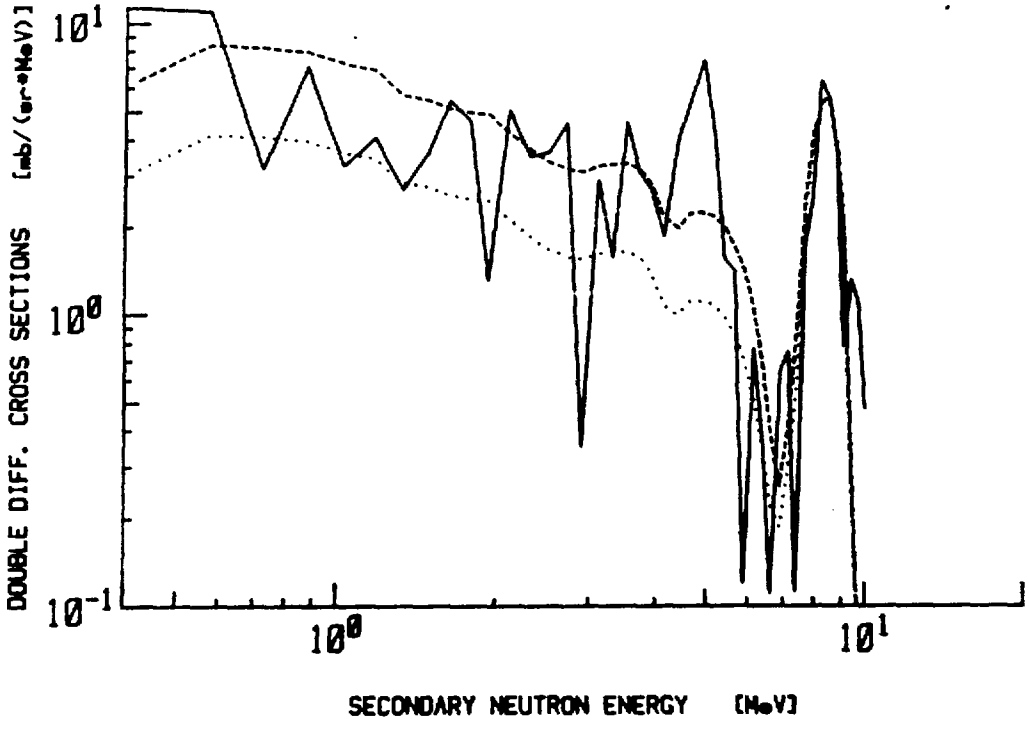

FIG. A-20. LITHIUM-7 143.0 DEG

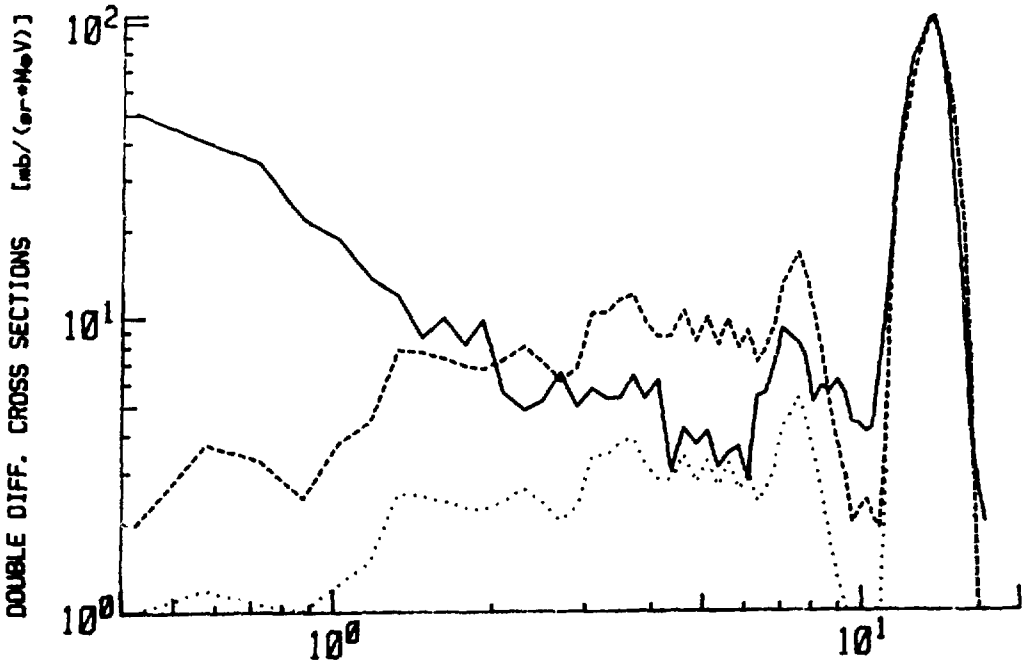

FIG. A-21. BORON-10 30.0 DEG

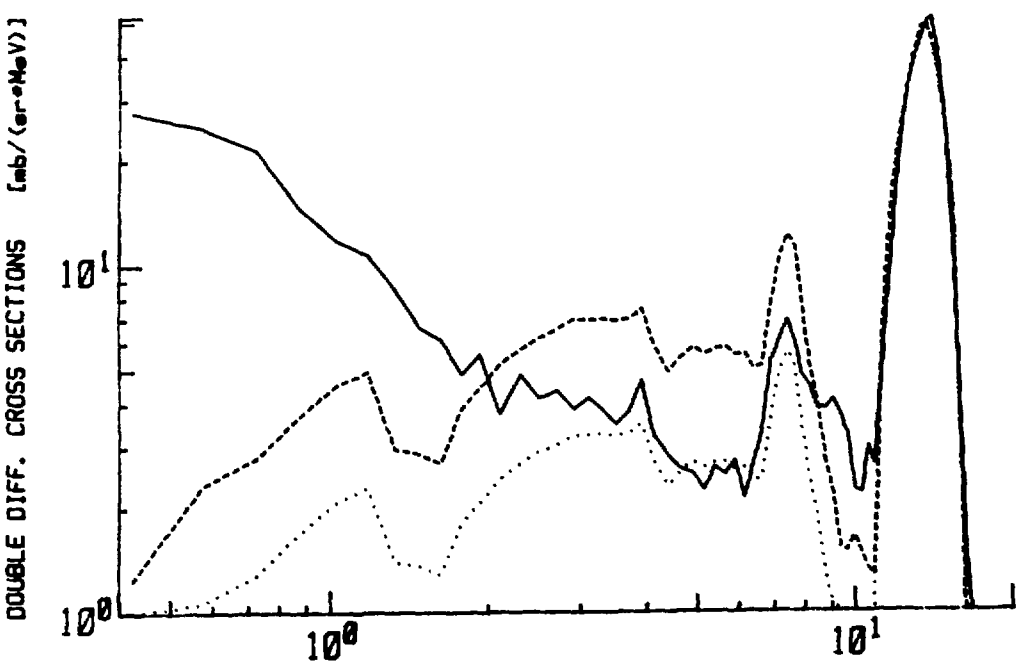

FIG. A-22. BORON-10 40.0 DEG

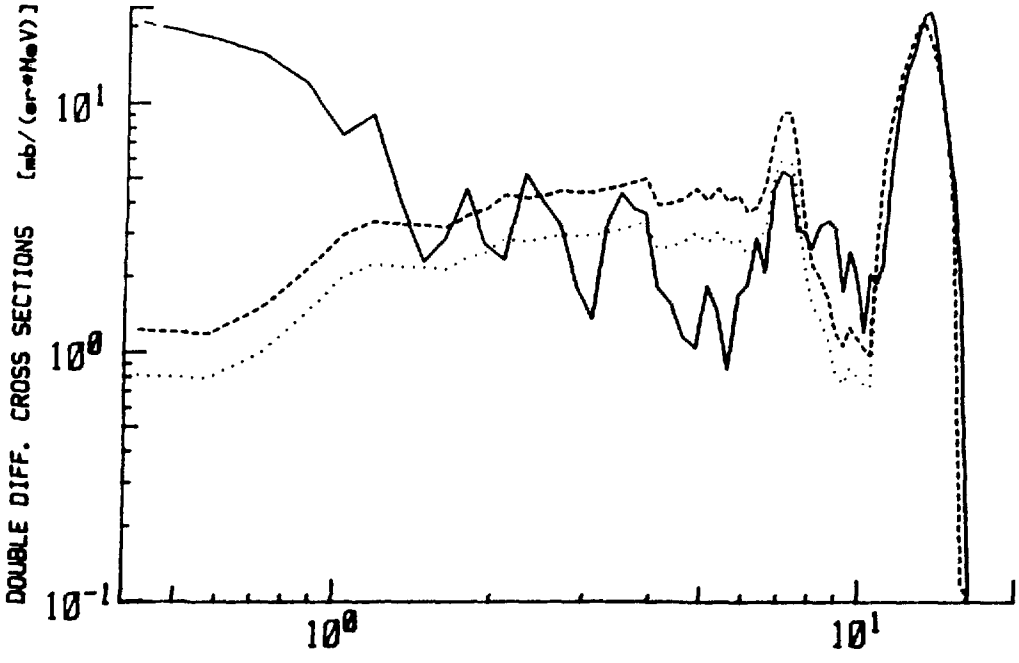

FIG. A-23. BORON-10 50.1 DEG

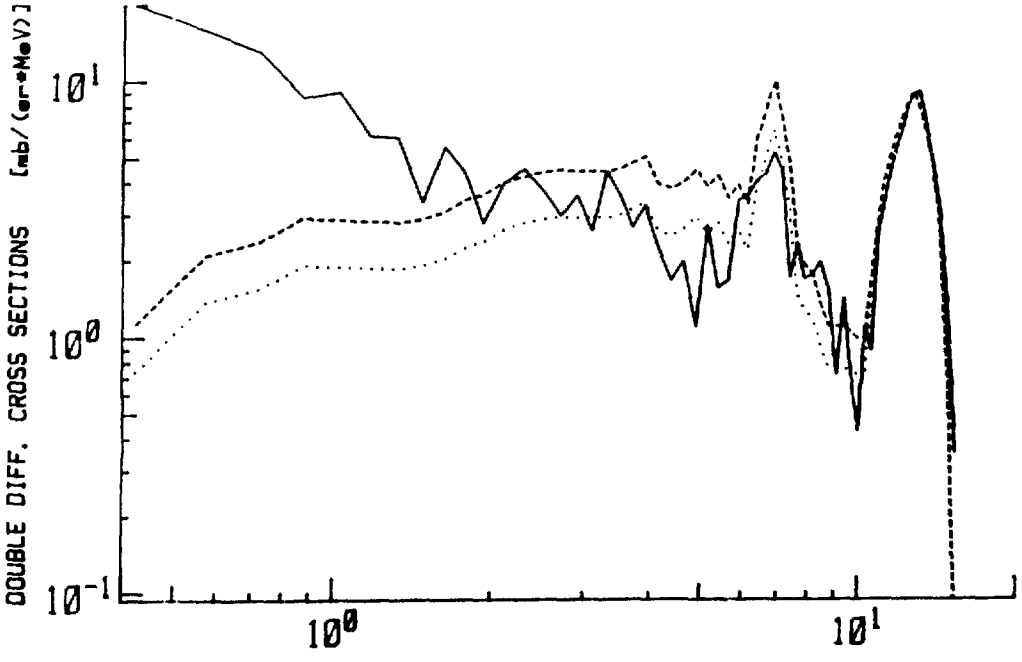

FIG. A-24. BORON-10 63.6 DEG

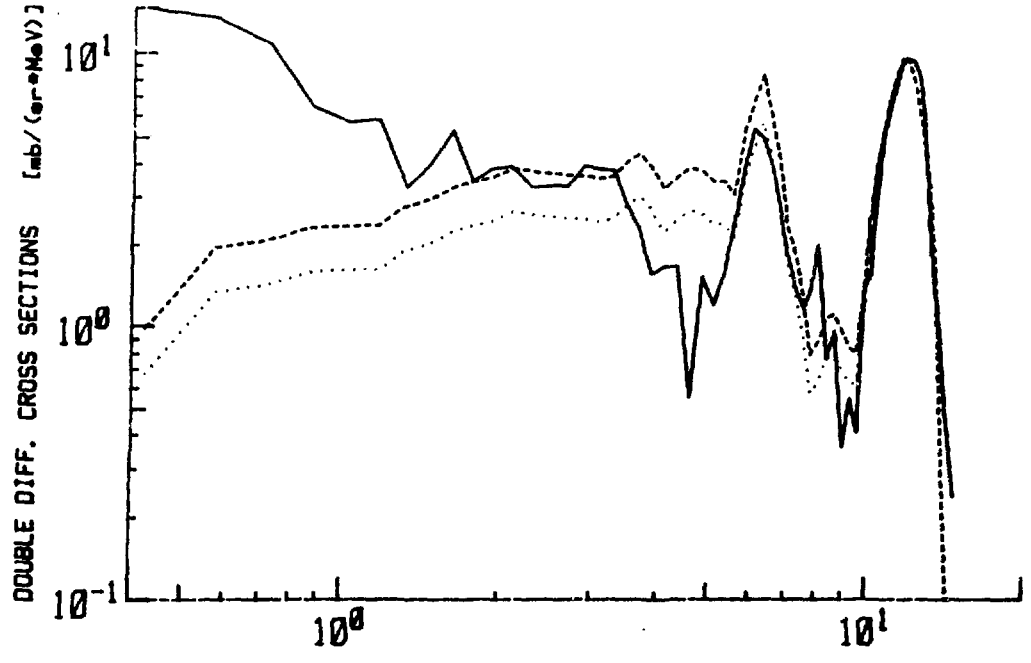

FIG. A-25. BORON-10 80.3 DEG

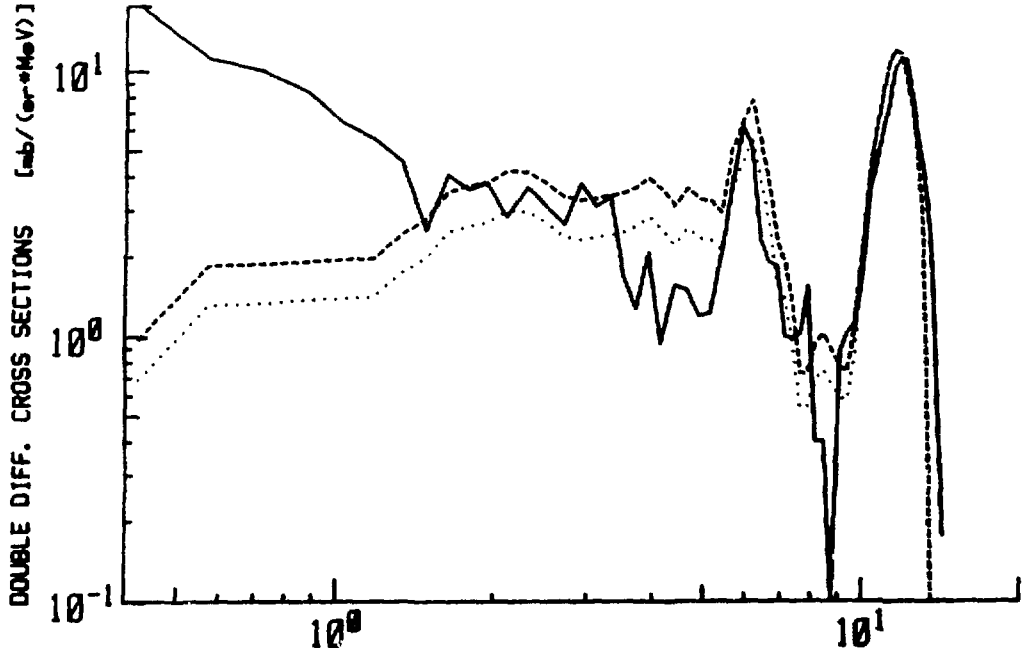

FIG. A-26. BORON-10 89.8 DEG

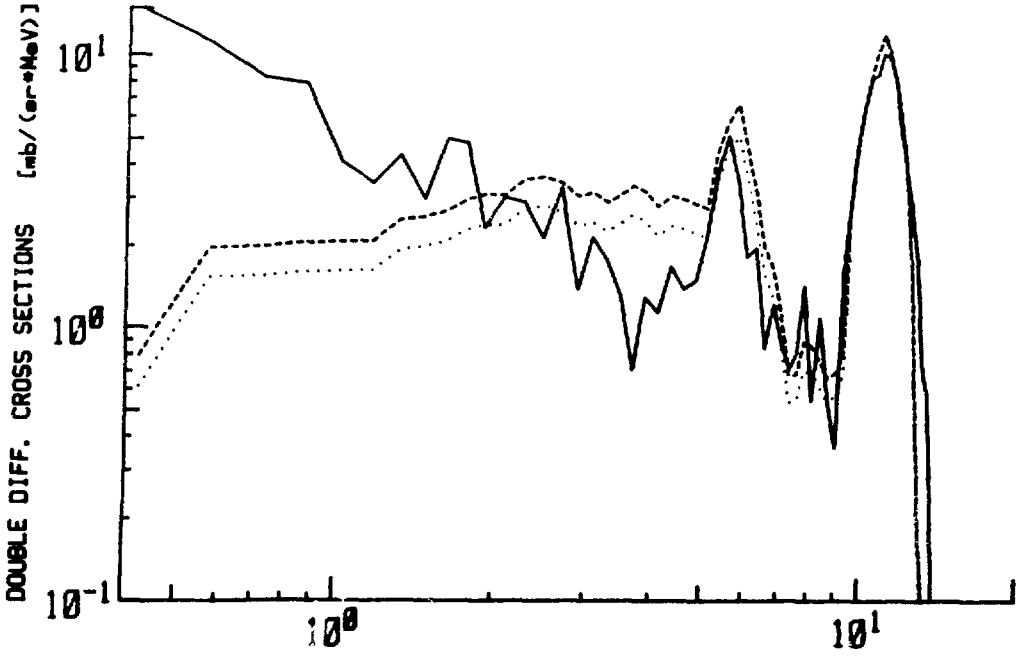

FIG. A-27. BORON-10 99.3 DEG

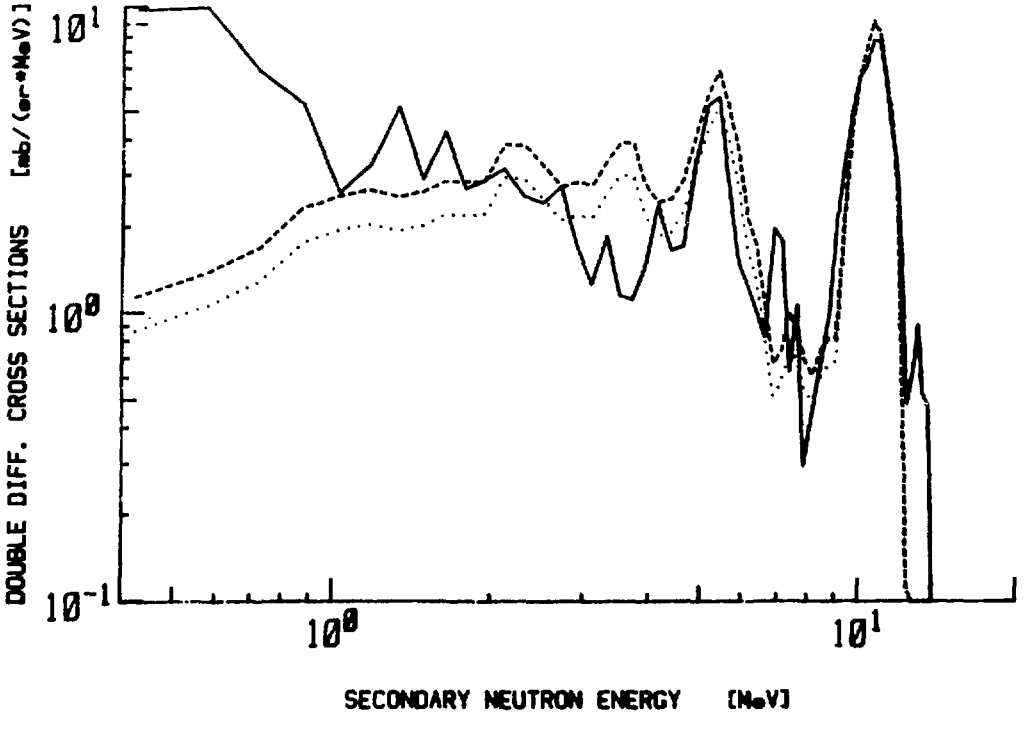

FIG. A-28. BORON-10 115.0 DEG

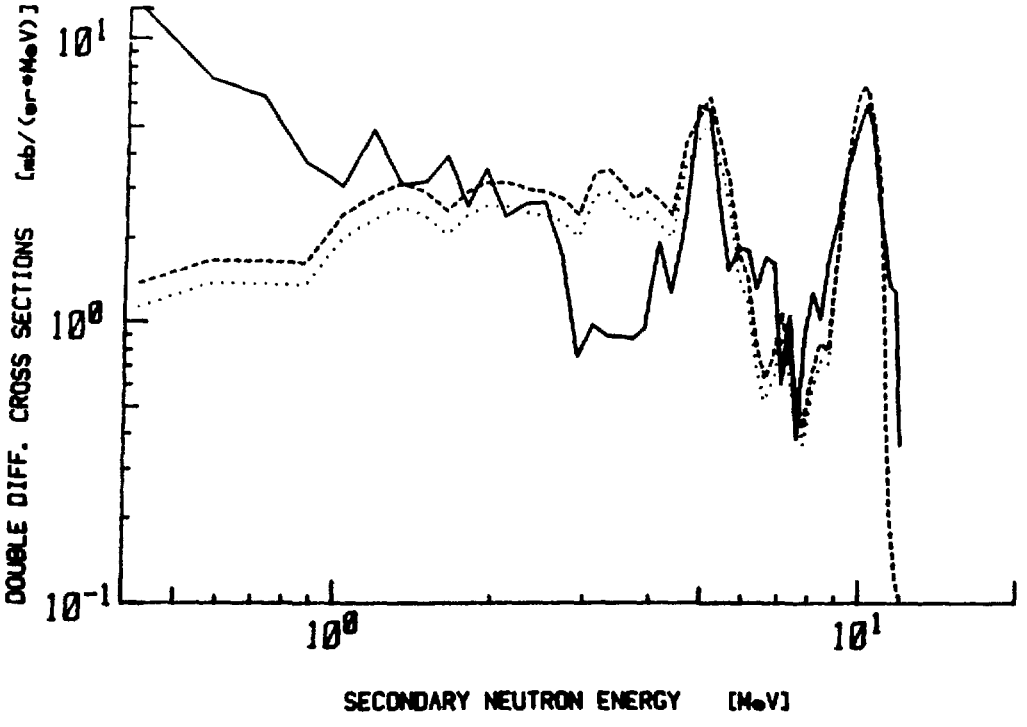

FIG. A-29. BORON-10 130.0 DEG

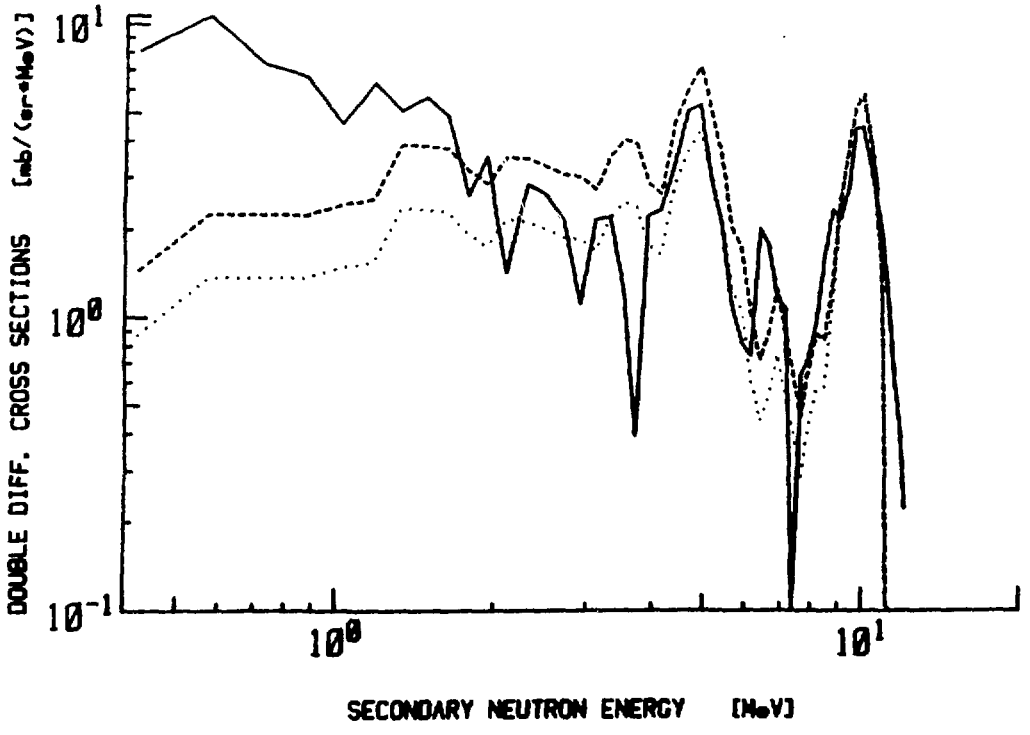

FIG. A-30. BORON-10 143.0 DEG

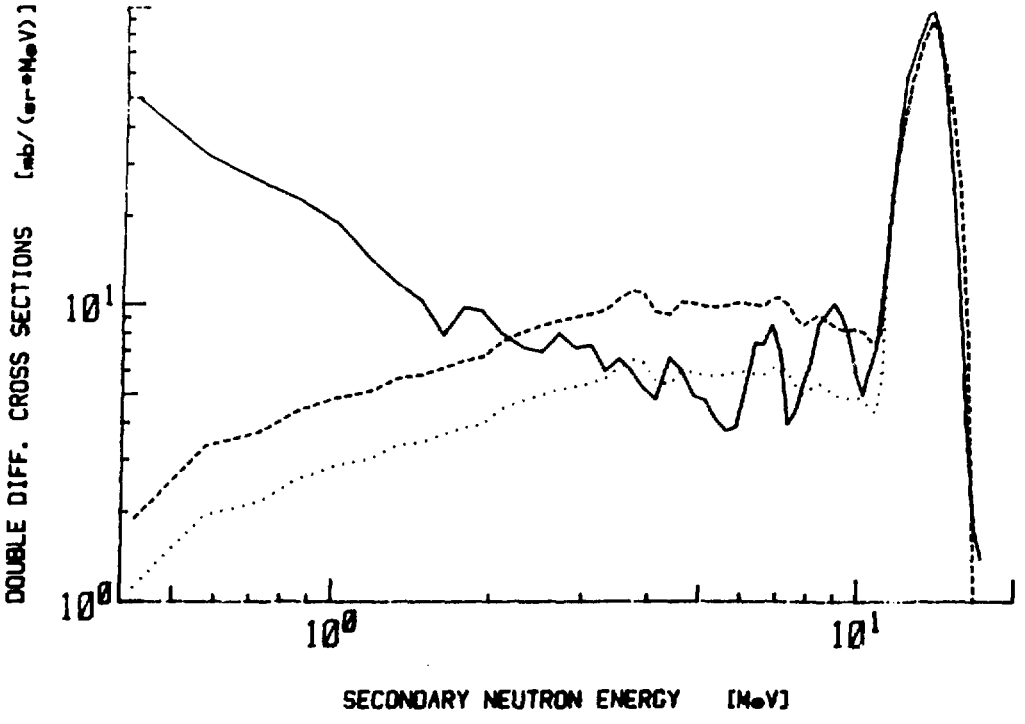

FIG. A-31. BORON-11 30.0 DEG

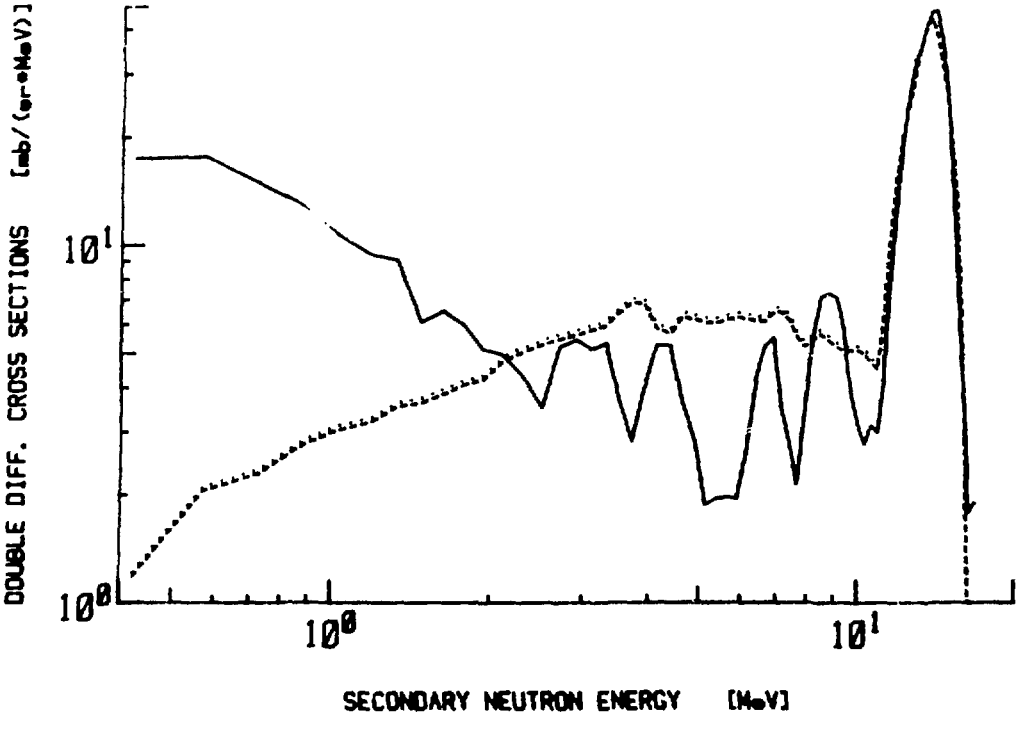

FIG. A-32. BORON-11 40.0 DEG

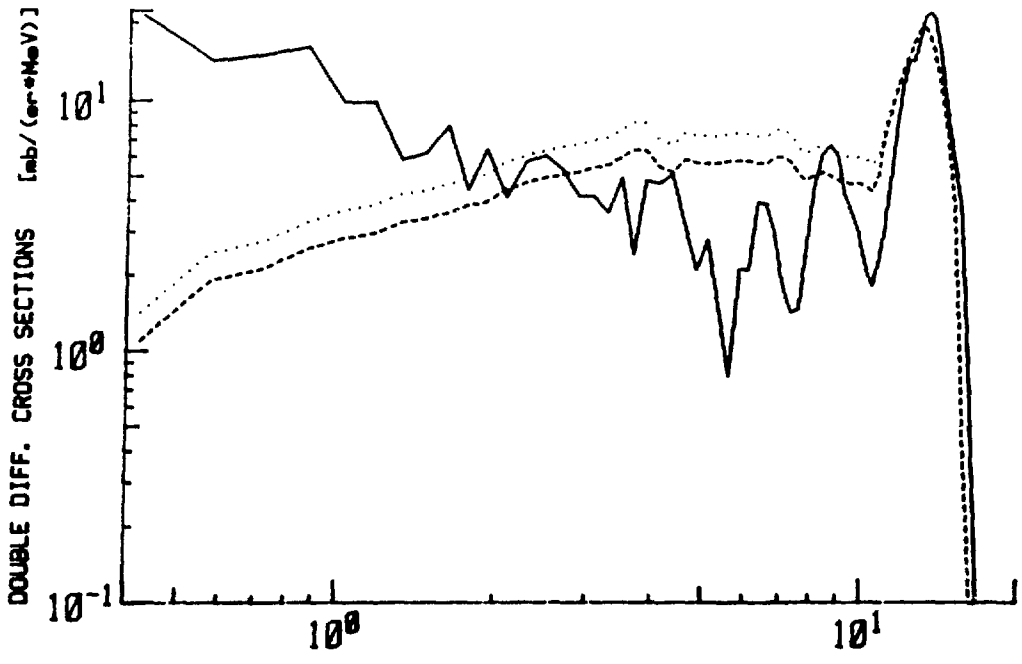

FIG. A-33. BORON-11 50.1 DEG

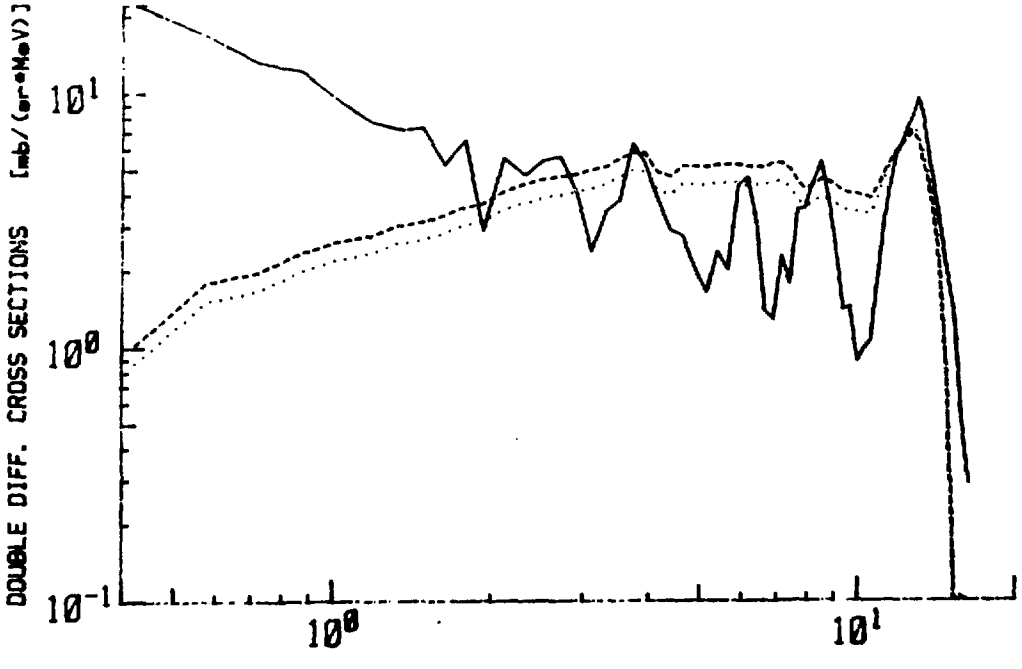

FIG. A-34. BORON-11 63.6 DEG

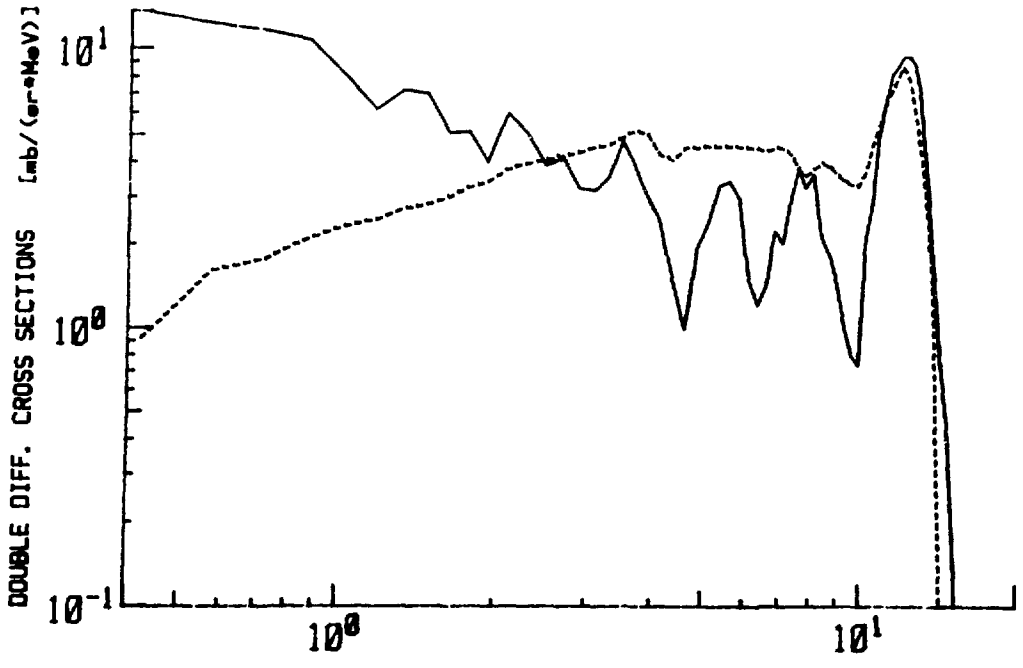

FIG. A-35. BORON-11 80.3 DEG

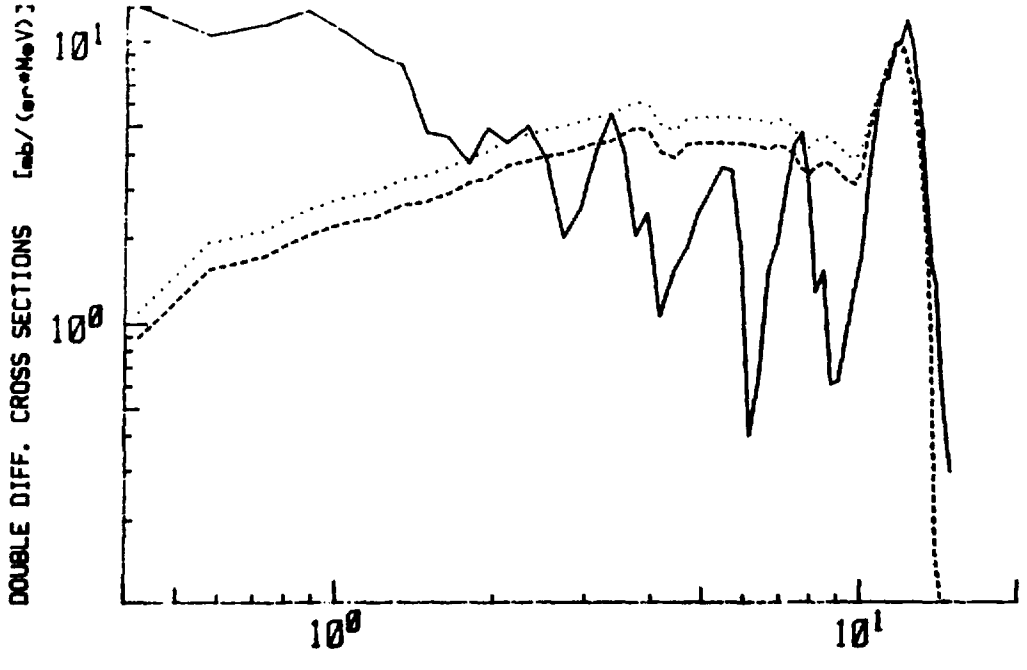

FIG. A-36. BORON-11 89.8 DEG

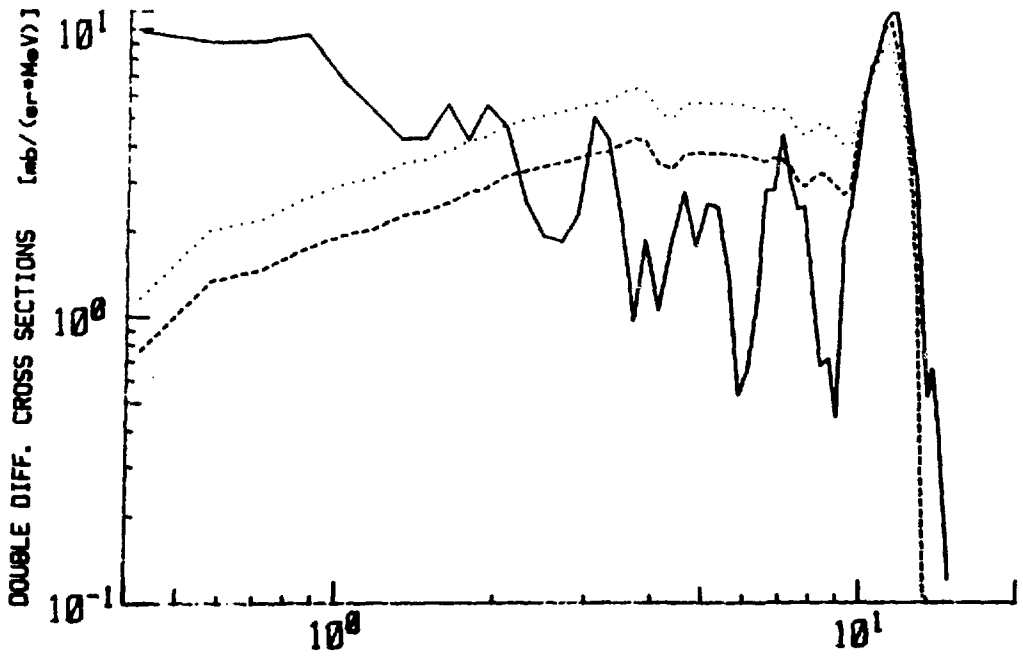

FIG. A-37. BORON-11 99.3 DEG

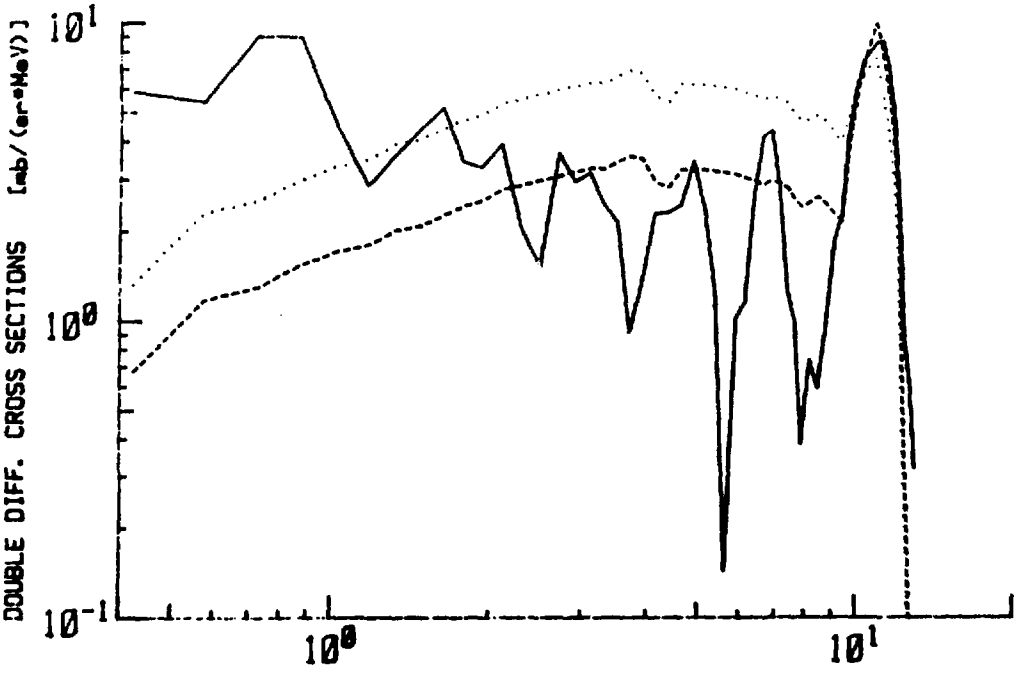

FIG. A-38. BORON-11 115.0 DEG

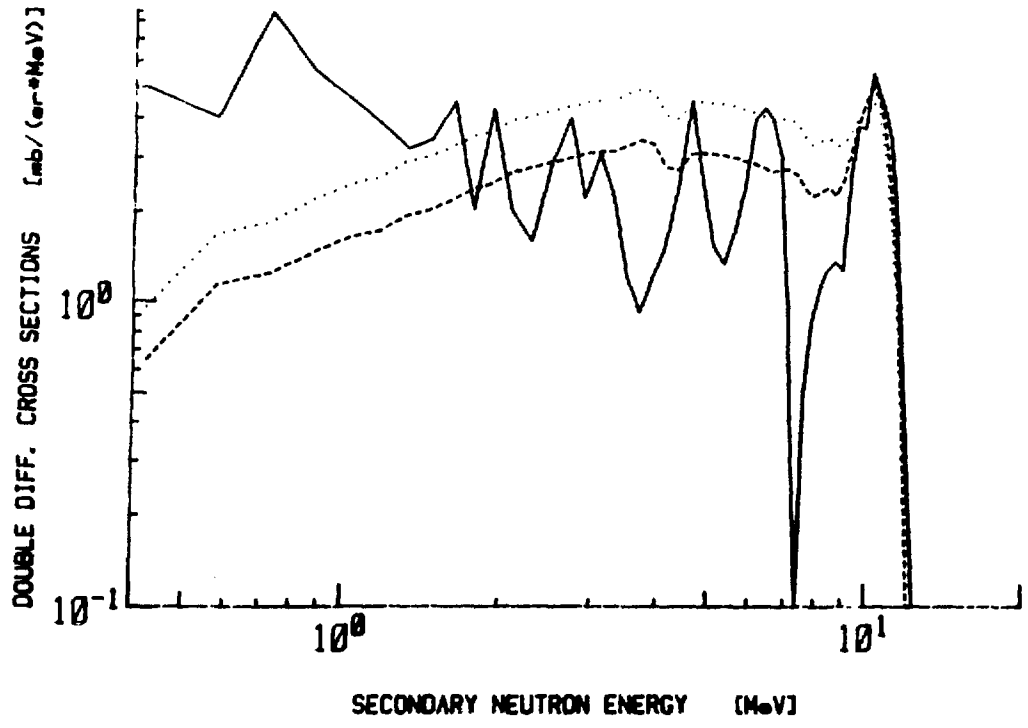

FIG. A-39. BORON-11 130.0 DEG

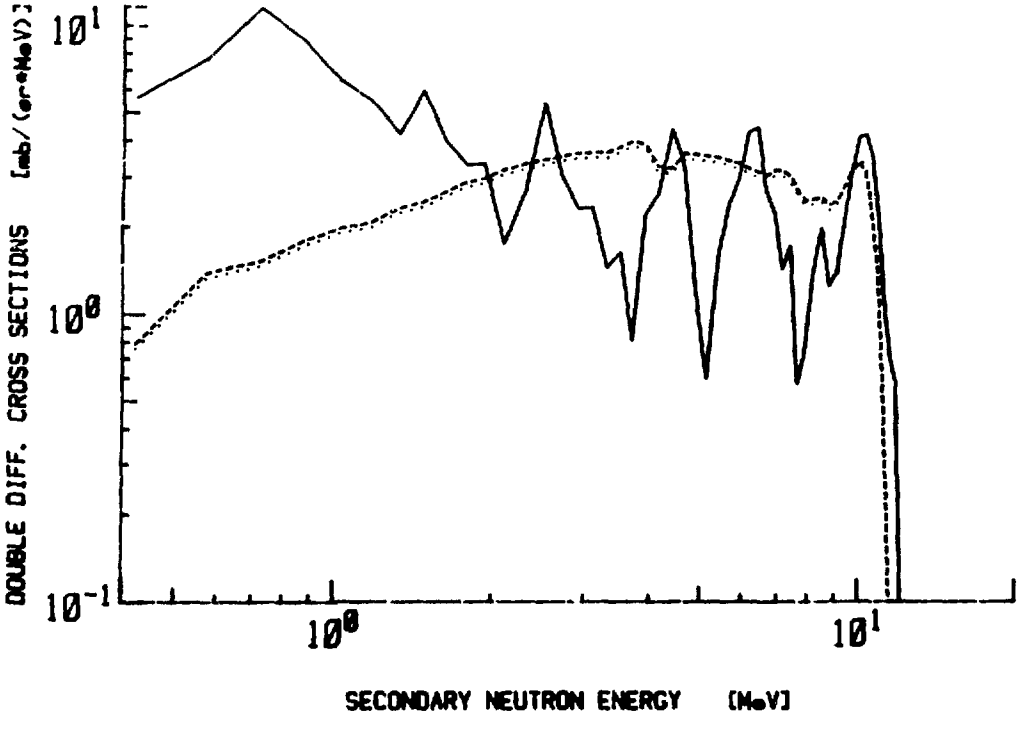

FIG. A-40. BORON-11 143.0 DEG

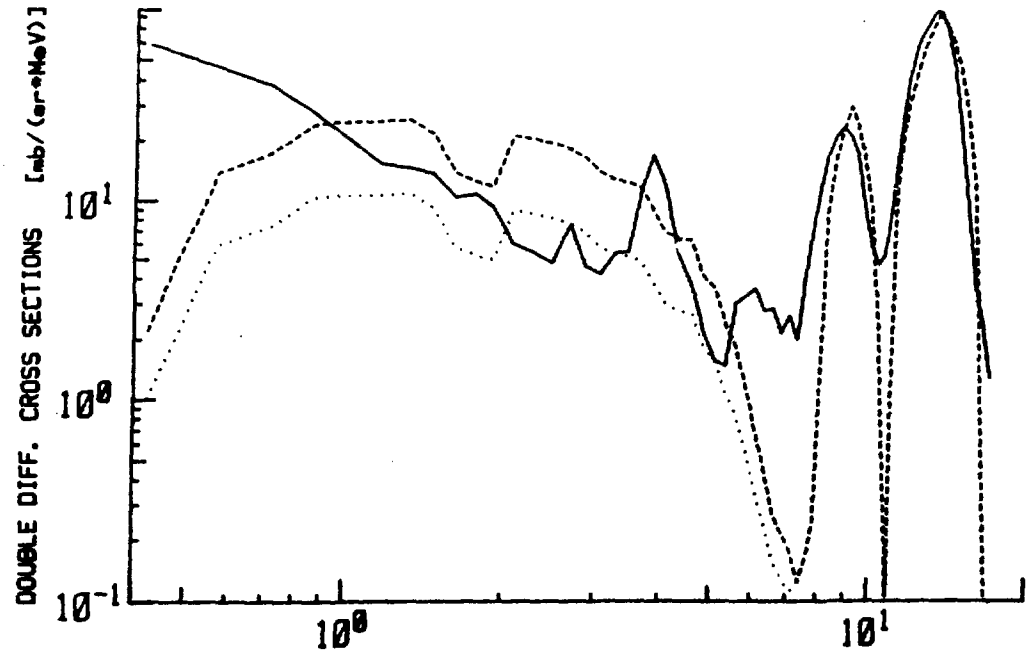

FIG. A-41. CARBON 30.0 DEG

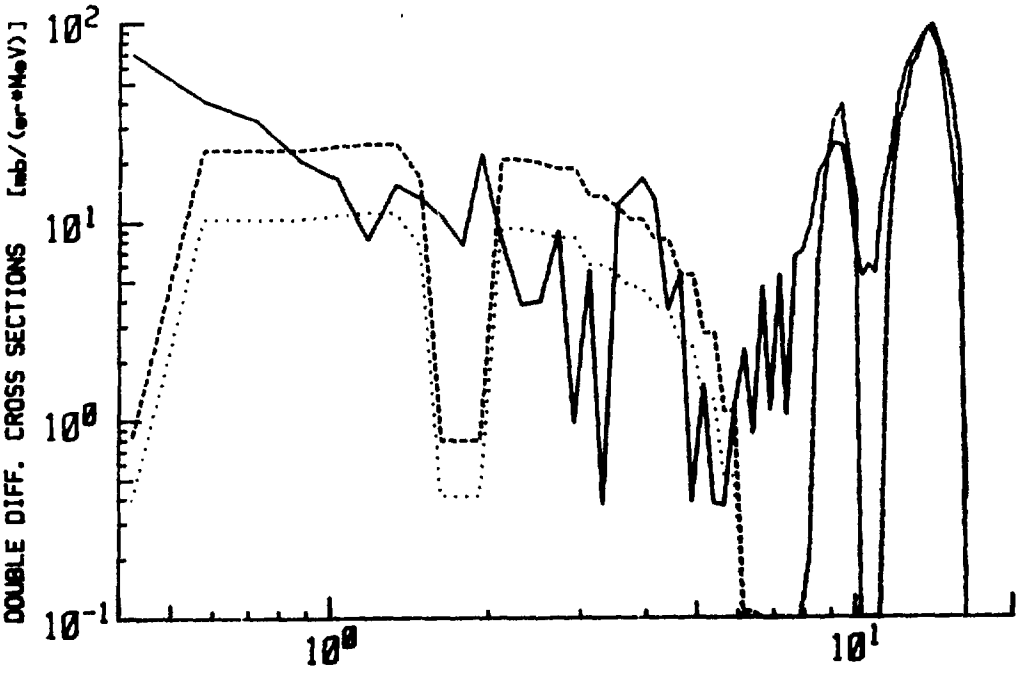

FIG. A-42. CARBON -30.0 DEG

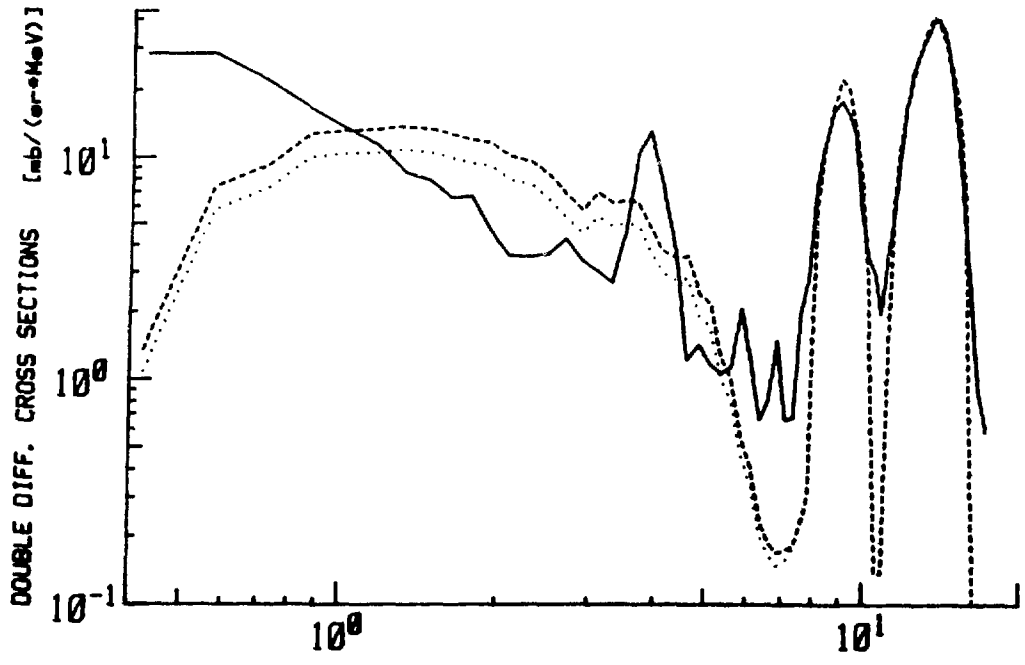

FIG. A-43. CARBON 40.0 DEG

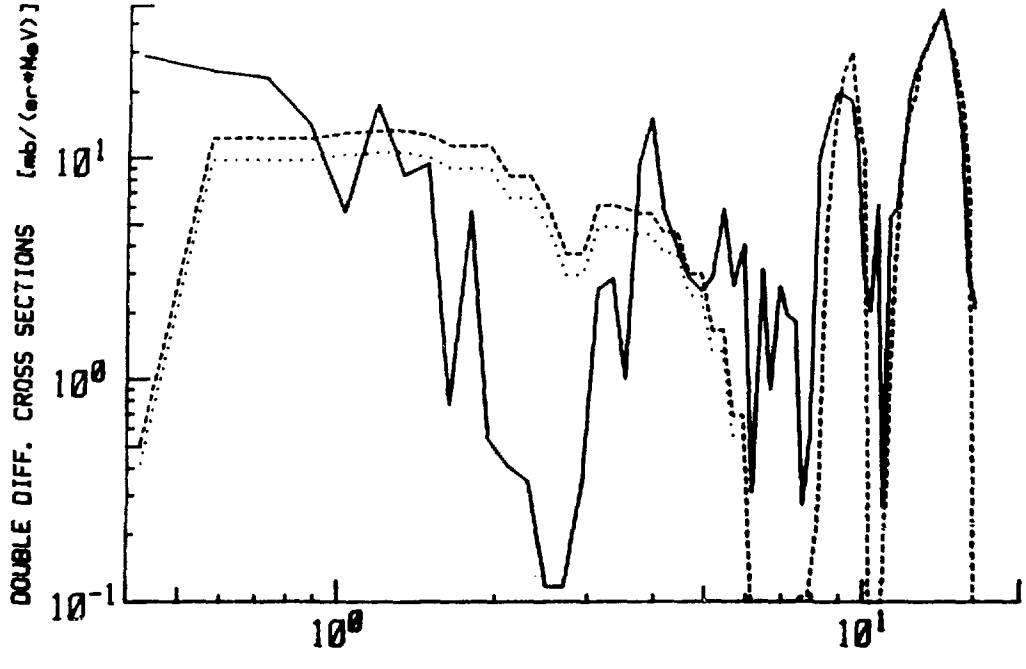

FIG. A-44. CARBON -40.0 DEG

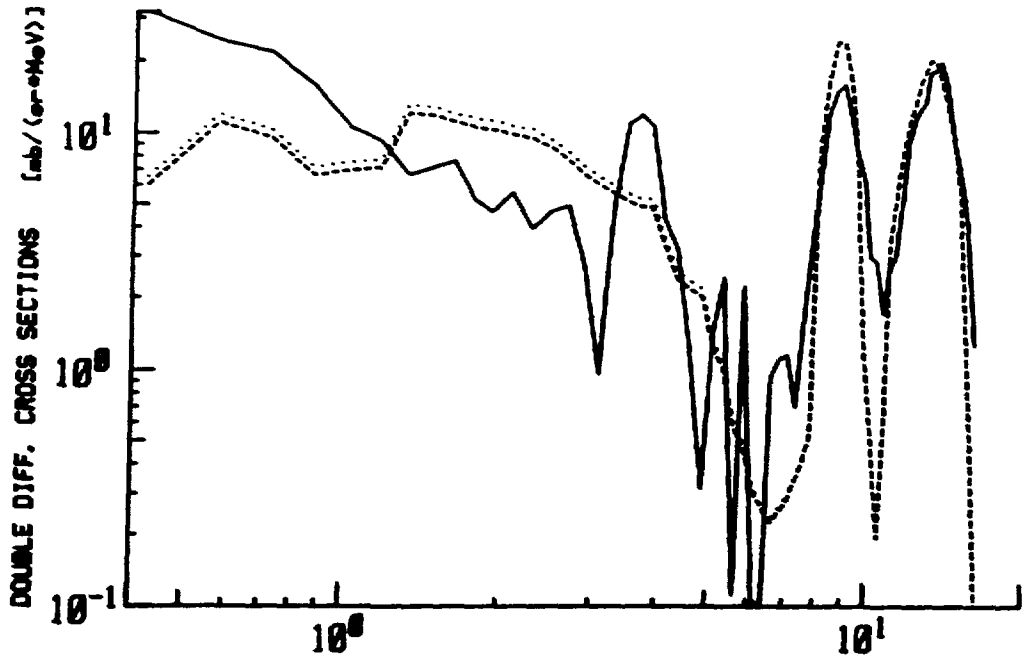

FIG. A-45. CARBON 50.1 DEG

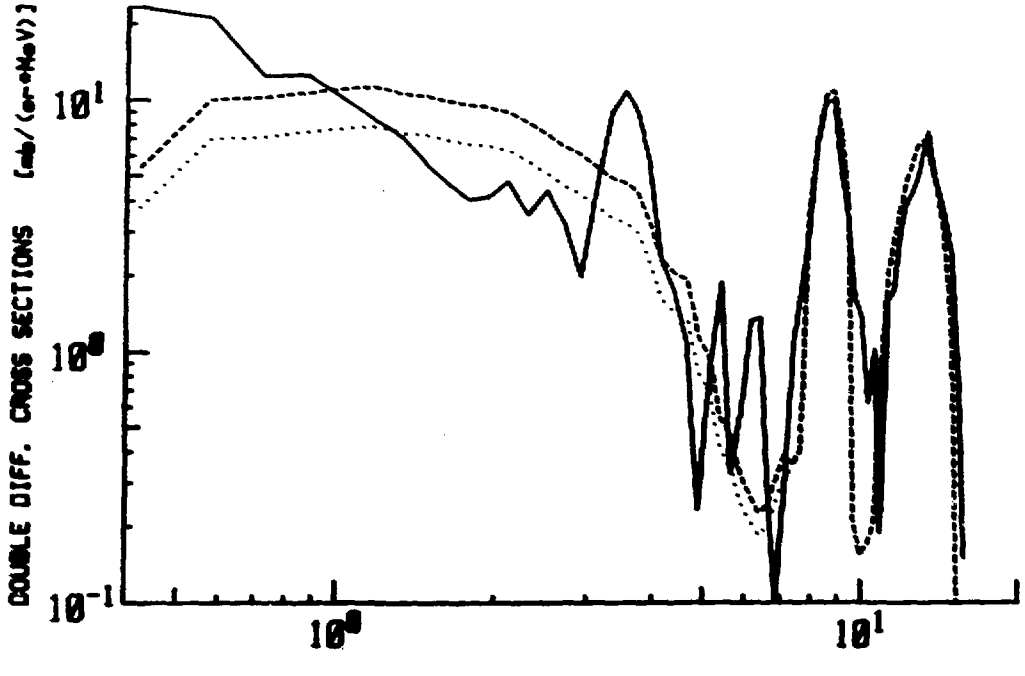

FIG. A-46. CARBON 63.6 DEG

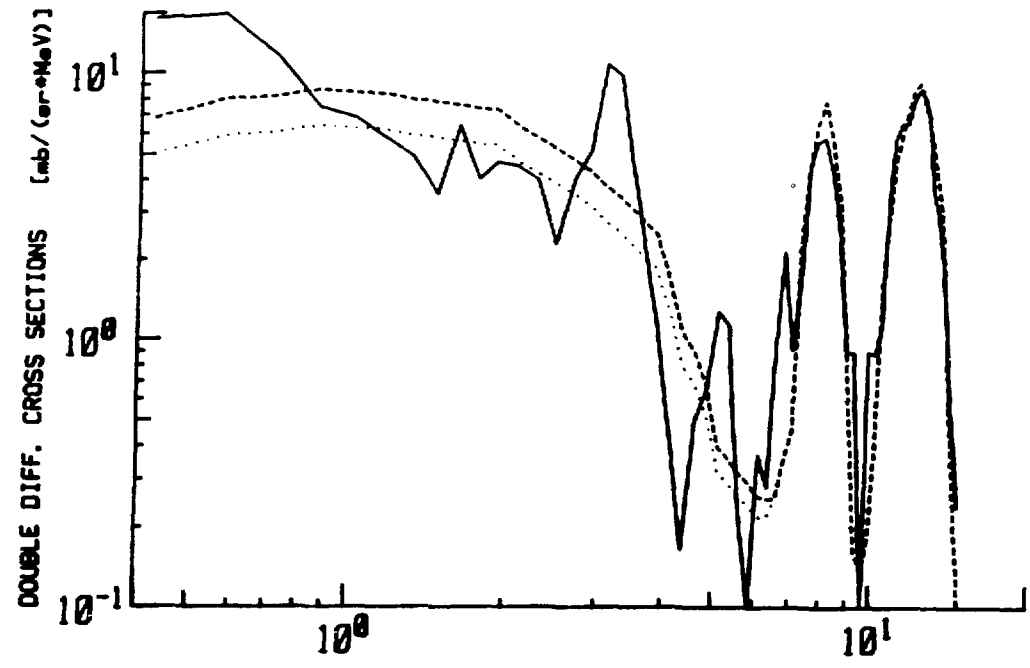

FIG. A-47. CARBON 80.3 DEG

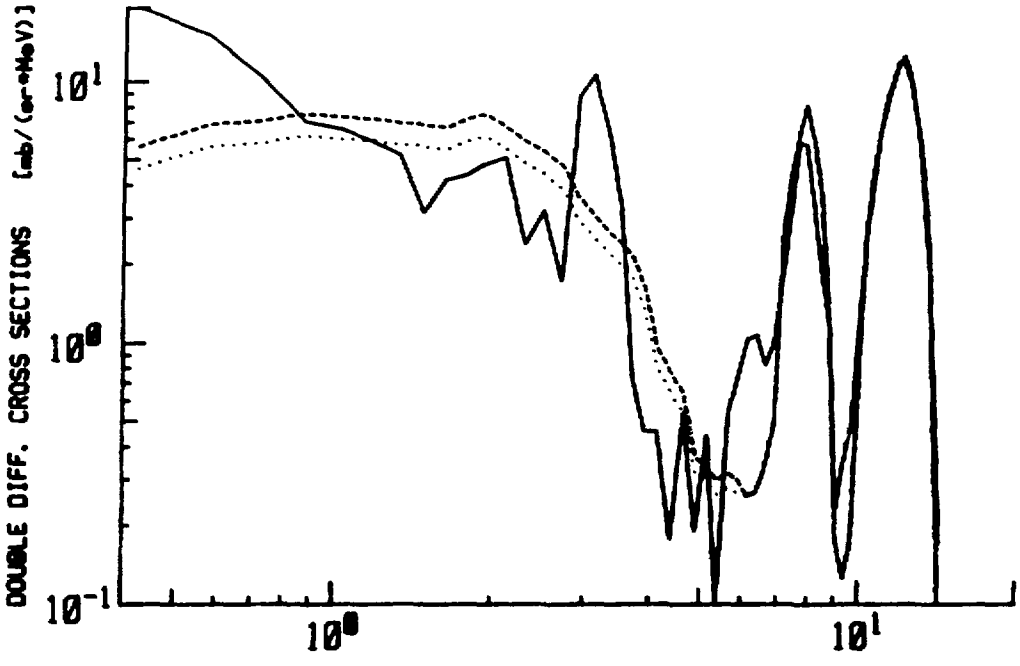

FIG. A-48. CARBON 89.8 DEG

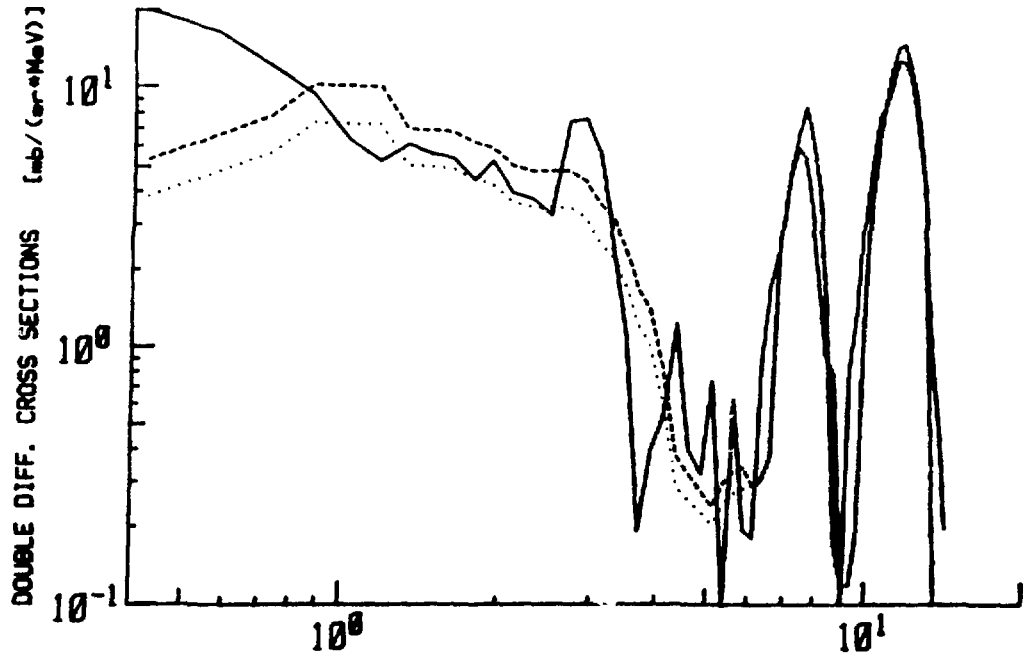

FIG. A-49. CARBON 99.3 DEG

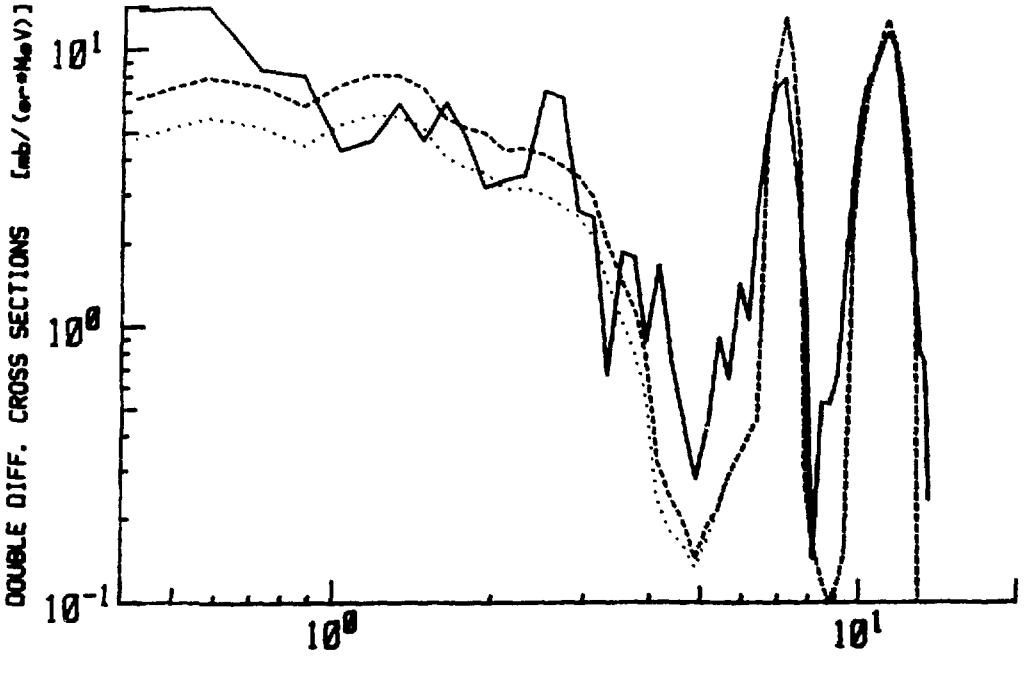

FIG. A-50. CARBON 115.0 DEG

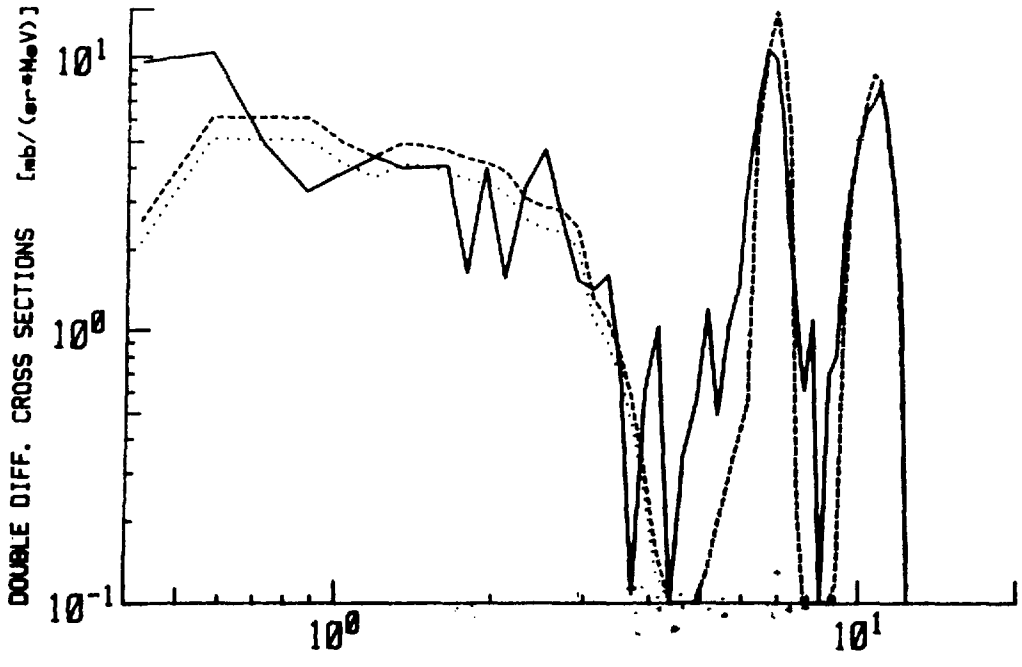

FIG. A-51. CARBON 130.0 DEG

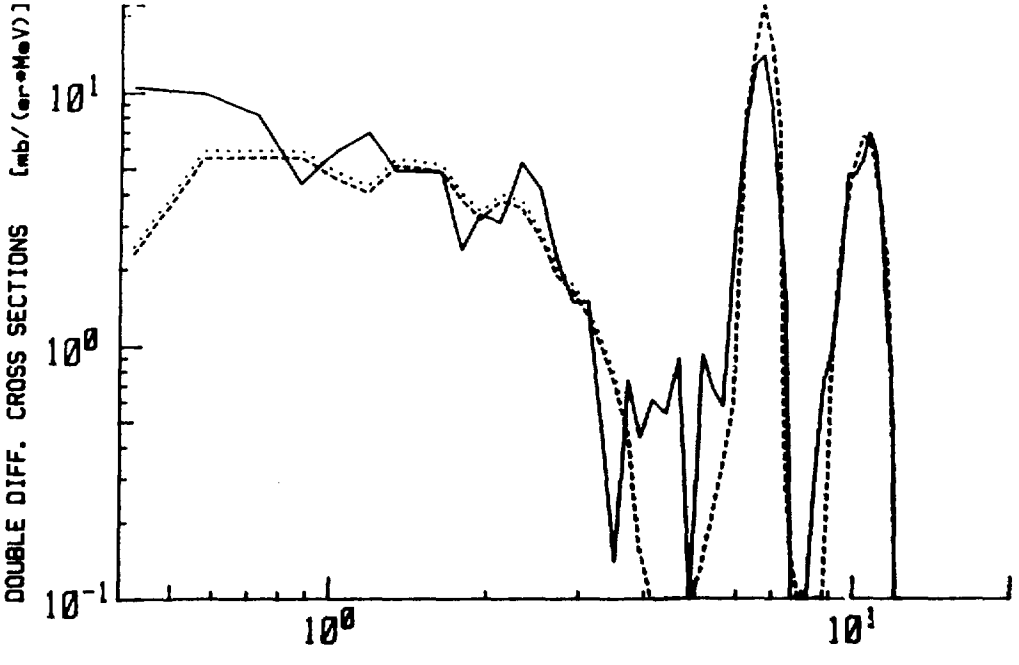

FIG. A-52. CARBON 143.0 DEG